Mississippi State University
Scholars Junction

Theses and Dissertations Theses and Dissertations

8-6-2021

Electric Vehicles Fast Charger Location-Routing Problem Under Ambient Temperature

Darweesh Ehssan A Salamah
darweesh.salamah@gmail.com

Follow this and additional works at: https://scholarsjunction.msstate.edu/td

Recommended Citation
Salamah, Darweesh Ehssan A, "Electric Vehicles Fast Charger Location-Routing Problem Under Ambient Temperature" (2021). *Theses and Dissertations*. 5197.
https://scholarsjunction.msstate.edu/td/5197

This Dissertation - Open Access is brought to you for free and open access by the Theses and Dissertations at Scholars Junction. It has been accepted for inclusion in Theses and Dissertations by an authorized administrator of Scholars Junction. For more information, please contact scholcomm@msstate.libanswers.com.

المنارة للاستشارات
www.manaraa.com

Electric vehicles fast charger location-routing problem under ambient temperature

By

Darweesh Ehssan A. Salamah

Approved by:

Mohammad Marufuzzaman (Major Professor)
Junfeng Ma
Imad Aleithawe
Mohannad Kabli
Linkan Bian (Graduate Coordinator)
Jason M. Keith (Dean, Bagley College of Engineering)

A Dissertation
Submitted to the Faculty of
Mississippi State University
in Partial Fulfillment of the Requirements
for the Degree of Doctor of Philosophy
in Industrial Engineering
in the Department of Industrial and Systems Engineering

Mississippi State, Mississippi

August 2021

المنارة للاستشارات
www.manaraa.com

Copyright by

Darweesh Ehssan A. Salamah

2021

المنارة للاستشارات

www.manaraa.com

Name: Darweesh Ehssan A. Salamah

Date of Degree: August 6, 2021

Institution: Mississippi State University

Major Field: Industrial Engineering

Major Professor: Mohammad Marufuzzaman

Title of Study: Electric vehicles fast charger location-routing problem under ambient temperature

Pages of Study: 113

Candidate for Degree of Doctor of Philosophy

Electric cars are projected to become the vehicles of the future. A major barrier for their expansion is range anxiety stemming from the limited range a typical EV can travel. EV batteries' performance and capacity are affected by many factors. In particular, the decrease in ambient temperature below a certain threshold will adversely affect the battery's efficiency. This research develops deterministic and two-stage stochastic program model for charging stations' optimal location to facilitate the routing decisions of delivery services that use EVs while considering the variability inherent in climate and customer demand. To evaluate the proposed formulation and solution approach's performance, Fargo city in North Dakota is selected as a tested.

For the first chapter, we formulated this problem as a mixed-integer linear programming model that captures the realistic charging behavior of the DCFC's in association with the ambient temperature and their subsequent impact on the EV charging station location and routing decisions. Two innovative heuristics are proposed to solve this challenging model in a realistic test setting, namely, the two-phase Tabu Search-modified Clarke and Wright algorithm and the Sweep-based

المنارة للاستشارات

www.manaraa.com

Iterative Greedy Adaptive Large Neighborhood algorithm. The results clearly indicate that the EV DCFC charging station location decisions are highly sensitive to the ambient temperature, the charging time, and the initial state-of-charge. The results provide numerous managerial insights for decision-makers to efficiently design and manage the DCFC EV logistic network for cities that suffer from high-temperature fluctuations.

For the second chapter, a novel solution approach based on the progressive hedging algorithm is presented to solve the resulting mathematical model and to provide high-quality solutions within reasonable running times for problems with many scenarios. We observe that the location-routing decisions are susceptible to the EV logistic's underlying climate, signifying that decision-makers of the DCFC EV logistic network for cities that suffer from high-temperature fluctuations would not overlook the effect of climate to design and manage the respective logistic network efficiently.

المنارة للاستشارات

www.manaraa.com

DEDICATION

To my parents and grandparents for their endless prayers, to my wife Dareen, who has been so supportive throughout my whole study, and my adorable daughter Dana.

المنارة للاستشارات

www.manaraa.com

ACKNOWLEDGEMENTS

I want to express my deep gratitude to everyone who has assisted me throughout my doctoral studies over the years. I want to thank my advisor Dr. Mohammad Marufuzzaman, for all the knowledge, support, and continuous encouragement and guidance throughout my doctoral studies. In addition, I will thank Dr. Mohannad Kabli. In 2005, he convinced me to be major in Industrial Engineering when we were studying undergraduate degree. The experience I gained from him is immense and invaluable and has prepared me to research in the best possible manner. I am also indebted to the other committee members, Dr. Linkan Bian, Dr. Junfeng Ma, and Dr. Imad Aleithawe, for their insightful comments and suggestions that helped to improve this research. I truly appreciate all their time and assistance. There are too many friends to name in the Department of Industrial and Systems Engineering who helped me for several years. Especially notable are Dr. Md Abdul Quddus, Dr. Sushil Poudel, Dr. Sudipta Chowdhury, Dr. Mojtaba Khanzadeh (MK), Dr. Farjana Nur, Dr. Jack Francis, Dr. Badr Aladwan, Amin Aghalari and Abdullah Battawi. They helped me with my research and made graduate school life and conferences fun. I also thank all other friends and colleagues at the McCain building and Starkville for not keeping me isolated and lonely. I also want to thank Holmes Cultural Diversity Center (HCDC), Graduate Students Association (GSA), TEDx MSSTATE, INFORMS student chapter at Mississippi State University, and Saudi Students Association . A special thanks to my friends Dr. Mohammad Hawasawi , and Dr. Salim Batiyah for sharing their electrical engineering experiences in my research. In addition,

المنارة للاستشارات
www.manaraa.com

I would like to thank my grandparents, my mother Dr. Hayam Badrshani, my father Ehssan, my brother Eyad, my sister Aya, my mother-in-law Aisha Kojah. They have always been a tremendous source of encouragement in each day of my life. They taught me how to love unconditionally and be more assertive. Then, I will show my deep and earnest thanks to my wife, Dareen Altayyar, and my daughter Dana. Dareen was very patient and encouraging me to work challenging during this whole process. She sacrificed a lot for my career development, and she was always there cheering me up and stood by me through the good times and bad. Finally, I want to thank my friends who support me in this journey around the world, especially Dr. Abdullah Aljubiri, Ghassan Gamal, Dr. Dalal Binmahfouz, Dr. Mahmoud Alaish, Dr. Sahar Awlya, Rayan Samman, Dr. Lujain Daghstani, Talal Alhafeez, Khadija Hussain, Ebtihal Shaban, Mohammad Alsaggaf, Mohammad Baghdadi, Mansour Ashmouni, and Dr. Manal Sunbul. I thank my sponsors, the Saudi Arabian Culture Mission (SACM) in the United States and King Abdullah City for Atomic and Renewable Energy (KA-CARE), for supporting me financially throughout my study.

المنارة للاستشارات
www.manaraa.com

TABLE OF CONTENTS

المنارة للاستشارات

www.manaraa.com

للاستشارات المنارة
www.manaraa.com

LIST OF TABLES

للاستشارات المنارة

www.manaraa.com

LIST OF FIGURES

المنارة للاستشارات

www.manaraa.com

CHAPTER I

DETERMINISTIC ELECTRIC VEHICLES FAST CHARGER LOCATION ROUTING PROBLEM UNDER AMBIENT TEMPERATURE

1.1 Introduction

In recent years, *electrical vehicles* (EV) have become an essential part of the manufacturing sector as the global day-by-day forced to future less dependent on nonrenewable fuel sources [61]. Sustainable transportation requires multiple efforts from different stakeholders (e.g., governments, car manufacturers, environmental advocates, and customers) to reduce the consumption of non-renewable resources (e.g., oil, coal, and gas). EV owners will increase to around 126 million in 2030 globally and 18.7 million in the USA [61]. As more EVs take to the road, the charging station system needs to be expanded accordingly. The large-scale adoption of EVs cannot be fully realized without the adequate deployment of publicly accessible charging stations. The problem of optimally locating the EV charging stations is not trivial due to simultaneous consideration of many factors, such as range anxiety, uncertainty in dwell time, frequency of charging, state of charge (SOC), and finally varieties of charging needs by different users (e.g., residential, visitors, employee, the fleet users) [13]. Even though separate or a combination of them is accounted for by a number of recent studies, none of the prior studies examined the impact of weather (e.g., hot or cold weather conditions) in designing the logistic network for the EV DCFC charging stations [97, 95].

المنارة للاستشارات

www.manaraa.com

EVs are typically equipped with small battery packs that can only offer a very limited driving range per charge. Cold temperature can significantly reduce the charging rate, which consequently prolongs the charging duration. Further, due to continuous heating needs in cold regions, the battery packs of EVs are always under stress, which substantially degrades the battery performance over time. A recent study from Idaho National Laboratory (INL) reported that the SOC of a 30-minute DC fast chargers (DCFC) could drop by as large as 36% from warm temperature ($25\circ C$) to cold temperature ($0\circ C$) [65], indicating the sensitivity of EVs routing performance in cold regions. Further, a number of relevant recent studies demonstrate that the performance of the Lithium-ion (Li-ion) battery is sensitive to the ambient weather (e.g., [18, 33, 32, 52]). Although very relevant, the temperature effect on EVs fast-charging is not considered and extensively examined. Thus, considering the effects of ambient temperature, specifically in the geographic areas that suffer from fluctuating temperatures throughout the year, on the EVs mobility network's planning is imperative.

To fulfill this knowledge gap, our study extends the traditional location-routing problems to develop an innovative mathematical model that examines the impact of ambient temperature on the EV DCFC charging station locations and the associated routing decisions. Given the problem is an extension of the traditional location-routing problems, which are already known to be an $\mathcal{NP}$-hard problem [70], we propose to develop two innovative heuristics, namely, the two-phase Tabu Search-modified Clarke and Wright and the Sweep based Iterated Greedy Adaptive Large Neighborhood algorithm, to efficiently solve the proposed model in a reasonable timeframe. The performance of the solution algorithms is validated via a series of computational experiments. In addition to proposing the mathematical model and the solution approaches, we demonstrate a real-life case study using the EV logistics network of Fargo city in North Dakota. The results

المنارة للاستشارات
www.manaraa.com

demonstrate the impact of ambient temperature on the EV DCFC location-routing decisions, which provide a number of managerial insights for efficiently designing and managing the EV logistic network in cities suffering from high-temperature fluctuations.

The exposition of this paper is as follows. Section 1.2 details the relevant literature review. Sections 2.3 and 2.4 introduce the proposed mathematical model formulation and the solution approaches. Finally, Section 2.5 presents the numerical experiments under different settings to assess the performance of our proposed methodologies. This study is providing a number of future research directions present in Chapter 3.

1.2 Literature Review

EV logistic literature, although it considers the charging station deployment along with the routing decisions, the effects of the ambient temperature on the maximum driving range of the EVs, which could potentially affect both the location-routing decisions, have not been adequately addressed. Most of the past studies assumed constant ambient temperature to simplify the modeling and computational efforts further. As this study is an extension of the location-routing problem to the EV area, which accounts for realistic features such as the impact of ambient temperature in the EVs' recharging process, we will first provide a detailed review of these problems.

Location-routing problems (LRP) simultaneously handle strategic-level (e.g., locating the charging stations) and operational-level (e.g., EV routing plans) decisions under the same decision-making framework. Quite a few variants of the LRP studies are available in the literature, such as single vs. multiple depots (e.g., [93],[103]), capacities on depots or vehicles (e.g., [51, 87]), and the time window restriction for the deliveries (e.g., [101, 21]). A comprehensive review

المنارة للاستشارات
www.manaraa.com

of the LRP can be found in [67] and [72]. Due to the challenges associated with solving LRP in commercial solvers (e.g., GUROBI/CPLEX), most of the past studies only able to find exact solutions to medium-sized capacitated or uncapacitated LRPs. The branch and bound algorithm, proposed by Laporte and Norbert [46], is considered the first study to provide an exact solution for an LRP consisting of only a depot and customers ranging from 20 to 50. In another study, Laporte et al. [47] developed a branch and cut algorithm to solve an uncapacitated LRP with 20 customers and 8 depots. Belenguer et al. [8] developed a new branch and cut algorithm, with a family of problem-specific valid inequalities, to exactly solve an uncapacitated LRP with 20-88 customers and 5-10 potential depots. Baldacci et al. [7] utilized set partitioning problems to reformulate the LRP, which then solved exactly by introducing a set of lower bounding techniques. The authors could solve the LRP up to 199 customers and 15 potential depot locations. Besides proposing the exact approaches, several heuristics are developed to solve realistic-size test instances in a reasonable timeframe. These heuristics decompose the LRP into two subproblems based upon the two decision levels, attempt to solve LRP sequentially and provide quality feasible solutions for large instances. For instance, Tuzun and Burke [88] developed a two-phase tabu search heuristic to solve an uncapacitated LRP. Wu et al. [93] combined a tabu search algorithm with a simulated annealing algorithm to solve a capacitated LRP. Prins et al. [71] developed a cooperative Lagrangian relaxation-granular tabu search heuristic to solve a capacitated LRP. Koç et al. [41] first introduced a family of valid inequalities and then developed a hybrid evolutionary algorithm, namely, the location-heterogeneous adaptive large neighborhood search procedure, to solve an LRP with heterogeneous fleet and time windows. Zhao et al. [106] proposed an iterated local search algorithm to solve an LRP with simultaneous pickup and delivery. Likewise, different heuristic

المنارة للاستشارات
www.manaraa.com

techniques are utilized to solve LRP applied in various applications, such as genetic algorithm with a new chromosome structure to solve a multimodal transportation network problem [22], variable neighborhood search algorithm along with a simulated annealing algorithm to solve a solid waste management problem [6], and many others.

Rather than adopting a LRP approach, another stream of research utilizes the maximum covering approach such that p refueling stations are opened to maximize the feasible round-trips between a set of source-destination pairs. This approach, proposed by Kuby and Kim [42], is referred to as the *flow refueling location model* (FRLM). Following this innovative approach, a number of extensions of the uncapacitated FRLM are made available, such as locating multiple facilities on the paths [43], capacitated FRLM [89], robust-counterpart of FRLM with battery-swapping network infrastructure and management [55], and capabilities for EV of making intentional deviation from the associated shortest path to refuel their batteries [40]. Besides adopting the FRLM approach, Mirchandani et al. [63] proposed a new formulation to capture the fleet scheduling and battery-swapping station in EV logistics. This study applies the shortest path concept to the EV routing problem such that several EVs with limited driving range could satisfy the customer demand in a single depot network. Yang and Sun [98] proposed a mathematical model for EV battery-swap stations-based LRP such that the EVs could revisit the same swapping stations multiple times. Schneider et al. [82] proposed an efficient heuristic to solve an EV LRP with a time window. Schiffer and Walther [81] proposed an EV LRP formulation with time windows capable of addressing a whole range of recharging options such as charging at customer sites and unique vertices, partial and full recharging. Most recently, Zhang et al. [105] proposed a hybrid heuristic algorithm that combines the binary particle swarm optimization with the variable neighborhood search to solve an EV LRP

المنارة للاستشارات
www.manaraa.com

under stochastic customer demand. Hof et al. [31] proposed an Adaptive Variable Neighborhood Search algorithm to solve a battery swap station-based LRP with capacitated EVs. Li et al. [50] proposed a bi-level programming approach, where the upper-level locates the charging stations and the lower-level decides the optimal routing plan to efficiently deploy the public recharging infrastructure in a given region.

Despite these notable developments, past studies (e.g., [104, 15, 102, 75, 73, 77, 34]), especially the studies that modeled the DCFC LRPs, ignore climate variability on location-routing decisions. A recent study by Motoaki et al. [65] showed that the ambient temperature could heavily impact the DCFC charging rate. The authors stressed that considering the ambient temperature in designing the EV DCFC infrastructure in large countries like the US, where the regional climate varies significantly, could not be neglected. Unfortunately, most of the past studies (e.g., [104, 15, 102, 75, 73, 77, 34]) assume that the charging process of the EVs, i.e., charging rate, as a constant factor in their formulation; hence, the obtained results for the EV logistics might be altered. To fill this gap in the literature, this study extends the traditional LRPs to account for the impact of ambient temperature on the DCFC infrastructure deployment and the associated EV routing decisions.

1.3 Mathematical Model Formulation

Because of the scarce research streams that include the ambient temperature, we start introducing the EV faster charger location-routing problem and discuss the potential interactions among simultaneous routing and siting decisions with the ambient temperature. Thus, in this section, we first proceed with the basic mathematical model formulation, referred to as **[EV]**, and then proceed to describe the model extension, referred to as **[EV-L]**. Finally, a number of variable fixing and

المنارة للاستشارات
www.manaraa.com

valid inequalities are introduced in an attempt to improve the computational performance of model **[EV-L]**.

1.3.1 Basic Model Formulation: [EV]

In this sub-section, the EV basic mathematical formulation (**[EV]**) is introduced as a mixed-integer linear programming (MILP) model. We assume that there exists a linear relationship between the (i) travel distance and the energy consumption and (ii) recharging time with the amount of energy recharged. Figure 1.1 delineates a simplified pictorial representation of the problem. Below is a summary of the sets, parameters, and decision variables of the optimization model. Our objective function is described in Section 1.3.1.1 and the constraints are introduced in Section 1.3.1.2.

Sets:

- I: set of customers, indexed by $i \in I$
- J: set of potential charging station locations, indexed by $j \in J$
- E: set of electrical vehicles, indexed by $e \in E$
- $\{o, o^{'}\}$: single depot and it's copy
- N: set of all nodes, indexed by $n \in N$, where $N = I \cup J \cup \{o, o^{'}\}$

Parameters:

- f_j: cost of installing a new charging station $j \in J$
- d_{ij}: distance between node $i \in N$ and $j \in N$
- c_{ije}: shipping cost per unit of distance between node $i \in N$ to $j \in N$ via EV $e \in E$
- w_i: demand weight for costumer $i \in I$
- k_e: weight capacity of EV $e \in E$

المنارة للاستشارات
www.manaraa.com

- soc: state of charge (SOC, in %) of an EV after getting charged in a DCFC station
- soc_0: initial SOC (%) of an EV at depot
- ϕ: conversion rate of vehicle $e \in E$ which is utilized to convert the state of charge to the respective maximum driving distance that an EV can travel after getting charged
- M: a big number
- d_{max}: the upper bound of driving distance once EVs are fully charged, where $d_{max} \geq soc$

Decision Variables:

- X_j: 1 if a charging station is built in $j \in J$; 0 otherwise
- Y_{ije}: 1 if EV $e \in E$ traverses from node $i \in N$ to $j \in N$; 0 otherwise
- R_{ije}: remaining weight capacity of $e \in E$ when it arrives node $i \in N$ after leaving node $j \in N$
- B^1_{ne}: the maximum distance that the remaining battery power allows when EV $e \in E$ arrives at node $n \in N$
- B^2_{ne}: the maximum distance that the remaining battery power allows when EV $e \in E$ leaves node $n \in N$

المنارة للاستشارات

www.manaraa.com

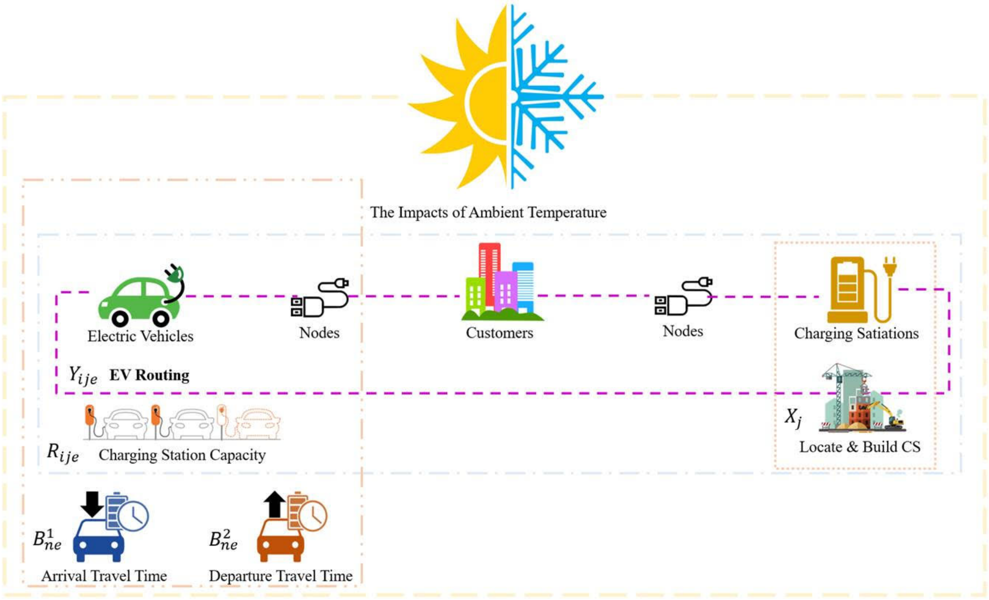

Figure 1.1

A simplified pictorial representation of the problem

1.3.1.1 Objective Function

The objective function of **[EV]** minimizes the total cost associated with opening EV charging stations and the driving distance costs within a planning horizon. The mathematical formulation is detailed as follows:

$$\textbf{[EV]}\ Minimize\ \underbrace{\overset{\text{Facility Cost}}{\sum_{j\in J} f_j X_j}} + \underbrace{\overset{\text{Total Driving Distance Cost}}{\sum_{i\in N}\sum_{j\in N}\sum_{e\in E} c_{ije} d_{ij} Y_{ije}}} \tag{1.1}$$

1.3.1.2 Constraints

Model **[EV]** is subject to a set of constraints, which are outlined below.

المنارة للاستشارات
www.manaraa.com

$$\sum_{n\in N\notin\{o'\}} \sum_{e\in E} Y_{nie} = 1 \qquad \forall i \in I \tag{1.2}$$

$$\sum_{n\in N\notin\{o'\},n\neq j} \sum_{e\in E} Y_{nje} \leq MX_j \qquad \forall j \in J \tag{1.3}$$

$$\sum_{n'\in N\notin\{o\},n'\neq n} Y_{nn'e} - \sum_{n'\in N\notin\{o'\},n'\neq n} Y_{n'ne} = 0 \qquad \forall n \in N \notin \left\{o, o'\right\}, e \in E \tag{1.4}$$

$$\sum_{n\in N\notin\{o\}} Y_{one} - \sum_{n\in N\notin\{o'\}} Y_{noe} = 0 \qquad \forall e \in E \tag{1.5}$$

$$\sum_{n\in N\notin\{o\}} Y_{one} \leq 1 \qquad \forall e \in E \tag{1.6}$$

$$\sum_{n\in N\notin\{o',j\}} R_{nje} = \sum_{n\in N\notin\{o,j\}} R_{jne} \qquad \forall j \in J, \forall e \in E \tag{1.7}$$

المنارة للاستشارات

www.manaraa.com

$$\begin{aligned}
\sum_{n\in N\notin\{o,i\}} R_{ine} &\le \sum_{n\in N\notin\{o',i\}} R_{nie} - w_i \sum_{n\in N\notin\{o',i\}} Y_{nie} \\
&+ k_e(1 - \sum_{n\in N\notin\{o',i\}} Y_{nie}) \quad \forall i \in I, \forall e \in E
\end{aligned} \tag{1.8}$$

$$\begin{aligned}
0 \le R_{nn'e} &\le k_e Y_{nn'e} \quad \forall n \in N \notin \left\{o'\right\}, \\
&n' \in N \notin \{o\}, n \neq n', e \in E
\end{aligned} \tag{1.9}$$

$$\begin{aligned}
B^1_{n',e} + d_{nn'} Y_{nn'e} &\le B^2_{ne} + d_{max}(1 - Y_{nn'e}) \quad \forall n \in N \notin \left\{o'\right\}, \\
&n' \in N \notin \{o\}, n' \neq n, e \in E
\end{aligned} \tag{1.10}$$

$$\begin{aligned}
B^1_{n'e} + d_{nn'} Y_{nn'e} &\ge B^2_{n,e} - d_{max}(1 - Y_{nn'e}) \quad \forall n \in N \notin \left\{o'\right\}, \\
&n' \in N \notin \{o\}, n' \neq n, e \in E
\end{aligned} \tag{1.11}$$

$$B^2_{oe} = \phi soc_0 \qquad \forall e \in E \tag{1.12}$$

$$B^2_{je} = \phi soc X_j \qquad \forall j \in J, e \in E \tag{1.13}$$

$$B^1_{ie} = B^2_{ie} \qquad \forall i \in I, e \in E \tag{1.14}$$

$$R_{ije}, B^1_{ne}, B^2_{ne} \ge 0 \qquad \forall (i,j) \in N, n \in N, e \in E \tag{1.15}$$

$$X_j, Y_{ije} \in \{0,1\} \qquad \forall i \in N, j \in N, e \in E \tag{1.16}$$

Constraints (1.2) ensure that each customer site $i \in I$ is visited by exactly one EV. Constraints (1.3) ensure that EVs could get recharged at a specific charging station $j \in J$ if only it is located. Constraints (1.4) enforce the flow balance for each EV's $e \in E$ in the customer sites and the charging stations. Constraints (1.5) guarantee that a utilized EV $e \in E$ should return to the depot at the end of the respective trip. Constraints (1.6) limit the number of trips that an EV $e \in E$ can start

المنارة للاستشارات
www.manaraa.com

from the depot. Constraints (1.7) ensure that at any charging station $j \in J$, the remaining weight capacity of the EVs does not change ($w_j = 0; \forall j \in J$). Constraints (1.8) update the remaining weight capacity of the EVs based on the nodes visited. Constraints (1.9) enforce that the remaining weight capacity of the EVs is less than the EV maximum weight capacity and also be greater than zero in all the visited nodes by the EVs. Constraints (1.10) and (1.11) update the battery power level of the EVs based on the nodes visited. Constraints (1.12) and (1.13) detail the SOC when the EV $e \in E$ starts its trip from the depot and when it visits a charging station. Constraints (1.14) ensure that the battery level of the EVs $e \in E$ remains unchanged when they visit a customer node $i \in I$ in the network. Constraints (1.15) and (1.16) enforce nonnegativity and binary resrictions for the decision variables.

1.3.2 Model Extension: [EV-L]

Model **[EV]** assumes that the SOC of a fast charger drops linearly. However, the actual fast charging process is non-linear and is a function of initial SOC and ambient temperature [65]. The simplified linearized SOC assumption may provide an overestimated duration for the DCFC's. As such, the resulting model, as in the case with **[EV]**, may overestimate the EV fast charger location-routing decisions. This sub-section introduces model **[EV-L]** by alleviating this drawback from model **[EV]**.

Let us define $\hat{soc}(c, t)$ to predict the SOC of an EV $e \in E$, which is a function of charging time t and ambient temperature c (in ^{o}Celsius). We further define $\lambda_0, \lambda_1, \lambda_2$ to be the coefficient estimates, and soc_0 the initial value of the SOC of an EV. Inspired from the study of [65], the following SOC estimation is provided.

المنارة للاستشارات
www.manaraa.com

$$s\hat{o}c(c,t) = \left(soc_0 + \frac{\lambda_0 + \lambda_1 c}{\lambda_2}\right)e^{\lambda_2 t} - \left(\frac{\lambda_0 + \lambda_1 c}{\lambda_2}\right)$$

After simplification, the above equation becomes:

$$s\hat{o}c(c,t) = e^{\lambda_2 t} soc_0 + \left(\frac{\lambda_0 + \lambda_1 c}{\lambda_2}\right)(e^{\lambda_2 t} - 1)$$

The ambient temperature is constant for all vehicles while they are in the charging process. We now replace the $e^{\lambda_2 t}$ and $\left(\frac{\lambda_0+\lambda_1 c}{\lambda_2}\right)(e^{\lambda_2 t} - 1)$ terms by μ_1 and μ_2, respectively, and obtained the following equation.

$$s\hat{o}c_{(}c,t) = \mu_1 soc_0 + \mu_2 \tag{1.17}$$

When an EV $e \in E$ arrives at a charging station, B^1_{je} captures the maximum distance that the EV can keep driving. Using the conversion rate (ϕ), the initial SOC (soc_0) of an EV at a charging station $j \in J$ can be defined as follows:

$$soc_0 \times \phi = B^1_{je} \longrightarrow soc_0 = \frac{B^1_{je}}{\phi} \tag{1.18}$$

Plugging (1.18) into (1.17), we obtain the following equation:

$$s\hat{o}c_{(}c,t) = \mu_1\left(\frac{B^1_{je}}{\phi}\right) + \mu_2 \tag{1.19}$$

Now, plugging (1.19) into constraints (1.13), we obtain the following:

$$B^2_{je} \leq soc\phi X_j \rightarrow B^2_{je} \leq \left(\mu_1 \frac{B^1_{je}}{\phi} + \mu_2\right)\phi X_j \rightarrow B^2_{je} \leq \mu_1 B^1_{je} X_j + \mu_2 \phi X_j \quad \forall j \in J, e \in E \tag{1.20}$$

المنارة للاستشارات
www.manaraa.com

Constraints (1.20) is nonlinear due to the presence of a product term between variables B^1_{je} and X_j, namely, $B^1_{je}X_j$. To linearize this product, we introduce a new variable $\{Z_{je} | \forall j \in J, e \in E\}$ to replace the $B^1_{je}X_j$ term. Knowing that d_{max} is an upper bound for the B^1_{je} variable, the following set of constraints are introduced.

$$Z_{je} \leq d_{max}X_j \qquad \forall j \in J, e \in E \tag{1.21}$$

$$Z_{je} \leq B^1_{je} \qquad \forall j \in J, e \in E \tag{1.22}$$

$$Z_{je} \geq B^1_{je} - d_{max}\left(1 - X_j\right) \qquad \forall j \in J, e \in E \tag{1.23}$$

$$Z_{je} \geq 0 \qquad \forall j \in J, e \in E \tag{1.24}$$

With this, model **[EV]** can be extended as follows, referred to as **[EV-L]**:

$$\textbf{[EV-L]}\ Minimize \sum_{j \in J} f_j X_j + \sum_{i \in N} \sum_{j \in N} \sum_{e \in E} c_{ije} d_{ij} Y_{ije} \tag{1.25}$$

subject to: (1.2)-(1.12), (1.14)-(1.16), and (1.20)-(1.24).

1.3.3 Variable Fixing and Valid Inequalities

To improve the computational performance of model **[EV-L]**, the following variable fixing and valid inequalities are introduced. We begin by introducing the variable fixing techniques first.

- The electric vehicle $e \in E$ is not able to traverse the arc between the nodes $n \in N$ and $n^{'} \in N$ if the respective traveling distance, i.e., d_{ij} is greater than the maximum distance that it can travel by a fully charged battery, namely, d_{max}.

المنارة للاستشارات
www.manaraa.com

$$Y_{nn'e} \quad = \quad 0 \qquad \forall n \in N, n^{'} \in N, e \in E | d_{nn'} > d_{max} \tag{1.26}$$

- The electric vehicle $e \in E$ is not able to traverse the arc between the nodes $n \in N$ and $n^{'} \in N$ if the sum of the demand of costumers in respective customer nodes exceeds the weight capacity of the EV.

$$Y_{nn'e} \quad = \quad 0 \qquad \forall n \in N, n^{'} \in N, e \in E | w_n + w_{n'} > k_e \tag{1.27}$$

In addition to the above-mentioned variable fixing techniques, the following valid inequalities are introduced.

- In our study, we assume that none of the EVs can travel more than d_{trip} each day. To capture this constraint, we add the following valid inequalities as a lazy constraint to model **[EV-L]**.

$$\sum_{n \in N} \sum_{n' \in N} d_{nn'} Y_{nn'e} \quad \leq \quad d_{trip} \qquad \forall e \in E \tag{1.28}$$

- To further tighten the proposed model **[EV-L]**, first, we approximate a lower bound, namely, N_{LB}^{total}, for the number of the EVs that are required to satisfy the customer demand. The lower bound on the number of EVs depends on two other factors, namely, the total weight associated with the requests of the costumers and maximum trip distance that each EV can traverse. Hence, in order to calculate N_{LB}^{total}, first, we find out the minimum number of EVs based on the freight limitation, $N_{LB}^{freight}$. To do so, we use a well-known bin packing problem [57] given by (1.29)-(1.33). Within this formulation, $\{Z_e | \forall e \in E\}$ denotes if EV $e \in E$ is used or not, and $\{H_{ie} | \forall i \in I, e \in E\}$ denotes if costumer i is served by EV e.

المنارة للاستشارات

www.manaraa.com

$$Minimize \quad N_{LB}^{freight} = \sum_{e \in E} Z_e \tag{1.29}$$

subject to

$$\sum_{i \in I} w_i H_{ie} \leq k_e Z_e \qquad \forall e \in E \tag{1.30}$$

$$\sum_{e \in E} w_i H_{ie} = 1 \qquad \forall i \in I \tag{1.31}$$

$$Z_e \in \{0, 1\} \qquad \forall e \in E \tag{1.32}$$

$$H_{ie} \in \{0, 1\} \qquad \forall i \in I, e \in E \tag{1.33}$$

The next lower bound on the number of EVs is based upon the maximum length of the trip, N_{LB}^{trip}, which utilizes the concept of the minimal spanning tree. To do so, given the feasible arcs in the network, we create a minimal spanning tree for the network consisting of the depot node and customer nodes, i.e., $I \cup \{o\}$. The total weight of this graph, where the weight is the traveling distance between vertices of the graph, provides us with an estimated minimum overall traveling distance of d_{est}. Hence, the second lower bound is computed as follow:

$$N_{LB}^{trip} = * \frac{d_{est}}{d_{trip}} \tag{1.34}$$

Having introduced these two lower bounds on the minimum number of required EVs, we use the best among them in the MILP settings, as shown below:

$$N_{LB}^{total} = max\{N_{LB}^{freight}, N_{LB}^{trip}\} \tag{1.35}$$

المنارة للاستشارات

www.manaraa.com

Finally, to tighten the solution space of model **[EV-L]**, we add the following valid inequality as a lazy constraint.

$$\sum_{e \in e} \sum_{n' \in N} Y_{on'e} \geq N_{LB}^{total} \tag{1.36}$$

1.4 Solution Methodology

Both basic (**[EV]**) and extended (**[EV-L]**) formulations developed in this study are indeed variants of the classical location-routing problems (LRP) [46]. It is worth mentioning that if the driving range of the EVs is a sufficiently large number, recharging the battery and constructing the charging stations will be unnecessary; therefore, model **[EV-L]** can be reduced to the classic vehicle routing problem (VRP) which is already known to be an $\mathcal{NP}$-hard problem [42]. As such, our proposed model **[EV-L]** can be considered as an $\mathcal{NP}$-hard problem.

Our initial experimentation with the GUROBI solver exposes its inability to solve the largest instances of problem **[EV-L]** in a reasonable timeframe, despite the additions of the variable fixing and valid inequalities introduced in Section 1.3.1. Given $\mathcal{NP}$-hard problems are hard or impossible to be solved using exact methods in a reasonable computational time [36], this section proposes two heuristic techniques, namely, the two-phase Tabu Search-modified Clarke and Wright Savings heuristic (TS-MCWS) and the Sweep-based Iterated Greedy Adaptive Large Neighborhood algorithm, to solve model **[EV-L]** efficiently.

المنارة للاستشارات

www.manaraa.com

1.4.1 The TS-MCWS Heuristic

This sub-section details the proposed hybrid algorithm referred to as the TS-MCWS heuristic, which combines the Tabu Search (TS) algorithm with a modified version of the Clarke and Wright Savings method. Within this two-phase algorithm, the TS algorithm is used to determine the location of the charging stations and then given the selected charging stations, the modified Clarke and Wright Savings method is used to finding the routing decisions. Two algorithms collaborate iteratively to provide an efficient solution for the model **[EV-L]**.

1.4.1.1 A radius covering procedure for initial location of the charging stations

To start the TS algorithm and find the charging station locations, an initial solution for selecting the charging stations is required. Let $d_{charge} = \phi \times \hat{soc}(c,t)$ represents the driving range of EVs after getting charged in a station after t minutes where the ambient temperature is c degree Celcius. Further, let N_J to represent the initial number of selected charging stations. The idea of this procedure is to select N_J stations that could cover as many as costumers within a radius of $r \times d_{charge}$ from each candidate station, where $0 \leq r \leq 1$ and is set to $r \leftarrow \frac{1}{3}$ in this study. This procedure is outlined as follows:

- **Step 1**: We generate a *covering list* (CL) for all the charging stations, which indicates the respective number of the customers that are located within the radius of $r \times d_{charge}$ from each charging station. To generate this list, we adopt two different strategies. In the first strategy, all the customers within the mentioned radius are counted for all the charging stations. However, in the second strategy, once a set of customers are covered by a specific charging station, they are removed from the customer list for the rest of the charging stations.

المنارة للاستشارات
www.manaraa.com

Before starting the TS procedure, first, we adopt the first strategy to come up with the initial location of the charging stations, and in case if the current list of charging stations does not lead to a feasible routing plan, we relocate the selected N_J charging stations using the second strategy.

- **Step 2**: Given the value of CL list for each candidate stations, we rank all the charging stations in descending order.

- **Step 3**: The first N_J stations based on the ordered CL list are selected as the initial location of the charging stations.

1.4.1.2 The modified version of the Clarke and Wright Savings method

Once the location of the charging stations using either the radius covering procedure or the TS algorithm is determined, we adopt a modified version of the Clarke and Wright Savings method to determine the optimal routing decisions within the selected charging stations. The original Clarke and Wright Savings method was first proposed by Clarke and Wright for classical VRP [11] and then Erdogan et al. [20] introduced the modified version of the algorithm for the green-VRP. The overall $MCWS$ framework is outlined as follows:

- **Step 1** (Initialization phase):

  Step 1.1: For each of the customers, $i \in I$, a back and forth route using the depot and its copy is generated $(o - i - o^{'})$.

  Step 1.2: The feasibility of each of the generated routes in the previous step is evaluated with respect to the battery driving range limitation. Those routes that are feasible are added

المنارة للاستشارات
www.manaraa.com

to *feasible route set* (FRS). However, for the routes in which the battery driving range is violated, one of the located stations, say j_1, with less insertion cost, is placed between the depot and the customer, such as $(o - j_1 - i - o^{'})$. If the modified route is feasible, it is added to the FRS; otherwise, another selected charging station, say j_2, is added between the customer and the copy of the depot, such as $(o - j_1 - i - j_2 - o^{'})$. If the modified route is still infeasible, it is discarded from the routing plan and added to *infeasible route set* (IRS); otherwise, it is added to the FRS. If the IRS is empty, then we directly go to **Step 2**; otherwise, the objective function of the infeasible routes in IRS are set to infinite.

- **Step 2** (Route merge phase):

  Step 2.1: For each pair of feasible routes in FRS, we compute the saving distances. First, for each feasible route ($k \in FRS$), the two adjacent nodes (n_k^1, n_k^2) to the depot and its copy are identified. Second, we create a saving pair $[n_1, n_2]$ which includes two nodes from two different routes, namely, k_1 and k_2, and add to a list called *SPL*. Then, we calculate the respective savings of each pair $s[n_1, n_2]$ using $s[n_1, n_2] = d_{o,n_1} + d_{o,n_2} - d_{n_1,n_2}$. All the saving pairs in *SPL* are sorted in a descending order with respect to the respective saving values, i.e., $s[n_1, n_2]$.

  Step 2.2: In this step, we attempt to merge the feasible routes in FRS considering the sorted savings obtained from the previous step. First, we choose the first element from *SPL*, i.e., $[n_1, n_2]$, and then introduce two new sets, namely R_1 and R_2, which include all the routes that visit node n_1 and n_2, respectively. For each route in $r_1 \in R_1$, we select route $r_2 \in R_2$ in order and merge two routes as follows: delete the arcs $(o, n_1) \in R_1$, $(o, n_2) \in R_2$ and

المنارة للاستشارات
www.manaraa.com

connect nodes (n_1, n_2) such that the two routes are connected. Once the new route resulted from merging r_1 and r_2 is obtained, it's feasibility concerning the weight capacity of the EVs is assessed. If the new merged route is infeasible, it is discarded and the next route from R_2 is taken into consideration. Otherwise, the feasibility of the merged route is assessed concerning the battery driving range of the EVs. If the route is still infeasible, a located charging station with less insertion cost is inserted between n_1 and n_2. If both constraints are met, then the merged route is added to the FRS and r_1 and r_2 are removed from R_1 and R_2, respectively. Then, we proceed with the next route in R_1. In case either R_1 or R_2 are empty, the merge process for these two nodes terminates. Finally, $[n_1, n_2]$ is removed from *SPL*, and the process is repeated until *SPL* is empty.

- **Step 3** (Improvement and termination phase):

  In this step for those routes in FS with more than one charging station, we check that if removing each of the inserted charging stations, the route remains feasible. If so, the redundant inserted charging stations are removed from the respective route. Finally, the objective function value of the network, considering the newly generated routes, is calculated.

1.4.1.3 The Tabu Search (TS) procedure

This algorithm attempts to update the location of the charging stations in such a way that the efficiency of the routing decisions improves. The overall framework of this algorithm is outlined as follows:

www.manaraa.com

- **Step 1**: Given the solution provided by the radius covering and MCWS algorithms, S_0, we calculate the respective objective function value $Z(S_0)$ and then initialize the current solution $S \leftarrow S_0$ and the best-known solution $S^* \leftarrow S_0$.

- **Step 2**: This step aims to use the neighborhood search to relocate the charging stations efficiently. Let J_l denotes the currently located charging stations, and $J_u = J \setminus J_l$ indicates the unlocated charging stations in the current solution S_0. Using a one-opt exchange operator, each located station in $j_l \in J_l$ is replaced by an unlocated charging station $j_u \in J_U$ and a set of neighboring solutions $N(S)$ are generated.

- **Step 3**: For each of the generated neighborhoods $S^{'} \in N(S)$, the MCWS procedure is applied to generate the corresponding routes.

- **Step 4**: In this step, by evaluating the objective function value of the routes generated by the MCWS for neighborhoods, the current solution S is updated using $argmin_{S' \in N(S)} [Z(S^{'})]$, where $S^{'}$ are not in the *tabu list*. However, if the objective function value of a neighborhood solution is less than the best-known value, the exchange is permitted even it is in the tabu list. Note that in our implementation, the length of the tabu list is set to 5. If $Z(S) < Z(S^*)$, set $Z(S^*) \leftarrow Z(S)$ and $S^* \leftarrow S$. Finally, if a given number of iteration has reached, stop the TS algorithm; otherwise, proceed to **Step 2**.

1.4.1.4 Framework of TS-MCWS

This section presents the overall framework of the TS-MCWS heuristic to solve model **[EV-L]**.

- **Step 1**: The initial number of the charging stations, N_j, is set to one.

المنارة للاستشارات
www.manaraa.com

- **Step 2**: Using the radius covering algorithm, N_j charging stations are selected. Then, using the MCWS procedure and considering the selected charging stations, the routing plan, S_0, to satisfy the customer demands, are obtained. By doing so, the current solution S and the best-known solution S^* are set to the initial solution S_0.

- **Step 3**: By applying the TS procedure on S, the current solution is updated. If $Z(S) < Z(S^*)$, the best-known solution is updated, $S^* \leftarrow S$.

- **Step 4**: If a pre-specified number of iterations without improvement in the objective function value of the best-known solution N_{itr} has reached or all the charging stations have located, the TS-MCWS heuristic is terminated. Otherwise, set $N_j \leftarrow N_j + 1$ and proceed to **Step 2**. In our experiments, if the number of costumers $|I| \leq 75$, we set $N_{itr} = 5$; otherwise, we set $N_{itr} = 10$.

1.4.2 The SIGALNS heuristic

This sub-section introduces the hybrid heuristic, referred to as SIGALNS heuristic, which is composed of three components, namely, the modified Sweep heuristic, the Iterated Greedy, and the Adaptive Large Neighborhood Search algorithm, to solve model **[EV-L]**. Below, we first discuss different components of the SIGALNS heuristic and then outlines the overall framework of the SIGALNS heuristic.

1.4.2.1 Modified Sweep Heuristic

Using the Modified Sweep (MS) heuristic, an initial solution for the SIGALNS algorithm is constructed. The objective of this algorithm is only to find an initial routing plan; thus, the battery

المنارة للاستشارات
www.manaraa.com

driving range limitation and charging station locations are ignored throughout that process. The sweep algorithm, proposed by Gillet and Miller [26], is used to solve vehicle routing problems, which consists of two subproblems, namely, the customer clustering and the traveling salesman problem (TSP). In the clustering subproblem, first, the costumers are sorted in an ascending order based upon their polar coordinate angles from the depot. Then, starting from the customer with the smallest angle, the customers are inserted in a single cluster as long as the weight capacity of the EV is not violated. Otherwise, a new cluster for the rest of the customers is generated and the process restarts. Once all the customers are assigned to the clusters, the procedure terminates. Then, in the second subproblem, for each one of the generated clusters, a TSP is solved to generate the corresponding routing plans. The modified Sweep heuristic is represented in **Algorithm 1**.

```
Algorithm 1: Modified Sweep heuristic
    Input: The longitude and latitude for customers and depot, the vehicle weight capacity, $K_e$,
      customer demand, $w_i$
    Rank customers in the ascending order of polar angles with respect to depot
    Create a cluster, $C_l \leftarrow$ , $l \leftarrow 1$
    for $i \in I$ do
        if $w_i + \sum_{n \in C_l} w_n \leq k_e$ then
            $C_l \leftarrow C_l \cup \{i\}$
        end
        else
            Start new cluster $C_{l+1} \leftarrow$
            $C_{l+1} \leftarrow C_{l+1} \cup \{i\}$
        end
    end
    for $C_l \in C$ do
        Solve a TSP on $C_l$ to obtain route $R_l$
    end
    Output: $S_0 \leftarrow \cup_{l=1}^{|R|} R_l$
```

المنارة للاستشارات
www.manaraa.com

1.4.2.2 Iterative Greedy Heuristic for Charging Station Selection

Once a routing plan is generated, using the iterative greedy (IG) heuristic, a subset of the candidate charging stations is selected and allocated into different routes with a minimal total construction and allocation cost. In this section, first, we discuss the allocation cost of charging stations into the constructed routes. Then, the procedure of the IG to determine the location of the charging stations and obtaining the feasible routes is described.

- ***Allocation Cost Analysis*:** In IG procedure, first, removes all the located charging stations from the current solution of the model **[EV-L]** and then relocates the charging stations in an attempt to find better location solutions. Given the candidate charging station set J and the solution for the routing phase represented by a set of routes $R = \{r_1, r_2, ..., r_{|R|}\}$, several stations with the least cost increment must be inserted to the current routes to improve the feasibility of the solution. Hence, first, we analyze the allocation cost strategy, which is used to select and insert a set of charging stations into the current partial routes.

  (a) *Breaking point:* Let $r_l = \{n_o = o, n_1, n_2, ...,, n_m = o'\}(r_l \in R)$ represents the visited nodes in the l^{th} route of the current solution. In this route, due to the battery driving range of the EVs, there might be some *breaking points* in r_l. Hence, a node $n \in r_l$ is called a *breaking point* if it satisfies the following condition:

$$\{n|B^1_{nl} < 0, n \in r_l\} \tag{1.37}$$

  This means that the node cannot be reached by the EV since its battery has been depleted before arriving at node n. The first *breaking point* in route r_l is represented

المنارة للاستشارات

www.manaraa.com

by $v^* = \{n|B^1_{n^*,l} < 0, B^1_{n',l} > 0, \forall n' < n^*, n', n^* \in r_l\}$, which signifies that all the nodes before v^* are reachable by EV.

(b) *Node feasibility state:* In model **[EV-L]**, B^1_{nl} represents the maximal distance that EV utilized in $r_l \in R$ could traverse after arriving at node $n \in N$. In order to further evaluate the feasibility status of the route r_l and its nodes, we define *node feasibility state*, denoted by q_{nl}, as follows:

$$q_{nl} = min\{n|B^1_{nl}, 0\}, \qquad n \in r_l \tag{1.38}$$

As can be observed, $q_{nl} \leq 0$. Using *node feasibility state*, it could be inferred that once $q_{nl} = 0$, the node is reachable in route r_l. However, $q_{nl} < 0$ indicates that the node is not reachable and the corresponding route is infeasible. Further, *node feasibility state* represents the further battery power required to visit node $n \in r_l$ and also indicates if a charging station is needed to recharge the battery before arriving $n \in r_l$. Additionally, using the *node feasibility states* in route r_l, we compute the *worst node feasibility state* in route r_l as $q^*_l = min_{n \in r_l \setminus \{o\}} q_{nl}$. In each route $r_l \in R$, the smaller the q^*_l is, the worse the solution feasibility becomes.

(c) *Allocation Cost:* Once a candidate charging station $j \in J$ is selected and inserted at position $\bar{n}$ after node n in the route r_l, the allocation cost $a^{\bar{n}}_{jl}$ is used to evaluate the improvement of the solution feasibility and calculate the objective function value increment. To minimize the allocation cost of the charging station, eliminating more *breaking points* and/or gaining larger improvement in the whole *node feasibility state*

www.manaraa.com

is preferred. To be concise, let $\bar{n}$ be an insertion position for a charging station after node n, $g^{\bar{n}}_{j,l}$ be the respective *insertion gain*, $h^{\bar{n}}_{j,l}$ be the respective *insertion loss*, and $p^{\bar{n}}_{j,l}$ be the *extra penalty*. The allocating and inserting the charging station $j \in J$ at node $\bar{n}$ after node n in the route r_l, denoted by $a^{\bar{n}}_{j,l}$, is defined as follows:

$$a^{\bar{n}}_{j,l} = \alpha_1(-g^{\bar{n}}_{j,l}) + \alpha_2 h^{\bar{n}}_{j,l} + \alpha_3 p^{\bar{n}}_{j,l}, \qquad j \in J, n \in r_l, r_l \in R \tag{1.39}$$

where

$$\begin{aligned}
&\alpha_1 + \alpha_2 + \alpha_3 = 1 \qquad \alpha_1, \alpha_2, \alpha_3 \geq 0 \\
&g^{\bar{n}}_{j,l} = \Bigg(\sum_{n \in r_l \setminus \{o\}} (q^{'}_{nl} - q_{nl}) \Bigg) \left(\frac{1 + |q^*_l|}{1 + |q^{*'}_l|} \right) && (1.40) \\
&h^{\bar{n}}_{j,l} = d_{n_i,\bar{n}} + d_{\bar{n},n_{i+1}} - d_{n_i,n_{i+1}}, \qquad n_i, n_{i+1} \in r_l && (1.41) \\
&p^{\bar{n}}_{j,l} = M|q_{\bar{n},l}| && (1.42)
\end{aligned}$$

In order to obtain the *insertion gain*, we utilize equation (2.45). Here, $g^{\bar{n}}_{j,l}$ measures the improvement regarding the solution of r_l when station j is placed at position $\bar{n}$ after node n. As discussed earlier, q_{nl} and q^*_l, respectively, represent the *node feasibility state* and *worst node feasibility state* before inserting the charging station j in route r_l. In addition, $q^{'}_{nl}$ and $q^{*'}_l$ represent the mentioned values after inserting the charging station j. The first component in the right hand side of equation (2.45) computes the total improvement with respect to the *node feasibility state* in route r_l. The second component, if $q^*_l < q^{*'}_l < 0$, which indicates the *worst node feasibility state* has

المنارة للاستشارات
www.manaraa.com

improved, becomes greater than one and thus increases the aggregate improvements in the first component. The *insertion loss* is calculated via equation (2.46), where n_i and n_{i+1}, respectively, are the *predecessor* and *successor* of node positioned at $\bar{n}$. Using this equation, the increment in traveling due to inserting charging station j after node n is calculated, which is then used as an *insertion loss* in the procedure. The *extra penalty*, $p^{\bar{n}}_{j,l}$, is calculated via equation (2.47), where M is an user-defined big number which we set to $M = 10^4$ in our experiments. In this equation, $q_{\bar{n},l}$ represents the feasibility state of station j at position $\bar{n}$. If $q_{\bar{n},l} < 0$, then the charging station j at position $\bar{n}$ is unreachable and the infeasible insertion is penalized. Let $B^2_{n,l}$ to represent the maximal distance that EV at route l could traverse after leaving node n. For all the nodes in route r_l, we define a reachable charging station set, denoted by $J^l_n \subset J$, which is obtained as $J^l_n = \{j \in J | B^2_{n,l} = s\hat{o}c(c, t) \geq d_{n,j}\}(n \in r_l)$. By doing so, for any charging station in J^l_n, if it is located after node n on route r_l, the extra penalty $p^{\bar{n}}_{j,l}$ is set to zero, i.e., $p^{\bar{n}}_{j,l} \leftarrow 0$.

The allocation cost is the main criterion to select and insert charging stations in the infeasible routes. Having comprehensively explained this cost, in the next section, we will describe the overall framework of the IG heuristic.

- ***The Iterated Greedy (IG) Heuristic**:* We now introduce the IG heuristic for solving the charging station location subproblem. This procedure aims to maintain or improve the feasibility of the routing decisions iteratively. Within this procedure, first, a set of infeasible routes is identified. Then, the best candidate charging stations and the respective positions of

المنارة للاستشارات
www.manaraa.com

insertion, given by the least allocation cost, are determined. These two phases are repeated until all the routes are feasible. Finally, by applying a *local heuristic*, the obtained solution is improved. **Algorithm 2** outlines the pseudo-code of this algorithm.

Algorithm 2: The Iterated Greedy (IG) algorithm

```
Input: Initial solution $S_0$, and the initial cost of building a charging station $f_0$
Initialize the cost of building a charging station $f_0$ and set $\Theta \leftarrow 0$
Eliminate all the located stations in the $S_0$
$S \leftarrow S_0$
while $\Theta = 0$ do
    for $r_l \in R$ do
        Compute the worst feasiblity state $q_l^*$
        if $q_l^* < 0$ then
            Select and insert the best stations
            Update the node feasibility state in $r_l$
            Update the station construction cost
        end
    end
    if all routes are feasible then
        $\Theta \leftarrow 1$
    end
end
$S \leftarrow$ Apply the local sarch procedure
Output: $S$
```

Let f_0 represents the initial construction cost of the charging stations and Θ signifies if a solution for model **[EV-L]** is feasible. The IG algorithm assumes that the initial solution for model **[EV-L]** is infeasible ($\Theta = 0$). Let the initial solution consist of vehicle routes, denoted by $R = \{r_1, ..., r_l, ..., r_R\}$. All the located stations in $r_l \in R$ are eliminated and then the current solution S is initialized as S_0. Then, for each of the routes, the feasibility of the routes concerning the battery driving range is evaluated and the worst feasibility state q_l^* is

المنارة للاستشارات
www.manaraa.com

determined. If $q_l^* < 0$, meaning that the route $r_l \in R$ is infeasible, the IG heuristic starts selecting and locating the charging station.

In this step to select the best possible charging station, first, a segment of nodes $\Psi_l \in r_l$, called the *search zone*, is introduced as follows: all the predecessor nodes of the first *breaking point* until a charging station or depot are added to Ψ_l. The Ψ_l represents all the possible positions to insert a charging station. Then, for each of the nodes in Ψ_l, $n \in \Psi_l$, we find the reachable charging station set J_n^l and then for each of the stations $j \in J_n^l$, we calculate the respective allocation cost $a_{jl}^{\bar{n}}$. Afterward, a node by empty reachable charging stations is discarded from Ψ_l. To obtain the best possible position to open the charging station, all the nodes in Ψ_l are sorted in ascending order of the summation of the allocation and construction costs and the position $\bar{n}$ after node n, indexed by $*\epsilon_1^{\rho_1} \times |\Psi_l|$, is selected, where ϵ_1 is a random number between 0 and 1, $\rho_1 \geq 1$ is a parameter to capture the randomness in the procedure and equal to 10 in our implementation. Likewise, to determine the best charging station in J_n^l and to insert in chosen position $\bar{n}$, the stations in J_n^l are sorted in ascending order based on the summation of the allocation and construction costs. From the sorted order, the station $\bar{j}$, indexed by $*\epsilon_1^{\rho_2} \times |J_n^l|$, is selected, where ϵ_2 is a random number between 0 and 1, and $\rho_2 \geq 1$ is a deterministic parameter which we set to 10 in our implementation. After placing the station $\bar{j}$ at position $\bar{n}$, the feasibility state of nodes in r_l are updated. Because a located charging station may be used by multiple routes, the construction cost of the inserted stations is set to zero.

After some iterations, the current solution is updated such that all the respective routes are feasible, concerning the battery driving range of the EVs. To further improve the solution

المنارة للاستشارات
www.manaraa.com

quality, a *local heuristic*, consisting of two neighborhood search operators, namely, *EXCHANGE* and *MOVE*, is applied to the current obtained solution. By using the *EXCHANGE* operator, a located station in a route is replaced by another located station. Further, by using the *MOVE* operator, a located station is replaced by an unlocated station. Each operator is applied to each of the located stations, and a new location strategy is accepted if it is still feasible and the objective function value is improved. As mentioned earlier, applying the IG procedure, all the located stations are first removed from the current solution; hence, the new location strategy strongly depends on the vehicle routes. On the other hand, the routing plan, obtained by the adaptive large neighborhood search (ALNS) heuristic which is discussed in the following section, is also strongly affected by the located stations. Therefore, the SIGALNS procedure is a cooperative method which exchanging information iteratively between locating and routing phases with an aim in solving model **[EV-L]** efficiently.

1.4.2.3 Adaptive Large Neighborhood Search (ALNS) Heuristic for EV Routing

The ALNS algorithm, proposed by Ropke and Pisinger [80], was developed to solve the vehicle pickup and delivery problems. The ALNS algorithm removes a set of costumes from the current solution and inserts them into other positions in an attempt to construct a new solution in the large neighborhood of the prior solution. In each iteration of the algorithm, a set of insertion and removal operators are selected given their historical success. In the following, we discuss the procedure of the ALNS algorithm, which is implemented in this study.

- **Overall framework**: This section describes the overall framework of the ALNS algorithm, proposed by Laporte et al. [45], which includes *large neighborhood*, *removal and insertion*

المنارة للاستشارات
www.manaraa.com

operators, *adaptive search mechanism*, *penalized objective function*, and *acceptance and termination criteria*.

The first component of this algorithm is known as *large neighborhood*. Within this component, in each iteration of the algorithm, using the removal operators, n_c number of costumers are removed from the current solution and are added into a request bank. Then, all the costumers in the request bank, using an insertion operator, are reinserted into the routes. We randomly select the n_c customers from the interval $[\eta_1 \times |I|, \eta_2 \times |I|]$, where $\eta_1, \eta_2 \in (0, 1)$ and $|I|$ denotes the number of the customers. The second component of the ALNS algorithm is *removal and insertion operators*, within which a set of removal operators are proposed and utilized to remove n_c customers from the current solution. Later, a set of insertion operators are proposed and used to reinsert all the costumers in the request bank to the best possible positions in the routes. The next component, known as the *adaptive search mechanism*, includes the adaptive selection of the removal-insertion operators and adaptive adjustment of the operators' weight. The search process within the ALNS algorithm is divided into a set of *segments*, where each segment consists of v (e.g., $v = 50$) iterations. Within each iteration of the ALNS algorithm, a *roulette-wheel* mechanism is utilized to choose the respective removal and insertion operators. Let γ_{ij} denotes the weight of operator i at segment j. The operator i is selected by a probability $p_{ij} = \gamma_{ij}/\sum_{h \in H} \gamma_{hj}$, where H denotes the entire list of either removal or insertion operators and $\sum_{h \in H} \gamma_{h,j}$ represents the total weight of the respective operators at segment j. The initial weight of each operator $h \in H$ is set to a deterministic number (10 in this study). Then, the value of the operator is updated at the end of each segment as follows: if $\chi_{ij} > 0$, $\gamma_{i,j+1} = (1-\Gamma)\gamma_{ij} + \Gamma\zeta_{ij}/\chi_{ij}$; otherwise, $\gamma_{i,j+1} = \gamma_{ij}$,

المنارة للاستشارات
www.manaraa.com

where ζ_{ij} and χ_{ij} represent the number of times the operator i has been selected at segment j, and the score of the operator i at segment j, respectively. Further, Γ, referred to as a *reaction factor*, is a deterministic parameter within the range $(0, 1)$, and it's value is set to 0.3 in this study. Finally, the score χ_{ij} is set to zero at the beginning of each segment, and then it's value is enhanced by $\Delta_{i,j}$ using the historical performance of the operator i at each iteration of segment j. For instance, given a pair of selected removal-insertion operators, if a new best-known solution is found, the respective score of the operators are increased by $\Delta_{ij} = 50$. If the current solution improves, the respective score of the operators are increased by $\Delta_{ij} = 20$, and if the new solution is not improved but it can be accepted based on the feasibility conditions, the respective score of the operators is increased by $\Delta_{ij} = 10$. Using the next component, referred to as the *penalized objective function*, rather than restricting the search in feasible region, we introduce a penalized objective function if the battery driving range of the EVs is violated.

$$Z_{penalized} = \sum_{j \in J} f_j X_j + \sum_{i \in N} \sum_{j \in N} \sum_{e \in E} c_{ije} d_{ij} Y_{ije} - M \sum_{l \in R} \sum_{n \in r_l} q_{nl} \qquad (1.43)$$

where M is a user-defined big number, such as 10^4, and $q_{nl} \leq 0$ is the *node feasibility state*, which is discussed earlier. The last element of the ALNS algorithm is *acceptance and termination criteria*. To implement this, we follow the Simulated Annealing (SA) criterion, as introduced by Adulyasak et al. [2]. With this, a new better solution is always accepted. Moreover, a worse solution is accepted by a probability of $e^{(Z(S^{'})-Z(S))/T}$, where S, $S^{'}$, and T represent, respectively, the current solution, new solution, and current temperature of the

المنارة للاستشارات
www.manaraa.com

SA. The initial value of the temperature of the SA is set to T_0 (10,000 in this study) and it's value is updated as $T_v = \Lambda T_{v-1}$, where Λ is the cooling rate of the SA method and is fixed to 0.995 in our implementation. Finally, the entire process of the ALNS algorithm terminates when either the maximum number of iteration (ITR^{ALNS}) or the time limit ($TIME^{ALNS}$) is reached. Given that S_0, S, $S^{'}$, and S^{*} represent the initial, current, neighborhood, and the best-known solution, respectively, the overall framework of the ALNS algorithm is presented in **Algorithm 3**.

Algorithm 3: Adaptive Large Neighborhood Search (ALNS) Algorithm

```
Input: Initial solution $S_0$
$S \leftarrow S_0, S^* \leftarrow S$
$iter \leftarrow 1$
while $iter < ITR^{ALNS}$ do
    Select a pair of removal and insertion operators
    $S^{'} \leftarrow S$
    Apply the removal operator to $S^{'}$
    Apply the insertion operator to $S^{'}$
    if the acceptance is satisfied then
        $S \leftarrow S^{'}$
    end
    if $Z(S) < Z(S^*)$ then
        $S^* \leftarrow S$
    end
    Update the score and weight of each operatore
    $iter \leftarrow iter + 1$
end
Output:
        The best-known solution: $S^*$
```

- **Removal operators:** This section provides detailed information on the removal operators that have been utilized in this study.

www.manaraa.com

- *Random removal:* This operator randomly selects n_c customers from the current solution and adds them to the request bank.

- *Basic worst removal:* This operator, first, ranks all the customers based on their respective *removal gains* in a descending manner, where the *removal gain* for customer n is the difference in the objective function value of the model when the customer is in the current solution and when it is removed, i.e., $(Z(S) - Z_{-n}(S))$ [30]. Since removing a customer from a route only affects the traveling distance of the route and it does not impact the location decisions, then it can be concluded that $Z(S) - Z_{-n}(S) := d_{n-1,n} + d_{n,n+1} - d_{n-1,n+1}$, where $n-1$ and $n+1$ are the predecessor and successor nodes of customer n, respectively. Next, the costumer, indexed by $*\epsilon_3^{\rho_w} \times |I|$, is eliminated from the respective route and added to the request bank, where ϵ_3 is a random number chosen from interval $(0, 1)$, the ρ_w is a pre-defined constant number, and $|I|$ is the total number of customers in the current solution.

- *Related removal:* This operator aims at removing the customers based on their similarity [83]. First, an initial seed customer n is randomly chosen from the current solution. Then, the similarity between the other customers $n^{'}$ and the seed customer n is calculated as $sim(n, n^{'}) := \beta_1 d_{n,n'} + \beta_2 |w_n - w_{n'}| + \varsigma_{n,n'}$, where β_1 and β_2 are weights chosen from interval $(0, 1)$ and $\beta_1 + \beta_2 = 1$, $d_{n,n'}$ denotes the respective distance between customers n and $n^{'}$, and $|w_n - w_{n'}|$ represents the absolute value of the difference in the demand of customers n and $n^{'}$. Further, the value of the $\varsigma_{n,n'}$ is fixed to one if two customers are on the same route; otherwise, $\varsigma_{n,n'} = 0$. The smaller the value of $sim(n, n^{'})$ is, the more similar customer n and $n^{'}$ becomes. Next, the customers are sorted based on the

المنارة للاستشارات
www.manaraa.com

respective similarity measurement in a descending manner, and the customer, indexed by $*\epsilon_4^{\rho_r} \times |I|$, are eliminated from the respective route and added to the request bank, where ϵ_4 is selected between 0 and 1, the ρ_r is a pre-defined constant number, and $|I|$ is the total number of customers in the current solution.

- *Advanced worst removal:* As a customer is removed from a route, not only the respective traveling distance decreases but also the feasibility of the solution concerning the battery driving range may improve. Hence, this operator, while calculating the *removal gain* for costumers, captures the improvement in feasibilty state of nodes as $Z(S) - Z_{-n}(S) := \theta_1(d_{n-1,i} + d_{n,n+1} - d_{n-1,n+1}) + \theta_2(\sum_{l \in R} \sum_{n \in r_l} q_{n,l} - \sum_{l \in R} \sum_{n \in r_l} q^{'}_{n,l})$, where $\theta_1 + \theta_2 = 1$, $q_{n,l}$, and $q^{'}_{n,l}$ denote the feasibility state of the nodes before and after the removal, respectively.

- *Station-based removal:* This operator first randomly chooses one of the charging stations, which is already located in the current solution. Next, all the customers, connected to the selected station, are removed from the respective routes until n_c number of customers are removed. For further information and illustrative examples, the interested readers could refer to [98].

- *Single point removal:* The partial routes between two charging stations or between a charging station and the depot or its copy are called the *service zone* of the charging stations [98]. The main idea of this operator is to destroy *service zone* such that the newly constructed routing plan maintains the feasibility condition as for the battery driving range. Within this operator, one of the routes, which have at least a located charging station, is randomly chosen. Afterward, one of the positions in the *service*

المنارة للاستشارات
www.manaraa.com

zone of the respective route is randomly selected. Finally, the customers between the selected position and either the respective charging station or the depot or its copy are removed from the selected route.

- **Insertion operators:** Using a removal operator, a set of customers are removed from the respective routes in the current solution and are added to the request bank. Then, the responsibility of the insertion operators, introduced below, is to reinsert all the customers in the best possible positions in the current solution.

  - *Basic greedy insertion:* This operator aims at inserting the removed customers in the current request bank (R_b) into the current solution in such a way that the insertion leads to the least objective function value increment at it's best-inserting position iteratively. To be concise, let $\Delta Z_{n,l} = Z_{n,l} - Z_{n-,l} = d_{n-1,i} + d_{n,n+1} - d_{n-1,n+1}$ represents the increment in the cost after inserting node n in route r_l at its best inserting position. The selected customer n^* is determined as: $n^* = argmin_{n \in R_b}\{min_{r_l \in R} \Delta Z_{n,l}\}$.
  - *Basic regret-k insertion:* The main idea of this operator, proposed by Ropke and Pisinger [80], is to reinsert the removed customers with the largest regret value in their respective best insertion position iteratively. For costumer $n \in R_b$, let $\Delta Z_{n,j}$ denotes the increment in the objective function value due to inserting it into the j^{th} best route in its best position, where the increment in objective function could be calculated with regard to added distance defined in *Basic greedy insertion*. For example, $\Delta Z_{n,1}$ indicates the change in the cost after adding cutomer n into the respective best route. Given *Basic regret-k insertion*, the selected customer n^* is determined as:

المنارة للاستشارات
www.manaraa.com

$n^* = argmax_{n \in R_b}\{\sum_{j=2}^{k}(\Delta Z_{n,j} - \Delta Z_{n,1})\}$. In this study, two cases of *Basic regret-k insertion* operator, namely, the *Basic regret-2 insertion* and the *Basic regret-3 insertion*, are implemented.

– *Advanced greedy insertion:* In order to calculate the change in the objective function value in the *Basic greedy insertion*, only the the difference due to the traveling distance, i.e., $d_{n-1,i} + d_{n,n+1} - d_{n-1,n+1}$, is utilized. However, inserting a customer in a route could affect the feasibility of the current solution due to the battery driving range and weight capacity limitations. To alleviate this problem, we utilize equation (2.49) to compute the increment in the objective function value due to the insertion of customer $n \in R_b$ in it's best position at route r_l as follows:

$$\Delta Z^{new} = \theta_3(d_{n-1,i} + d_{n,n+1} - d_{n-1,n+1}) + \theta_4(\sum_{l \in L}\sum_{n \in r_l} q_{n,l} - \sum_{l \in L}\sum_{n \in r_l} q'_{n,l})$$

$$+max\left\{\left(\sum_{n \in r_l} w_n - k_l\right), 0\right\} \times M \tag{1.44}$$

where $\theta_3 + \theta_4 = 1$, $q_{n,l}$ and $q'_{n,l}$ are the node feasibility state before and after the insertion. Using equation (2.49), the *Advanced greedy insertion* is motivated to construct new routes such that they satisfy the battery driving range limitation and the vehicle capacity constraints.

– *Advanced regret-k insertion:* Similar to the *Advanced greedy insertion*, the equation used for calculating the regret values in *Basic regret-k insertion* is replaced by equation (2.49), i.e., $\Delta Z_{n,j} = \Delta Z^{new}$. Note that in our implementation, two cases of the *Advanced*

المنارة للاستشارات
www.manaraa.com

regret-k insertion, namely, the *Advanced regret-2 insertion* and the *Advanced regret-3 insertion*, are utilized as insertion operators.

1.4.2.4 Algorithmic Framework of the SIGALNS Algorithm

The SIGALNS algorithm consists of three phases: *initialization*, *location*, and *routing* phases. After the initialization phase, the location and routing phases are implemented successively to generate the best-known solution for model **[EV-L]**. A pseudocode of the hybrid algorithm is presented in **Algorithm 4**. In the beginning, an initial solution S_0, using the modified sweep algorithm, is generated, which is then provided to the location and routing phases. At this point, the current solution S and the best-known solution S^* are fixed to S_0. In the next step, the weights associated with different operators of the ALNS algorithm are initialized. With this, the operator weights are recorded globally which could improve the performance of the ALNS algorithm. Afterward, at the beginning of each iteration of the SIGALNS algorithm, the located stations are eliminated from the current solution in model **[EV-L]**. In the following steps, the location and routing subproblems are solved successively, wherein each iteration, similar to the ALNS algorithm, the acceptance criterion from the Simulated Annealing (SA) algorithm is used to accept newly constructed routes as a current solution. Subsequently, the best-known solution to the problem is updated. Note that, the entire process of the SIGALNS algorithm terminates after $ITR^{SIGALNS}$ iterations or reaching to a maximum time limit.

المنارة للاستشارات
www.manaraa.com

Algorithm 4: The framework of SIGALNS algorithm

```
**Input**: The distance between all the nodes $d_{n,n'}$, $\forall(n, n') \in N$, customers' demand $w_i$,
the wight capacity of EVs $k_e$, $\forall e \in E$, battery driving range of EVs $s\hat{o}c(c, t)$, where $c$ is charging
  time and $t$ is the ambient temperature
Implement modified sweep algorithm to obtain a initial solution $S_0$
$S \leftarrow S_0, S^* \leftarrow S_0$
Starting the initial value of the removal and insertion operators for the ALNS algorithm
$iter \leftarrow 1$
**while** $iter < ITR^{SIGALNS}$ **do**
    $S' \leftarrow S$
    Remove all the located charging stations from $S'$
    Apply the iterated greedy algorithm to $S'$ to find out the updated located charging stations
    Apply the ALNS algorithm to $S'$ to update the routing plans
    **if** *the acceptance criterion is satisfied* **then**
        $S \leftarrow S'$
    **end**
    **if** $Z(S) < Z(S^*)$ **then**
        $S^* \leftarrow S$
    **end**
    $iter \leftarrow iter + 1$
**end**
**Output**:
        The best-known solution: $S^*$
```

1.5 Computational Study

In this section, we first describe the data utilized for generating the test instances. Next, the performance of the proposed heuristics, namely, the SIGALNS and TC-MCWS techniques, in solving model **[EV-L]** over GUROBI are discussed. Further, using Fargo, North Dakota (ND), as a testbed, the performance of the proposed model is discussed. More specifically, the impact of temperature in the EV location-routing decisions is demonstrated. All numerical experiments are coded in Python 2.7 on a desktop computer equipped with an Intel Core i7 processor 3.60 GHz and a 32 GB RAM. The optimization solver used is GUROBI Optimizer 9.0.

المنارة للاستشارات

www.manaraa.com

1.5.1 Data description and parameter settings

In this subsection, a concise description of the utilized data and parameters is provided. Our study considers a fixed depot location, which is positioned at the center of the test region (see Figure 1.2(a)). Using a 200 miles squared distance from the depot location, 150 customer locations are selected (see Figure 1.2(a)). These customer locations are selected from different neighborhoods in Fargo, which has a population of more than 4,000. Further, 100 neighborhoods, with a population size of more than 7,000, are selected as potential charging station locations. Figure 1.2 visualizes the depot, customer, and potential charging station locations considered in this study. We utilize a *google* tool, *Distance Matrix API*[1], to calculate the distance between each origin-destination pairs. The tool provides travel distance and time, in the form of a matrix, between each origin-destination pairs. We consider *Tesla Model 3 Long Range* EV to satisfy customer demands. When fully charged, this vehicle can travel up to $d_{max} = 322$ miles and with a maximum weight capacity of w_i =417 kg[2]. The weight of the customer demands (w_i) are randomly generated using a uniform distribution between 50 and 100. The unit distance cost is set to be $c_{ije} = 1$ [98]. The fixed installation cost of a single port DCFC is set to be $2,750, which is amortized over 10 years [84].

After running several preliminary experiments, the parameters utilized in the two proposed heuristics are fixed as follows. The α_1, α_2, and α_2 utilized in allocation cost calculation of the SIGALNS algorithm are fixed to 0.07, 0.92, 0.01, respectively. The values of η_1 and η_2, utilized for generating n_c in the ALNS algorithm, are fixed to 0.1 and 0.3, respectively. The parameters ρ_w and ρ_r, utilized in the *basic worst* and *related removal* operators, are fixed to 10. The β_1 and β_2 parameters, utilized in the *related removal* operator, are set to 0.6 and 0.4, respectively. In advanced

[1] Available from: `https://developers.google.com/maps/documentation/distance-matrix/start`
[2] Available from: `https://www.tesla.com/model3`

www.manaraa.com

worst removal and *insertion* operators, the weights are set as: $\theta_1 = \theta_3 = 0.9$ and $\theta_2 = \theta_4 = 0.1$. Finally, the maximum number of iterations of ALNS and SIGALNS algorithms, for instances with less than 50 customers, are fixed to 40 and 200, respectively. On the hand, for larger instances, these two values are fixed to $ITR^{ALNS} = 50$ and $ITR^{SIGALNS} = 400$.

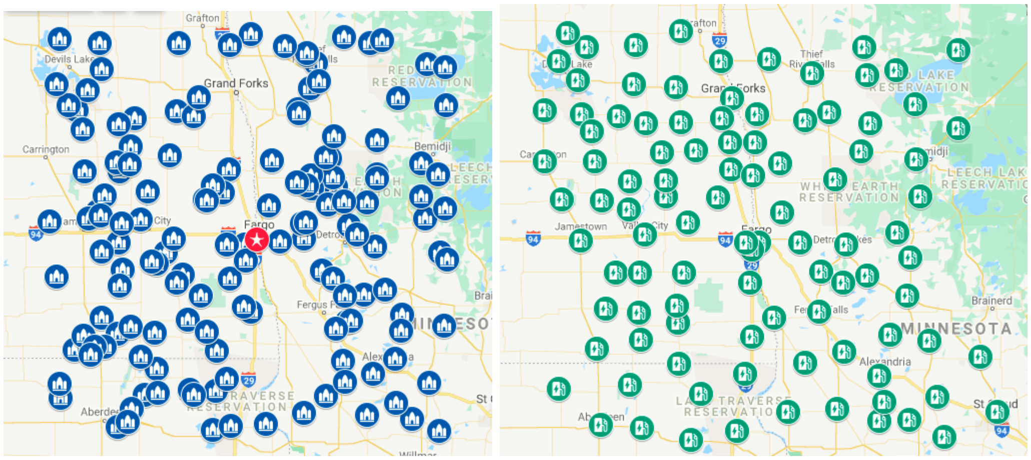

(a) Location of customers and depot

(b) Potential location of the charging stations

Figure 1.2

Illustration of the dataset

1.5.2 Computational performance of the proposed algorithms

Based on the parameter setting and algorithmic configuration, the efficiency of the proposed algorithms in solving model **[EV-L]** are evaluated on different test instances. To do so, a new set of problem instances with various sizes, in terms of the number of the customers and the available EVs, are generated. As discussed earlier, in total 150 locations with a considerable population are considered as the potential locations of the customers. Next, varying the size of the customers, 10 different test instances are generated. In these instances, the respective customers' locations are

المنارة للاستشارات
www.manaraa.com

randomly chosen out of 150 potential locations, given the corresponding number of the customers in each instance. Table 1.1 reports the number of variables (continuous and binary) and constraints for each of the generated test instances of model **[EV-L]**. In the following, the computational performance of the proposed algorithms under these generated test instances are discussed.

Table 1.1

Test instances for model **[EV-L]**

Instance	$\|I\|$	$\|E\|$	variables			Total constraints
			Binary	Continous	Total	
S1	5	3	4,026	303	4,329	3,291
S2	10	5	8,640	780	9,420	25,880
S3	15	8	6,866	968	7,834	51,829
S4	20	11	29,202	2,046	31,248	87,258
S5	25	15	47,910	3,015	50,925	143,050
S6	50	22	146,154	6,072	152,226	435,856
S7	75	29	328,948	10,179	339,127	981,262
S8	100	36	622,542	15,336	637,878	1,858,018
S9	125	43	1,053,186	21,543	1,074,729	3,144,874
S10	150	50	1,647,130	28,800	1,675,930	4,920,580

Having introduced the test instances, we first evaluate GUROBI's performance in solving model **[EV-L]** (see Table 1.2). Next, the performance of GUROBI, enhanced with variable fixing and valid inequalities, in solving model **[EV-L]**, is discussed (see Table 1.3). Note that the performance of the GUROBI solver in solving model **[EV-L]**, with and without using the variable fixing and valid inequalities, are tested under three different temperatures: -10^{o}C, 10^{o}C, and 30^{o}C. In Tables 1.2 and 1.3, $T(s)$, $gap(\%)$, and $Best$ represent the solution time, the obtained gap, and the best objective function value obtained by GUROBI, respectively. In running the experiments, the optimality gap and time limit for GUROBI are set to 3% and 14,400 seconds, respectively. Table 1.2 shows that basic GUROBI is able to find feasible solutions for only 1, 2, and 2 test instances, when the temperature is $-10\circ C$, $10\circ C$, and $30\circ C$, respectively. However, the performance of the

المنارة للاستشارات
www.manaraa.com

GUROBI solver improves slightly when GUROBI is enhanced with different variable fixing and valid inequalities. Under such a situation, GUROBI was able to find feasible solutions for 2, 2, and 3 problem instances under $-10\circ C$, $10\circ C$, and $30\circ C$ temperatures, respectively (see Table 1.3). From these results, it can be concluded that enhancing the basic GUROBI via variable fixing and valid inequalities, the performance of the GURUBI solver increases by 18.4%, 36.3%, 7.9%, when the temperature is $-10\circ C$, $10\circ C$, and $30\circ C$, respectively. Despite these benefits, we must note that even the enhanced GUROBI cannot serve more than 15 customers, which drastically limits its practicability from a real-world viewpoint.

Table 1.2

Performance of the GUROBI solver

	Temperature = $-10\circ C$			Temperature = $10\circ C$			Temperature = $30\circ C$		
instance	$T(s)$	$gap(\%)$	$Best$	$T(s)$	$gap(\%)$	$Best$	$T(s)$	$gap(\%)$	$Best$
s1	14,400	22.4	14,287.1	14,400	24.1	11,175.2	14,400	14.0	6875.5
s2	TL[1]	-	-	14,400	56.1	13,601.3	14,400	49.1	6607.1
s3	TL	-	-	TL	-	-	TL	-	-
s4	TL	-	-	TL	-	-	TL	-	-
s5	TL	-	-	TL	-	-	TL	-	-
s6	TL	-	-	TL	-	-	TL	-	-
s7	TL	-	-	TL	-	-	TL	-	-
s8	OM[2]	-	-	OM	-	-	OM	-	-
s9	OM	-	-	OM	-	-	OM	-	-
s10	OM	-	-	OM	-	-	OM	-	-
Average	14,400	22.4	14,287.1	14,400	40.1	12,388.2	14,400	31.6	6,741.3

[1] TL: No feasible solution within time limit

[2] OM: Out of memory

We now present the computational performances of TS-MCWS and SIGALNS algorithms in solving the larger instances of model **[EV-L]** under varying temperatures (see results in Tables 1.4-1.6 for the performance of the algorithms under $-10\circ C$, $10\circ C$, and $30\circ C$ temperatures). The first two columns in Tables 1.4-1.6 represent the problem instances and the number of respective customers. Next, $|J_l|$, $Best$, $Average$, and T to represent the number of charging stations opened,

المنارة للاستشارات

www.manaraa.com

Table 1.3

Performance of GUROBI enhanced with variable fixing and valid inequalities

	Temperature = $-10\circ C$			Temperature = $10\circ C$			Temperature = $30\circ C$		
instance	$T(s)$	$gap(\%)$	$Best$	$T(s)$	$gap(\%)$	$Best$	$T(s)$	$gap(\%)$	$Best$
S1	10,077	2.6	11,378.8	8,025	2.4	8,690.5	3,282	2.9	6,089.5
S2	14,400	9.4	12,377.4	14,400	5.1	6,292.5	14,400	6.7	3,604.5
S3	TL	-	-	TL	-	-	14,400	61.5	9,262.3
S4	TL	-	-	TL	-	-	TL	-	-
S5	TL	-	-	TL	-	-	TL	-	-
S6	TL	-	-	TL	-	-	TL	-	-
S7	TL	-	-	TL	-	-	TL	-	-
S8	OM	-	-	OM	-	-	OM	-	-
S9	OM	-	-	OM	-	-	OM	-	-
S10	OM	-	-	OM	-	-	OM	-	-
Average	12,238.5	6	11878.1	11,212.5	3.75	7,491.5	10,695.1	23.7	6,318.8

the best feasible solution, the average feasible solution, and the average running time (in seconds) of the investigated algorithms, respectively. The last column, $gap(\%)$, in Tables 1.4-1.6 represents the difference between the best feasible solution found by the two heuristics and is computed as follows: $(Best_2 - Best_1)/Best_1$. It is worth mentioning that we run each test instance *five* times to obtain the average solution and running time reported in Tables 1.4-1.6.

Table 1.4 presents the computational performance of the SIGALNS and TS-MCWS algorithms under $-10\circ C$ temperature. It can be observed that besides instances S5 and S6 (25 and 50 customers), the SIGALNS algorithm is capable of providing high-quality feasible solutions in all the other instances (8 out of 10 instances). The exception could be attributed due to the special distribution of the customers, which influences the ALNS performance [80]. Besides, such quality solutions in the SIGALNS algorithm can be obtained in 2.7 times faster than the TS-MCWS algorithm. Finally, we observe that at least one fewer charging stations are required to be constructed in three instances of the SIGALNS algorithm, namely, instances S4, S7, and S9, over the TS-MCWS algorithm.

www.manaraa.com

Table 1.4

Performance of SIGALNS and TS-MCWS when temperature is $-10\circ C$

		SIGALNS				TS-MCWS				
instance	$\|I\|$	$\|J_l\|$	$Best_1$	$Average_1$	$T1(s)$	$\|J_l\|$	$Best_2$	$Average_2$	$T2(s)$	$gap(\%)$
S1	5	4	**11,083.2**	11,083.2	2.1	4	11,168.5	11,168.5	1.6	0.8
S2	10	4	**11,214.7**	11,264.7	1.9	4	11,243.9	11,243.9	2.2	0.3
S3	15	3	**8,861.9**	8,861.9	2.8	3	8,889.3	8,889.3	2.2	0.3
S4	20	6	**17,119.2**	17,119.2	3.5	7	19,684.6	19,745.7	3.5	14.9
S5	25	6	17,255.6	17,257.8	4.0	6	**17,231.2**	17,269.7	3.5	-0.2
S6	50	13	37,689.3	37,713.5	15.2	13	**37,368.1**	37,557.6	48.1	-0.9
S7	75	14	**41,347.2**	41,513.4	22.6	15	43,918.1	44,119.8	33.5	6.2
S8	100	16	**48,505.7**	48,750.0	86.7	16	48,778.3	48,903.9	141.2	0.6
S9	125	22	**66,866.2**	67,182.0	140.1	24	72,211.7	72,420.0	312.0	7.9
S10	150	22	**67,794.6**	67,862.9	220.2	22	68,584.9	69,034.7	779.4	1.2
Average	57.5	11	**32,773.6**	32,860.8	49.9	11.4	33,907.9	34,035.3	132.7	3.1

To demonstrate the computation superiority of the SIGALNS algorithm over the TS-MCWS algorithm, we further experiment with temperatures $10\circ C$ and $30\circ C$, as shown in Tables 1.5 and 1.6. To summarize, we observe that when the temperature is $10\circ C$ (Table 1.5), 8 out of 10 problem instances SIGALNS algorithm provides a high-quality feasible solution over the TS-MCWS algorithm. This improvement in solution quality in the SIGALNS algorithm is achieved in 2.7 times faster than the TS-MCWS algorithm. Further, when the temperature is $30\circ C$ (Table 1.6), 9 out of 10 problem instances SIGALNS algorithm provides a high-quality feasible solution over the TS-MCWS algorithm. This improvement in solution quality in the SIGALNS algorithm is achieved in 2.4 times faster than the TS-MCWS algorithm. Overall, the SIGALNS algorithm consistently provides high-quality feasible solutions in a reasonable timeframe within our experimental ranges.

1.5.3 Sensitivity Analysis

This subsection performs a set of sensitivity analysis to evaluate the performance of the proposed model and to draw managerial insights for the respective policy-makers. To perform these experiments, three instances, namely, $S6$ (50 customers), $S8$ (100 customers), and $S10$ (150

المنارة للاستشارات
www.manaraa.com

Table 1.5

Performance of SIGALNS and TS-MCWS when temperature is $10\circ C$

		SIGALNS				TS-MCWS				
instance	$\|I\|$	$\|J_l\|$	$Best_1$	$Average_1$	$T1(s)$	$\|J_l\|$	$Best_2$	$Average_2$	$T2(s)$	$gap(\%)$
S1	5	3	**8,482.9**	8,523.3	0.4	3	8,513.3	8,513.3	0.3	0.4
S2	10	2	**5,971.6**	5,990.6	1.6	2	5,985.3	5, 985.3	1.7	0.3
S3	15	3	8,841.7	8,882.5	4.1	3	**8,838.8**	8,838.8	2.9	-0.1
S4	20	3	**9,130.6**	9,152.1	4.2	4	9,178.3	9,240.1	4.4	0.6
S5	25	3	9,352.9	9,384.7	3.9	4	**9,331.0**	9,370.8	3.1	-0.3
S6	50	7	**21,652.5**	21,711.8	13.4	8	24,353.7	24,442.9	42.1	12.4
S7	75	5	**17,831.2**	17,983.5	28.9	6	20,462.1	20,544.6	45.1	14.7
S8	100	9	**30,136.4**	30,159.4	68.1	9	30,577.0	30,827.7	113.7	1.5
S9	125	6	**24,524.4**	24,563.7	134.4	6	24,738.0	25,006.1	298.1	0.9
S10	150	9	**32,742.3**	32,904.1	179.6	10	35,534.5	35,737.9	657.5	8.5
Average	57.5	5	**16,866.6**	16,925.5	43.9	5.5	17,751.2	17,850.7	116.9	3.8

Table 1.6

Performance of SIGALNS and TS-MCWS when temperature is $30\circ C$

		SIGALNS				TS-MCWS				
instance	$\|I\|$	$\|J_l\|$	$Best_1$	$Average_1$	$T1(s)$	$\|J_l\|$	$Best_2$	$Average_2$	$T2(s)$	$gap(\%)$
S1	5	2	**5,913.7**	5,913.7	0.4	2	5,921.0	5,921.0	0.3	0.2
S2	10	1	**3,363.0**	3,363.0	1.4	1	3,411.3	3,411.3	1.6	1.4
S3	15	1	**3,566.6**	3,566.9	5.0	1	3,585.6	3,585.6	4.0	0.6
S4	20	1	**3,875.9**	3,875.9	5.4	2	3,902.1	3,924.9	5.3	0.7
S5	25	2	6,681.4	6,693.2	6.6	2	**6,661.4**	6,702.1	5.5	-0.3
S6	50	1	**5,859.5**	5,859.5	11.1	1	5,386.9	5,967.3	36.1	0.5
S7	75	2	**10,788.2**	10,934.0	29.3	3	12,443.2	12,507.5	44.3	15.3
S8	100	3	**13,948.9**	14,056.5	71.2	3	14,261.6	14,519.8	111.9	2.2
S9	125	2	**12,739.0**	12,970.6	64.8	3	14,349.6	15,531.1	152.1	12.6
S10	150	2	**13,822.1**	13,853.2	84.5	2	14,183.0	14,296.9	308.7	2.6
Average	57.5	1.7	**8,055.8**	8,108.6	28	1.8	8,460.6	8,636.7	67	3.5

المنارة للاستشارات

www.manaraa.com

customers), are used as representative instances. In all the experiments, we study the impact of ambient temperature and charging time variation on the overall system performance. The key lessons learned from the experiments are summarized below.

- From Figure 1.3, it can be observed that the EV DCFC charging station location decisions are sensitive to the ambient temperature and charging time. For instance, when the charging time of the EVs is set to its base value (80 minutes) and the ambient temperature decreases from $10 \circ C$ (base ambient temperature) to $-10 \circ C$, the selection of the charging stations increases by approximately 100%, 110%, and 141% for 50, 100, and 150 customers, respectively. Figure 1.4 visualizes the EV DCFC charging station location decisions under different ambient temperatures (only for 150 customers). Likewise, if the ambient temperature remains fixed, but the charging time decreases, then more EV charging stations are getting selected. For instance, when the ambient temperature is set to its base value ($10 \circ C$) and the charging time of EVs drops from 80 minutes (base value) to 40 minutes, the selection of the charging stations increases by approximately 71.4%, 90%, and 100% for 50, 100, 150 customers, respectively. The results clearly indicate that the EV DCFC charging station location decisions are highly sensitive to the ambient temperature and charging time.

- Figure 1.5 indicates the impact of variation in the ambient temperature on the overall system cost, where the box of the boxplot indicates the first quartile, median, and third quartile borders, and the whiskers show the highest and lowest values found. As can be seen from the figure, increasing the ambient temperature, the median value of the overall system cost decreases. For instance, when the ambient temperature increases from $-10 \circ C$ to $10 \circ C$,

المنارة للاستشارات
www.manaraa.com

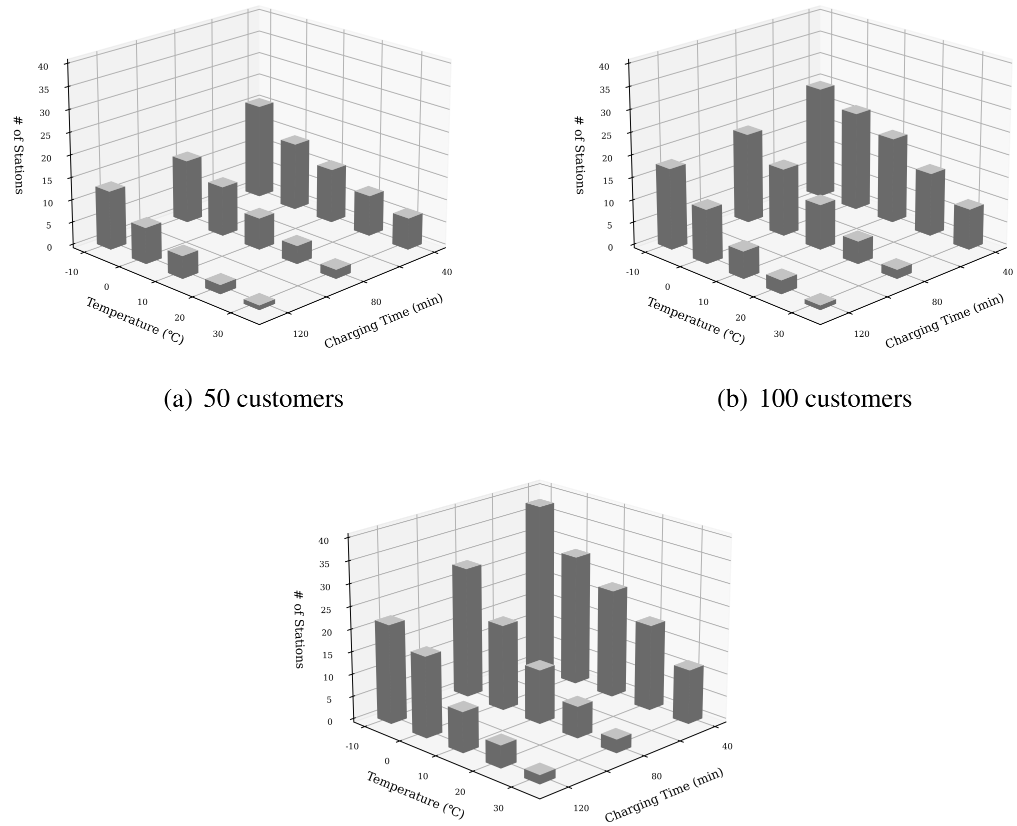

(a) 50 customers

(b) 100 customers

(c) 150 customers

Figure 1.3

Impact of temperature and charging time on EV DCFC charging station selection

www.manaraa.com

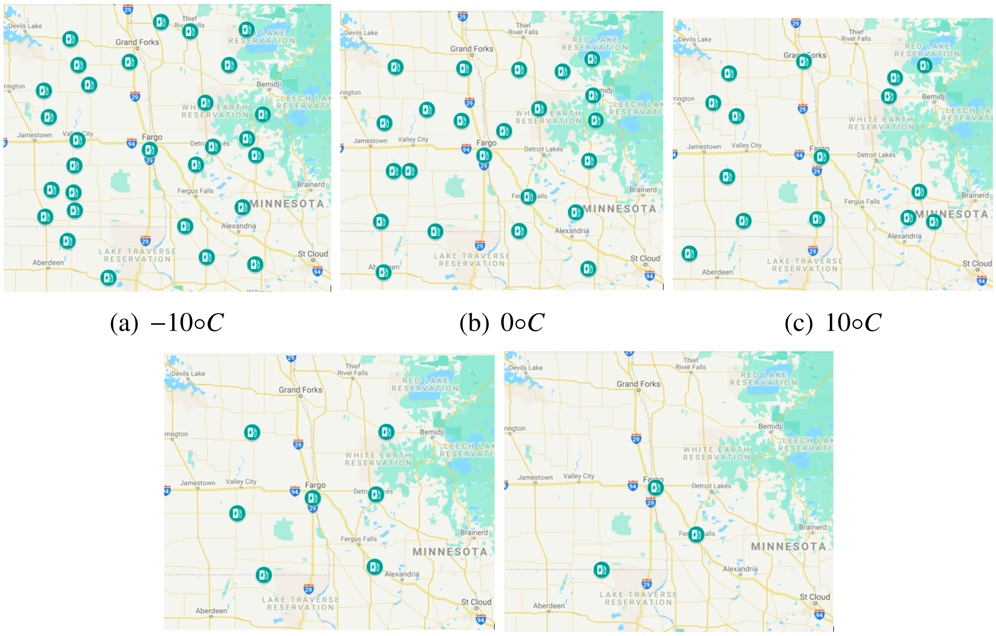

(a) $-10\circ C$ (b) $0\circ C$ (c) $10\circ C$

(d) $20\circ C$ (e) $30\circ C$

Figure 1.4

Illustration of charging station location decisions under different ambient temperatures

the overall system cost drops by approximately 27.2%, 19.7%, and 23.1% for 50, 100, 150 number of customers, respectively. This is quite intuitive, given fewer EV DCFC charging stations would be necessary at the higher temperatures (see Figure 1.3).

- Figure 1.5 shows the impact of ambient temperature and initial state of charge of EVs (soc_0) on the DCFC charging station selection decisions. To run the experiments, we vary the ambient temperature between $-10\circ C$ and $30\circ C$ and soc_0 between 100 and 250 miles while keeping the recharging time fixed at 80 minutes (base value). The results in Figure 1.5 clearly indicates that the EV DCFC charging station location decisions are highly sensitive to both the ambient temperature and soc_0. For instance, assuming that the ambient temperature is $10\circ C$ and the soc_0 decreases from 200 miles to 100 miles, the number of EV DCFC charging

المنارة للاستشارات
www.manaraa.com

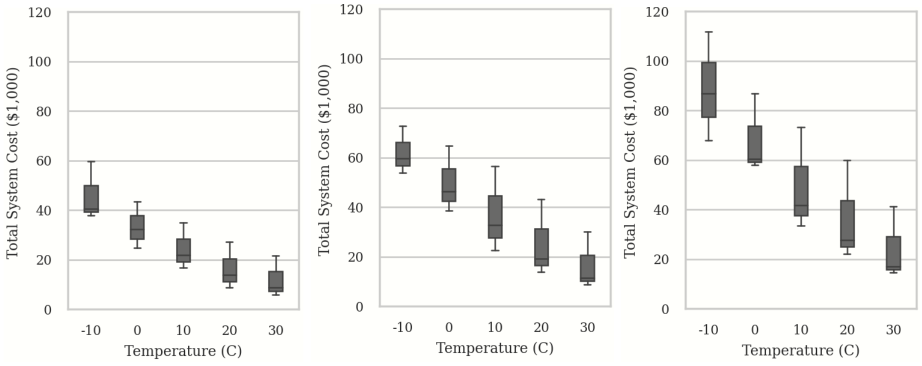

(a) 50 customers (b) 100 customers (c) 150 customers

Figure 1.5

Impact of ambient temperature on overall system cost

station location decisions increases by approximately 60%, 100%, and 133.1% for 50, 100, 150 customers, respectively. In summary, it can be concluded that both the initial state of the charging and the ambient temperature are of high importance in properly modeling and planning the EV DCFC location routing problems.

- Figure 1.7 visualized how the EV routing decisions are impacted with and without considering the ambient temperature. For demonstration purposes, we use the instance with 20 customers (instance $S4$) and set the recharging time and soc_0 to their base values, namely, 80 minutes and 150 miles. From Figure 1.7, we observe a noticeable change in the location-routing decisions when the ambient temperature is considered. In both cases, 5 EVs are utilized to satisfy the customer's demand. However, an additional 5 charging stations need to be installed, and 81 more miles need to be traveled by the EVs to satisfy the customer's demand when the ambient temperature is considered.

المنارة للاستشارات
www.manaraa.com

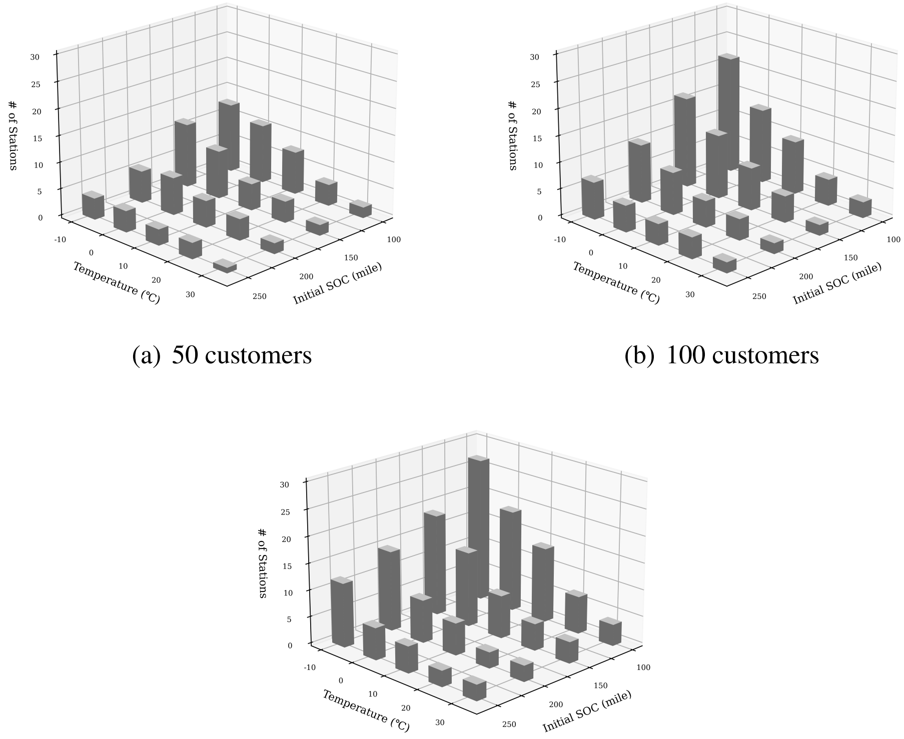

(a) 50 customers

(b) 100 customers

(c) 150 customers

Figure 1.6

Impact of ambient temperature and soc_0 on EV DCFC charging station selection

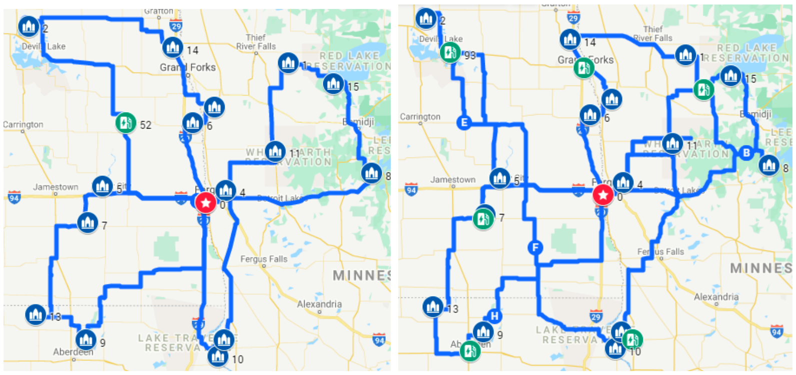

(a) Without temperature

(b) Temperature = $-10\circ C$

Figure 1.7

Illustration of routing decisions with and without considering the ambient temperature

المنارة للاستشارات
www.manaraa.com

CHAPTER II

TWO-STAGE STOCHASTIC ELECTRIC VEHICLES FAST CHARGER LOCATION ROUTING PROBLEM UNDER AMBIENT TEMPERATURE

2.1 Introduction

According to the 2019 world energy outlook report [69], energy systems' future estimation indicates that severe environmental damages will occur by 2040 if no policies are adopted worldwide to reduce the fossil fuel consumption rate. This forthcoming failure in fossil energy accessibility and the pollution produced by unnatural sources drive several efforts to avoid the loss by overcoming the pollution resulting from fossil fuel consumption. Cost drops in renewable energy sources and advances in digital technologies, while eliminating some energy security problems, offer incredible energy transition opportunities. As such, shifting towards more sustainable transportation, electric vehicles (EVs) are becoming more popular in urban transport and logistics systems. In 2030, EV owners will continue to grow to around 18.7 million in the USA and 126 million worldwide [62]. As more EVs take to the road, the appropriate deployment of publicly accessible charging stations becomes an important issue to resolve. However, the problem of optimally locating the EV charging stations is not trivial due to the simultaneous consideration of many factors such as uncertainty in charging time, range anxiety, frequency of charging, state of charge (SOC), and finally, varieties of charging needs by different users (e.g., visitors, employee,residential, the fleet users) [14].

المنارة للاستشارات
www.manaraa.com

Recent EVs rely on lithium-ion and lithium-polymer battery packs as the primary power source [64], which can only offer a minimal driving range per charge. Low ambient temperature can significantly reduce the charging rate, thereby prolonging the charging time [99]. Due to the need for continuous heating in most cold areas, EV battery packs frequently get stressed, which significantly degrading the battery charging performance over time. Even though an individual or a combination of the aforementioned factors are taken into account by a number of past studies, none of the prior studies examined the impact of weather variability (e.g., hot or cold weather conditions) in designing the EV DC Fast Charging (DCFC) stations [96, 94]. Idaho National Laboratory (INL) recently found that the SOC of a 30-minute DCFC charger could drop by 36% from warm temperature ($25\circ C$) to low temperature ($0\circ C$), indicating the sensitivity of EVs routing performance in cold areas [104]. The sensitivity of Lithium-ion and Lithium-polymer battery performance to the ambient temperatures is also supported by a number of recent studies, such as [17, 33, 32, 52].

Over the past few decades, many studies have investigated the vehicle routing problem under a stochastic environment [44, 37, 49]. However, investigating the impact of uncertainty in EV-specific attributes, such as battery depletion, SOC level, and other related parameters, are not extensively investigated in the literature. As such, several studies in EV logistic planning pointed out the importance of addressing such issues in future studies [38, 68]. Due to the challenges associated with solving stochastic optimization problems, most of the past studies related to the location-routing problems (LRPs) on EVs ignore the input parameters' uncertainty. To the best of the author's knowledge, apart from [105], other studies related to the EV LRPs do not consider the effect of uncertain input parameters on the location-routing decisions. With all these

المنارة للاستشارات
www.manaraa.com

taken into account, planning the EVs transportation network that could appropriately consider the ambient weather and related uncertain parameters (e.g., demand uncertainty), especially in specific geographic areas that suffer from fluctuating temperatures around the year or during the day, is imperative.

To fill the gap in the literature, this study proposes developing an innovative two-stage stochastic mixed-integer linear programming model, which optimizes the EV DCFC charging station locations and the associated routing decisions under stochastic customer demand and ambient temperature fluctuations. The proposed mathematical model is an extension of the classical location-routing problems, which are already known to be an $\mathcal{NP}$-hard problem [46]. To deal with this problem's computational burden, we developed a hybrid algorithm that first utilizes the Progressive Hedging algorithm to decompose the original problem by scenarios. Subsequently, an innovative heuristic, namely, the Sweep-based Iterated Greedy Adaptive Large Neighborhood algorithm, is developed to solve the scenario-specific subroblems in a reasonable timeframe. The performance of the proposed algorithm is compared with the state-of-the-art solvers, such as GUROBI. Finally, by designing a real-life case study using Fargo city in North Dakota, we aim to evaluate the proposed model's performance and to draw a number of managerial insights for the decision-makers to a region with high ambient temperature fluctuations.

The exposition of this paper is as follows. Section 2.2 details the related literature review. Sections 2.3 and 2.4 introduce the proposed mathematical model formulation and solution approaches. Finally, section 2.5 presents the numerical experiments under different settings to assess the performance of our proposed methodologies. This study is providing a number of future research directions present in Chapter 3.

المنارة للاستشارات
www.manaraa.com

2.2 Literature Review

To assess the impact of ambient temperature and other stochastic parameters (e.g., customer demand), this study integrates the facility location decisions (e.g., charging stations) and the associated EV routing decisions via solving a vehicle routing problem. As such, in this section, we first review the related location-routing studies.

The LRP is a hybrid problem that integrates the location-allocation problem and vehicle routing problem, and its objective is to solve the two problems concurrently to achieve a better solution compared to the case where problems are solved independently [16]. In literature, different variants of the LRP, such as single vs. multiple depots (e.g., [48, 93]), capacities on depots or vehicles (e.g., [54, 51]), and the time window restriction for the deliveries (e.g., [100, 101]) have been investigated. A comprehensive review of the LRP can be found in [67] and [72]. Laporte and Nobert [46] developed an exact solution method to address the LRP under smaller instances which only included 20-50 customers. Belenguer et al. [8] proposed an exact solution method based upon the branch-and-cut algorithm to address the capacitated LRP. Their method was able to tackle problems with 5-10 potential depots and 20-88 customers. Due to the challenges associated with solving LRP using exact solution methods, various heuristic solution techniques (e.g., simulated annealing, tabu search, particle swarm optimization) were developed to tackle the LRP (e.g., [56, 91, 53, 23]). Lately, several studies have incorporated energy and environmental factors in the LRPs. Ebrahimi [19] developed a multi-objective optimization model for a tire distribution system that minimizes the effects of environmental emission and maximizes the total costs of the integrated network's responsiveness. Yang and Sun [98] proposed a mixed-integer linear programming model to address the battery swap station location-routing problem. The authors then provided an extended

المنارة للاستشارات
www.manaraa.com

formulation that enables EVs to revisit a specific battery swap station more than once. Later, Hof et al. [31] developed a mixed-integer linear programming model to address the EV battery swap station location-routing problem, which accounted the possibility of intermediate stops. Schiffer and Walther [81] proposed an LRP formulation for EV logistics, which considers the time windows and enables the EVs to be partially charged after visiting the charging stations. Li et al.[50] utilize a bi-level programming approach to generate public recharging infrastructure location strategy in which the location strategy is optimized in the upper-level model and the corresponding routing plan in the lower-level model. Finally, Zhang et al. [105] developed a mixed-integer linear programming model to address the EV battery swap station LRP with stochastic demands. This study develops a hybrid variable neighborhood search algorithm to solve the location and routing problems interactively. In summary, although many studies related to the LRP and LRP with EVs are carried out, the majority of them assumed that the model input parameters are known in advance, which may limit their applications under stochastic environment.

As discussed earlier, the generalization of the LRP requires solving a vehicle routing problem (VRP), which is already known to be a challenging problem from a solution standpoint [12]. Over the years, many variants of the VRP are developed, such as capacitated VRP (CVRP), customer time windows (VRPTW), multiple depots (MDVRP), pickup and delivery (VRPPD), time-dependent travel time (TD-VRP), and heterogeneous fleet (MFVRP) [90]. All these different variants of the VRP could be investigated under both deterministic and stochastic settings under the LRP. The literature related to stochastic Vehicle Routing Problems (SVRPs) aims to find the routing decisions where some parameters of the problem, such as customers' demands (e.g., [10, 28]), the number of customers (e.g., [9, 25]), travel times (e.g., [44, 29]), etc., are not known in advance.

المنارة للاستشارات
www.manaraa.com

Besides, a number of EV-specific factors are also required to be considered to obtain a robust EV logistic network, such as uncertain waiting times at the public recharging stations (e.g., [39, 86, 1]), uncertainty in battery depletion (e.g., [85]), and many others.

It shall be noted that even though the past studies have done a phenomenal job in addressing different EV-specific challenges, the studies ignored the effect of climate variability on the DCFC siting selection and the associated EV routing decisions (e.g., [15, 102, 76, 74, 78, 35]). Motoaki et al. [65] presented findings claiming that ambient temperature might heavily affect the DCFC charging rate. The authors stressed that considering the ambient temperature in designing the EV DCFC infrastructure in large countries like the US, where the regional climate varies significantly, could not be neglected. Unfortunately, most of the past studies (e.g., [15, 102, 76, 74, 78, 35]) assumed a constant charging rate in their formulations; hence, the obtained EV logistical solutions might be inaccurate. As such, this study fills the gap in the literature by extending the traditional LRPs to account for the impact of ambient temperature on the DCFC infrastructure deployment and the associated EV routing decisions.

2.3 Mathematical Model Formulation

The effect of variation in ambient temperature on the battery's charging process is a major concern for planning the delivery routes of the EVs. As shown in [65], the SOC of a fast charger does not drop linearly. Indeed, the actual fast charging process is non-linear, which is a function of initial SOC, charging time, and the ambient temperature. As such, the simplified linearized SOC assumption may provide an overestimated duration for the DCFC's, and the resulting model may overestimate the EV fast charger location-routing decisions. In the following development,

المنارة للاستشارات
www.manaraa.com

the inclusion of temperature effects in the proposed EV location-routing mathematical model is explained.

Let us define $s\hat{o}c(c,t)$ to predict the SOC of an EV, which is a function of charging time t and ambient temperature c (in ^{o}Celsius). We further define λ_0, λ_1, and λ_2 to be the coefficient estimates, and soc_i the initial value of the SOC of an EV. Inspired from the study of [65], the following SOC estimation is provided.

$$s\hat{o}c(c,t) = \left(soc_i + \frac{\lambda_0 + \lambda_1 c}{\lambda_2}\right)e^{\lambda_2 t} - \left(\frac{\lambda_0 + \lambda_1 c}{\lambda_2}\right)$$

After simplification, the above equation becomes:

$$s\hat{o}c(c,t) = e^{\lambda_2 t} soc_i + \left(\frac{\lambda_0 + \lambda_1 c}{\lambda_2}\right)(e^{\lambda_2 t} - 1)$$

The ambient temperature is constant for all vehicles while they are in the charging process. We now replace the $e^{\lambda_2 t}$ and $\left(\frac{\lambda_0+\lambda_1 c}{\lambda_2}\right)(e^{\lambda_2 t} - 1)$ terms by μ^1 and μ^2, respectively, and obtain the following equation.

$$s\hat{o}c(c,t) = \mu^1 soc_i + \mu^2 \tag{2.1}$$

Note that Figure 2.1 visualizes $\mu_1$and μ_2 that equation (2.1) utilizes to estimate the level of SOC in this study.

Having introduced the underlying equation to estimate the SOC, it is observed that the value of two new defined parameters, μ^1 and μ^2, depends on the value of λ_0, λ_1, and λ_2, which are estimated using statistical approaches and historical data for a specific type of EV [65]. To

www.manaraa.com

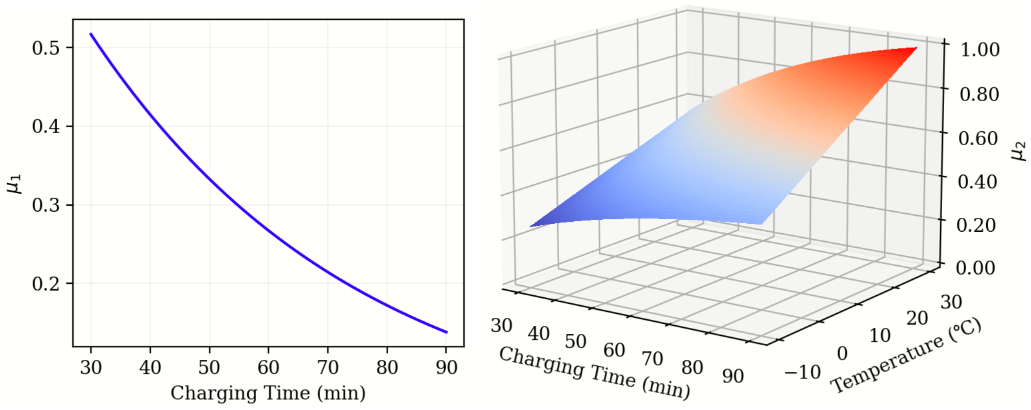

(a) μ_1 visualization

(b) μ_2 visualization

Figure 2.1

Illustration of the parameters used for SOC estimation

capture the variability in the data and reflect a sound SOC estimation, the value of these two terms is modeled as an uncertain parameter in this study. Moreover, we assume the stochasticity of customer demands at individual customer locations. Given the EV facility location decisions need to be made now prior to realizing the uncertainty, we formulated this problem as a two-stage stochastic mixed-integer linear programming (MILP) model and referred to as **[EV-SAT]**. The summary of the sets, parameters, and decision variables used in the proposed mathematical model **[EV-SAT]** are listed below.

Sets:

- $\mathcal{I}$: set of customers, $i \in \mathcal{I}$
- $\mathcal{J}$: set of potential charging station locations, $j \in \mathcal{J}$
- $\mathcal{E}$: set of electrical vehicles, $e \in \mathcal{E}$
- $\{o, o^{'}\}$: A single depot and it's duplicate dummy
- $\mathcal{N}$: set of all nodes, $n \in \mathcal{N}$, where $\mathcal{N} = \mathcal{I} \cup \mathcal{J} \cup \{o, o^{'}\}$

www.manaraa.com

- Ω: set of all possible scenarios of ambient temperature $\omega \in \Omega$

Parameters:

- s_j: cost of installing a new charging station at location $j \in \mathcal{J}$
- d_{ij}: distance between node $i \in \mathcal{N}$ and $j \in \mathcal{N}$
- c_{ije}: shipping cost per unit of distance from node $i \in \mathcal{N}$ to $j \in \mathcal{N}$ using EV $e \in \mathcal{E}$ under scenario $\omega \in \Omega$
- $\gamma_{i\omega}$: demand weight for costumer $i \in \mathcal{I}$ under scenario $\omega \in \Omega$
- δ_e: maximum weight capacity of EV $e \in \mathcal{E}$
- soc_0: initial state of charge (SOC, in %) of an EV at depot
- θ: a conversion factor to calculate the maximum distance an EV can travel at its current SOC
- M: a big number
- d_{max}: the maximum driving distance at a 100% SOC, where $d_{max} \geq \theta s\hat{o}c(c, t)$
- μ^1_ω, μ^2_ω: stochastic parameters used for SOC estimation under sceanario $\omega \in \Omega$
- ρ_ω: the probability of occurrence of a scenario $\omega \in \Omega$ and $\sum_{\omega \in \Omega} \rho_\omega = 1$

Decision Variables:

- X_j: 1 if a charging station is located in $j \in \mathcal{J}$; 0 otherwise
- $V_{ije\omega}$: 1 if the road connecting node $i \in \mathcal{N}$ to $j \in \mathcal{N}$ is traversed by EV $e \in \mathcal{E}$ under scenario $\omega \in \Omega$; 0 otherwise
- $P_{ije\omega}$: remaining weight capacity of EV $e \in \mathcal{E}$ after delivery fulfillment at node $j \in \mathcal{N}$ as soon as it arrives at node $i \in \mathcal{N}$ under scenario $\omega \in \Omega$
- $D^1_{ne\omega}$: the maximum distance an EV $e \in \mathcal{E}$ can travel as it arrives at node $n \in \mathcal{N}$ under scenario $\omega \in \Omega$

www.manaraa.com

- $D^2_{ne\omega}$: the maximum distance an EV $e \in \mathcal{E}$ can travel as it leaves at node $n \in \mathcal{N}$ under scenario $\omega \in \Omega$

As defined earlier, $D^1_{ne\omega}$ denotes the maximum distance an EV can travel under the current SOC level when arrives node $n \in \mathcal{N}$ in the underlying logistic network. We now use the conversion rate (θ) to find the initial SOC (soc_i) of an EV $e \in \mathcal{E}$ at a charging station $j \in \mathcal{J}$ under scenario $\omega \in \Omega$ as follows:

$$soc_i \times \theta = D^1_{je\omega} \longrightarrow soc_i = \frac{D^1_{je\omega}}{\theta} \tag{2.2}$$

Substituting (2.2) into (2.1), given that μ^1_ω and μ^2_ω represent the scenario-specific value of the parameters needed for SOC estimation, we obtain the following equation to estimate the the scenario-specific SOC:

$$s\hat{o}c^{\omega}(c,t) = \mu^1_\omega \left(\frac{D^1_{je\omega}}{\theta}\right) + \mu^2_\omega \tag{2.3}$$

To calculate the maximum distance an EV $e \in \mathcal{E}$ can travel as it leaves a charging station $j \in \mathcal{J}$ under scenario $\omega \in \Omega$, we define the following constraints:

$$\begin{array}{rcll} D^2_{je\omega} & = & \theta s\hat{o}c^{\omega}(c,t)X_j & \forall j \in \mathcal{J}, e \in \mathcal{E}, \omega \in \Omega \\ \rightarrow D^2_{je\omega} & = & \theta\left(\mu^1_\omega \frac{D^1_{je\omega}}{\theta} + \mu^2_\omega\right)X_j & \forall j \in \mathcal{J}, e \in \mathcal{E}, \omega \in \Omega \\ \rightarrow D^2_{je\omega} & = & \mu^1_\omega D^1_{je\omega} X_j + \mu^2_\omega \theta X_j & \forall j \in \mathcal{J}, e \in \mathcal{E}, \omega \in \Omega \end{array} \tag{2.4}$$

www.manaraa.com

Constraints (2.4) are nonlinear. To linearize, we first introduce a new variable $\{Z_{je\omega} | \forall j \in \mathcal{J}, e \in \mathcal{E}, \omega \in \Omega\}$ to substitute the $D^1_{je\omega} X_j$ term. Since we know that d_{max} is an upper bound for the $D^1_{je\omega}$ variable, the following set of linear constraints are introduced to substitute constraints (2.4):

$$
\begin{aligned}
D^2_{je\omega} &= \mu^1_\omega Z_{je\omega} + \mu^2_\omega \theta X_j && \forall j \in \mathcal{J}, e \in \mathcal{E}, \omega \in \Omega && (2.5)\\
Z_{je\omega} &\leq d_{max} X_j && \forall j \in \mathcal{J}, e \in \mathcal{E}, \omega \in \Omega && (2.6)\\
Z_{je\omega} &\leq D^1_{je\omega} && \forall j \in \mathcal{J}, e \in \mathcal{E}, \omega \in \Omega && (2.7)\\
Z_{je\omega} &\geq D^1_{je\omega} - d_{max}\left(1 - X_j\right) && \forall j \in \mathcal{J}, e \in \mathcal{E}, \omega \in \Omega && (2.8)\\
Z_{je\omega} &\geq 0 && \forall j \in \mathcal{J}, e \in \mathcal{E}, \omega \in \Omega && (2.9)
\end{aligned}
$$

With this, we are now ready to introduce our proposed mathematical model **[EV-SAT]**, as shown below. In **[EV-SAT]**, charging station location decision $\{X_j\}_{\forall j \in \mathcal{J}}$ is considered as a first-stage decision variable. Following this decision, a number of second-stage routing-related decisions are made (e.g., $V_{ije\omega}$, $P_{ije\omega}$, $D^1_{ne\omega}$, and $D^2_{ne\omega}$) after the uncertainty is revealed. The objective function (2.25) of the model **[EV-SAT]** minimizes the first-stage EV charging station location cost and the expected second-stage routing-related costs across all possible uncertain realizations.

$$
\textbf{[EV-SAT]}\ Minimize \sum_{j \in \mathcal{J}} s_j X_j + \sum_{\omega \in \Omega} \rho_\omega \sum_{i \in \mathcal{N}} \sum_{j \in \mathcal{N}} \sum_{e \in \mathcal{E}} c_{ije} d_{ij} V_{ije\omega} \qquad (2.10)
$$

subject to constraints (2.5)-(2.9) and

المنارة للاستشارات
www.manaraa.com

$$\sum_{n\in\mathcal{N}\notin\{o'\}}\sum_{e\in\mathcal{E}} V_{nie\omega} = 1 \qquad \forall i\in\mathcal{I},\omega\in\Omega \tag{2.11}$$

$$\sum_{n\in\mathcal{N}\notin\{o'\},n\neq j}\sum_{e\in\mathcal{E}} V_{nje\omega} \leq MX_j \qquad \forall j\in\mathcal{J},\omega\in\Omega \tag{2.12}$$

$$\begin{aligned}\sum_{n'\in\mathcal{N}\notin\{o\},n'\neq n} V_{nn'e\omega} - \sum_{n'\in\mathcal{N}\notin\{o'\},n'\neq n} V_{n'ne\omega} &= 0 \ \ \forall n\in\mathcal{N}\notin\left\{o,o'\right\}, e\in\mathcal{E},\\ \omega\in\Omega &\end{aligned} \tag{2.13}$$

$$\sum_{n\in\mathcal{N}\notin\{o\}} V_{one\omega} - \sum_{n\in\mathcal{N}\notin\{o'\}} V_{noe\omega} = 0 \qquad \forall e\in\mathcal{E},\omega\in\Omega \tag{2.14}$$

$$\sum_{n\in\mathcal{N}\notin\{o\}} V_{one\omega} \leq 1 \qquad \forall e\in\mathcal{E},\omega\in\Omega \tag{2.15}$$

$$\begin{aligned}\sum_{n\in\mathcal{N}\notin\{o',j\}} P_{nje\omega} &= \sum_{n\in\mathcal{N}\notin\{o,j\}} P_{jne\omega}\ \forall j\in\mathcal{J},\forall e\in\mathcal{E},\\ &\qquad\qquad \omega\in\Omega\end{aligned} \tag{2.16}$$

$$\begin{aligned}\sum_{n\in\mathcal{N}\notin\{o,i\}} P_{ine\omega} &\leq \sum_{n\in\mathcal{N}\notin\{o',i\}} P_{nie\omega} - \gamma_{i\omega}\sum_{n\in\mathcal{N}\notin\{o',i\}} V_{nie\omega}\\ +\delta_e(1-\sum_{n\in\mathcal{N}\notin\{o',i\}} V_{nie\omega}) &\qquad \forall i\in\mathcal{I}, e\in\mathcal{E},\omega\in\Omega\end{aligned} \tag{2.17}$$

$$\begin{aligned}P_{nn'e\omega} &\leq \delta_e V_{nn'e\omega}\ \ \forall n\in\mathcal{N}\notin\left\{o'\right\}, n'\in\mathcal{N}\notin\{o\},\\ n\neq n', e\in\mathcal{E},\omega\in\Omega &\end{aligned} \tag{2.18}$$

المنارة للاستشارات

www.manaraa.com

$$\begin{aligned} D^1_{n'e\omega} + d_{nn'}V_{nn'e\omega} &\leq D^2_{ne\omega} + d_{max}(1 - V_{nn'e\omega}) \ \ \forall n \in \mathcal{N} \notin \left\{o'\right\}, \\ &\qquad n' \in \mathcal{N} \notin \{o\}, n' \neq n, e \in \mathcal{E}, \omega \in \Omega \end{aligned} \tag{2.19}$$

$$\begin{aligned} D^1_{n'e\omega} + d_{nn'}V_{nn'e\omega} &\geq D^2_{ne\omega} - d_{max}(1 - V_{nn'e\omega}) \ \ \forall n \in \mathcal{N} \notin \left\{o'\right\}, \\ &\qquad n' \in \mathcal{N} \notin \{o\}, n' \neq n, e \in \mathcal{E}, \omega \in \Omega \end{aligned} \tag{2.20}$$

$$D^2_{oe\omega} = \theta soc_0 \qquad \forall e \in \mathcal{E}, \omega \in \Omega \tag{2.21}$$

$$D^1_{ie\omega} = D^2_{ie\omega} \qquad \forall i \in \mathcal{I}, e \in \mathcal{E}, \omega \in \Omega \tag{2.22}$$

$$P_{ije\omega}, D^1_{ne\omega}, D^2_{ne\omega} \geq 0 \qquad \forall (i,j) \in \mathcal{N}, n \in \mathcal{N}, e \in \mathcal{E}, \omega \in \Omega \tag{2.23}$$

$$V_{ije\omega} \in \{0,1\} \qquad \forall i \in \mathcal{N}, j \in \mathcal{N}, e \in \mathcal{E}, \omega \in \Omega \tag{2.24}$$

$$X_j \in \{0,1\} \qquad \forall j \in \mathcal{J} \tag{2.25}$$

Constraints (2.11) ensure that each customer location $i \in \mathcal{I}$ is served by atleast one EV. Constraints (2.12) limit the number of EVs that can visit a charging station $j \in \mathcal{J}$. Constraints (2.13) and (2.14) ensure flow balance of EVs within the logistic network. Constraints (2.15) ensure that each EV $e \in \mathcal{E}$ can leave the depot at most once. Constraints (2.16) enforce that no deliveries are made when an EV stops at a charging station. Constraints (2.17) update the weight capacity of an EV as it leaves a customer node $i \in \mathcal{I}$. Constraints (2.18) limit the weight capacities of the EVs. Constraints (2.19) and (2.20) update the battery level of an EV after each node is visited. Constraints (2.21) initiate the SOC of an EV $e \in \mathcal{E}$ as it leaves the depot. Constraints (2.22) keep

المنارة للاستشارات
www.manaraa.com

the battery level unchanged as an EV fulfills a delivery at a customer node. Finally, constraints (2.23), (2.24), and (2.25) are the nonnegativity and binary restrictions for the decision variables.

2.3.1 Variable Fixing and Valid Inequalities

To improve the computational performance of the proposed mathematical model **[EV-SAT]**, the following variable fixing and valid inequalities are introduced. We begin by introducing the variable fixing techniques first.

- The electric vehicle $e \in \mathcal{E}$ is not able to traverse the arc between the nodes $n \in \mathcal{N}$ and $n^{'} \in \mathcal{N}$ if the respective traveling distance, i.e., $d_{nn'}$ is greater than the maximum distance that it can travel by a fully charged battery, namely, d_{max}.

$$V_{nn'e\omega} \quad = \quad 0 \qquad \forall n \in \mathcal{N}, n^{'} \in \mathcal{N}, e \in \mathcal{E}, \omega \in \Omega | d_{nn'} > d_{max} \tag{2.26}$$

- The electric vehicle $e \in \mathcal{E}$ is not able to traverse the arc between the nodes $n \in N$ and $n^{'} \in N$ if the sum of the demand of costumers in respective customer nodes exceeds the weight capacity of the EV.

$$V_{nn'e\omega} \quad = \quad 0 \qquad \forall n \in \mathcal{N}, n^{'} \in \mathcal{N}, e \in \mathcal{E}, \omega \in \Omega | (\gamma_{n\omega} + \gamma_{n'\omega}) > \delta_e \tag{2.27}$$

In addition to the above-mentioned variable fixing techniques, the following valid inequalities are introduced.

المنارة للاستشارات
www.manaraa.com

- In our study, we assume that none of the EVs can travel more than d_{trip} each day. To capture this constraint, we add the following valid inequalities as a lazy constraint to model **[EV-SAT]**.

$$\sum_{n \in \mathcal{N}} \sum_{n' \in \mathcal{N}} d_{nn'} V_{nn'e\omega} \quad \leq \quad d_{trip} \qquad \forall e \in \mathcal{E}, \omega \in \Omega \tag{2.28}$$

- In this technique, we approximate a lower bound, namely, $N^{total}_{LB,\omega}$, to determine the number of EVs that are required to satisfy the customer demand under each scenario $\omega \in \Omega$. We believe generation of this lower bound will further tighten the solution space for model **[EV-SAT]**. To estimate $N^{total}_{LB,\omega}$, the following two factors need to be considered: (i) the total weight associated with the requests of the costumers in each scenario $\omega \in \Omega$ and (ii) the maximum trip distance that each EV $e \in \mathcal{E}$ can traverse. First, we need to estimate the minimum number of EVs that are required under each scenario $\omega \in \Omega$ based on the freight limitation, $N^{freight}_{LB,\omega}$, which can be obtained by solving a well-known bin packing problem [57] given by (2.29)-(2.33). Within this formulation, we define the following two decision variables: $\{Z_{e\omega} | \forall e \in \mathcal{E}, \omega \in \Omega\}$ denotes if EV $e \in \mathcal{E}$ is used under scenario $\omega \in \Omega$ or not and $\{H_{ie\omega} | \forall i \in \mathcal{I}, e \in \mathcal{E}, \omega \in \Omega\}$ denotes if costumer $i \in \mathcal{I}$ is served by EV $e \in \mathcal{E}$ under scenario $\omega \in \Omega$. Under each scenario $\omega \in \Omega$, we then solve the following optimization model.

$$Minimize \quad N^{freight}_{LB,\omega} = \sum_{e \in \mathcal{E}} Z_{e\omega} \tag{2.29}$$

subject to

المنارة للاستشارات
www.manaraa.com

$$\sum_{i \in \mathcal{I}} \gamma_{i\omega} H_{ie\omega} \leq \delta_e Z_{e\omega} \quad \forall e \in \mathcal{E}, \omega \in \Omega \tag{2.30}$$

$$\sum_{e \in \mathcal{E}} \gamma_{i\omega} H_{ie\omega} = 1 \quad \forall i \in \mathcal{I}, \omega \in \Omega \tag{2.31}$$

$$Z_{e\omega} \in \{0, 1\} \quad \forall e \in \mathcal{E}, \omega \in \Omega \tag{2.32}$$

$$H_{ie\omega} \in \{0, 1\} \quad \forall i \in \mathcal{I}, e \in \mathcal{E}, \omega \in \Omega \tag{2.33}$$

The next lower bound is computed based on the maximum length of the trip, N_{LB}^{trip}, that an EV $e \in \mathcal{E}$ can traverse. To do so, we create a minimal spanning tree based on the feasible arcs contained by the depot and the customer nodes, i.e., $\mathcal{I} \cup \{o\}$. The total weight of this graph, where the weight is the traveling distance between vertices of the graph, provides us with an estimated minimum overall traveling distance d_{est}. Hence, the second lower bound is computed as follow:

$$N_{LB}^{trip} = *\frac{d_{est}}{d_{trip}} \tag{2.34}$$

Having introduced these two lower bounds on the minimum number of EVs required under each scenario $\omega \in \Omega$, we use the best among them in the MILP settings, as shown below:

$$N_{LB,\omega}^{total} = max\{N_{LB,\omega}^{freight}, N_{LB}^{trip}\} \tag{2.35}$$

المنارة للاستشارات

www.manaraa.com

Finally, to tighten the solution space of model **[EV-SAT]**, we add the following valid inequality as a lazy constraint.

$$\sum_{e\in\mathcal{E}}\sum_{n'\in\mathcal{N}} V_{on'e\omega} \geq N^{total}_{LB,\omega} \qquad \forall\omega\in\Omega \tag{2.36}$$

2.4 Solution Methodology

Model **[EV-SAT]** is an extension of the classical location-routing problems (LRP) [46]. Note that if the EVs' driving range is set to be a sufficiently large number, then recharging the battery and constructing the charging stations will be unnecessary in this logistic network. With such an assumption, model **[EV-SAT]** can be reduced to the classic vehicle routing problem (VRP) with stochastic demands [24], which is already known as an $\mathcal{NP}$-hard problem. Therefore, it could be inferred that model **[EV-SAT]** is also an $\mathcal{NP}$-hard problem. As such, despite the additions of the variable fixing and valid inequalities introduced in Section 2.3.1, our initial experimentation with the `GUROBI` solver exposes its inability to solve the larger instances of model **[EV-SAT]** in a reasonable timeframe. To alleviate this challenge, we propose to develop a customized hybrid solution approach, which combines Progressive Hedging Algorithm (PHA) and a Sweep-based Iterated Greedy Adaptive Large Neighborhood search algorithm (SIGALNS) to efficiently solve model **[EV-SAT]** in a reasonable timeframe. The following subsections detail the proposed hybrid algorithm.

2.4.1 Progressive Hedging Algorithm

Model **[EV-SAT]** is a two-stage stochastic mixed-integer linear programming model. Evaluating such a model with a large scenario set, Ω, poses a serious computational challenge. To alleviate

المنارة للاستشارات
www.manaraa.com

this challenge, we apply the PHA procedure, proposed by Rockafellar and Wets [79], to efficiently solve model **[EV-SAT]**. This algorithm adopts an augmented Lagrangian relaxation method to decompose the two-stage stochastic programming model by individual scenarios. As a result, the subproblems corresponding to the scenarios could be solved in a much shorter time [92]. The PHA algorithm has shown a good capability in solving a broad range of problems, including applications in financial planning [66], surgery planning [27], inland waterway port management [5, 4, 3], and many others. As can be seen in the model **[EV-SAT]**, constraints (2.5), (2.6), and (2.12) connect the first-stage decision variables, $\{X_j\}_{j \in \mathcal{J}}$, with the second-stage decision variables. The connection between the decision variables of the two stages restricts model **[EV-SAT]** to be decomposed by scenarios. To overcome this issue, we introduce a new *copy* variable $\{X_{j\omega}\}_{j \in \mathcal{J}, \omega \in \Omega} \in \{0, 1\}$, which allows model **[EV-SAT]** to be separable by scenarios. Having introduced this new variable, we reformulate **[EV-SAT]** as follows:

$$Minimize \sum_{\omega \in \Omega} \rho_\omega \left(\sum_{j \in \mathcal{J}} s_j X_{j\omega} + \sum_{i \in \mathcal{N}} \sum_{j \in \mathcal{N}} \sum_{e \in \mathcal{E}} c_{ije} d_{ij} V_{ije\omega} \right) \tag{2.37}$$

subject to (2.6)-(2.9), (2.11), (2.13)-(2.24), and

المنارة للاستشارات
www.manaraa.com

$$D^2_{je\omega} = \mu^1_{\omega} Z_{je\omega} + \mu^2_{\omega}\theta X_{j\omega} \qquad \forall j \in \mathcal{J}, e \in \mathcal{E}, \omega \in \Omega \tag{2.38}$$

$$Z_{je\omega} \leq d_{max} X_{j\omega} \qquad \forall j \in \mathcal{J}, e \in \mathcal{E}, \omega \in \Omega \tag{2.39}$$

$$\sum_{n\in\mathcal{N}\notin\{o'\}, n\neq j} \sum_{e\in\mathcal{E}} V_{nje\omega} \leq M X_{j\omega} \qquad \forall j \in \mathcal{J}, \omega \in \Omega \tag{2.40}$$

$$X_{j\omega} = X_{j\omega'} \qquad \forall j \in \mathcal{J}, (\omega, \omega^{'}) \in \Omega, \omega \neq \omega^{'} \tag{2.41}$$

$$X_{j\omega} \in \{0, 1\} \qquad \forall j \in \mathcal{J}, \omega \in \Omega \tag{2.42}$$

Constrraints (2.41), known as *nonanticipativity* constraints, compel the scenario-dependent first-stage variables to take the same values for different scenarios. However, such constraints in the model still hinder the problem from being separable by scenarios. As such, we introduce $\{\bar{X}_j\}_{j\in\mathcal{J}} \in \{0, 1\}$, referred to as *overall design vectors*, and replace constraint (2.41) with the following set of constraints:

$$X_{j\omega} = \bar{X}_j \qquad \forall j \in \mathcal{J}, \omega \in \Omega \tag{2.43}$$

$$\bar{X}_j \in \{0, 1\} \qquad \forall j \in \mathcal{J} \tag{2.44}$$

المنارة للاستشارات

www.manaraa.com

With the introduction of constraints (2.43) and (2.44), problem (2.37) can now be decomposed by scenarios. We adopt the *augmented Lagrangian* strategy, proposed by Rockafellar et al. [79], to obtain the following objective function:

$$\begin{aligned} Minimize \sum_{\omega\in\Omega} \rho_\omega \Bigg(\sum_{j\in\mathcal{J}} s_j X_{j\omega} + \sum_{i\in\mathcal{N}} \sum_{j\in\mathcal{N}} \sum_{e\in\mathcal{E}} c_{ije} d_{ij} V_{ije\omega} + \\ \sum_{j\in\mathcal{J}} \Big(\zeta_{j\omega}(X_{j\omega} - \bar{X}_j) + \frac{1}{2}\kappa(X_{j\omega} - \bar{X}_j)^2 \Big) \Bigg) \end{aligned} \tag{2.45}$$

where $\{\zeta_{j\omega}\}_{\forall j\in\mathcal{J},\omega\in\Omega}$ and κ are known as *Lagrangian multiplier* and *penalty ratio*, respectively. In (2.45), since both $\{X_{j\omega}\}_{j\in\mathcal{J},\omega\in\Omega} \in \{0,1\}$ and $\{\bar{X}_j\}_{j\in\mathcal{J}} \in \{0,1\}$ are binary, we can reduce the quadratic term $\sum_{j\in\mathcal{J}} \kappa(X_{j\omega} - \bar{X}_j)^2$ as follows:

$$\sum_{j\in\mathcal{J}} \kappa(X_{j\omega} - \bar{X}_j)^2 = \sum_{j\in\mathcal{J}} \Big(\kappa(X_{j\omega})^2 - 2\kappa X_{j\omega}\bar{X}_j + \kappa(\bar{X}_j)^2 \Big) \approx \sum_{j\in\mathcal{J}} \Big(\kappa X_{j\omega} - 2\kappa X_{j\omega}\bar{X}_j + \kappa\bar{X}_j \Big)$$

With this simplification, the objective function (2.45) can be re-written as follow:

$$\begin{aligned} Minimize \sum_{\omega\in\Omega} \rho_\omega \Bigg(\sum_{j\in\mathcal{J}} (s_j + \zeta_{j\omega} + \frac{\kappa}{2} - \kappa\bar{X}_j) X_{j\omega} + \\ \sum_{i\in\mathcal{N}} \sum_{j\in\mathcal{N}} \sum_{e\in\mathcal{E}} c_{ije} d_{ij} V_{ije\omega} + \sum_{j\in\mathcal{J}} (\frac{1}{2}\kappa\bar{X}_j - \zeta_{j\omega}\bar{X}_j) \Bigg) \end{aligned} \tag{2.46}$$

Note that when the value of $\{\bar{X}_j\}_{j\in\mathcal{J}}$ is fixed, the last term in (2.46) becomes a constant and can be eliminated from (2.46). With this, (2.46) can be reduced to the following.

$$\textbf{[EV-SAT(PHA)]}\ Minimize \sum_{\omega\in\Omega} \rho_\omega \Bigg(\sum_{j\in\mathcal{J}} \hat{s}_{j\omega} X_{j\omega} + \sum_{i\in\mathcal{N}} \sum_{j\in\mathcal{N}} \sum_{e\in E} c_{ije} d_{ij} V_{ije\omega} \Bigg) \tag{2.47}$$

www.manaraa.com

subject to (2.6)-(2.9), (2.11), (2.13)-(2.24), (2.38)-(2.40), and (2.42). where $\hat{s}_{j\omega} = (s_j + \zeta_{j\omega} + \frac{\kappa}{2} - \kappa\bar{X}_j)$ is the revised installation cost for installing the charging station at location $j \in J$ under scenario $\omega \in \Omega$.

Let $\zeta^r_{j\omega}$ and κ^r, respectively, denote the value of the *lagrangian multipliers* and the *penalty parameters* at iteration r of the PHA. In each iteration of the PHA, $|\Omega|$ deterministic subproblems **[EV-SAT(PHA)]** are solved, and the consensus value for the overall design vectors, $\{\bar{X}_j\}_{j\in\mathcal{J}}$, is calculated. The algorithm continues to find a better solution until some pre-specified conditions are satisfied (shown below). Otherwise, we update the values of $\{\zeta^r_{j\omega}\}$ and κ^r using the following equations:

$$\zeta^r_{j\omega} \longleftarrow \zeta^{r-1}_{j\omega} + \kappa^{r-1}(X^r_{j\omega} - \bar{X}^{r-1}_j) \qquad \forall j \in \mathcal{J}, \omega \in \Omega \tag{2.48}$$

$$\kappa^r \longleftarrow \Delta^p \kappa^{r-1} \tag{2.49}$$

where $\Delta^p > 1$ is a given constant and the values of the parameters $\{\zeta^{r=0}_{j\omega}\}_{\forall j\in\mathcal{J},\omega\in\Omega}$ and $\kappa^{r=0}$ are initially set to zero and a positive number, respectively. Finally, the following criteria are followed to terminate the PHA implementation.

Termination criteria: The PH algorithm terminates upon satisfying one of the following conditions:

- $\sum_{\omega\in\Omega}\rho_\omega\left(\sum_{j\in\mathcal{J}}\left(\frac{|X^r_{j\omega}-\bar{X}^r_j|}{|\mathcal{J}|}\right)\right) \le \epsilon$; where ϵ is a pre-specified tolerance gap
- 10 consecutive non-improvement iterations
- Maximum iteration limit is reached (e.g., $iter^{max} = 50$)

المنارة للاستشارات
www.manaraa.com

- Maximum time limit is reached (e.g., $t^{max} = 36,000$ CPU seconds)

2.4.2 The SIGALNS Heuristic

Having decomposed the original problem **[EV-SAT]** by scenarios, the size of corresponding subproblems decreases considerably. However, the subproblem **[EV-SAT(PHA)]** is still a variant of the classical location-routing problems (LRP) [46] that is already known as an $\mathcal{NP}$-hard problem. The preliminary experiments reveal that solving subproblems **[EVSAT(PHA)]** using `GUROBI` is computationally challenging. To overcome this challenge, we introduce a hybrid heuristic, referred to as SIGALNS heuristic, which is composed of *three* components, namely, the modified Sweep heuristic, the Iterated Greedy, and the Adaptive Large Neighborhood Search algorithm. Below, we first discuss different SIGALNS heuristic components and then outline the overall framework of the SIGALNS heuristic. Note that the subproblems of **[EV-SAT]** can be viewed as a deterministic mixed-integer linear programming model, which are solved for each scenario $\omega \in \Omega$. Therefore, to reduce the notation burden, the following subsection omits ω for any newly introduced sets and parameters.

2.4.2.1 Modified Sweep Heuristic

We first develop a Modified Sweep (MS) heuristic to construct an initial solution for the SIGALNS algorithm. Given this algorithm's purpose is to find an initial routing plan, the battery driving range limitation and charging station locations are ignored in this process. We initially utilize the sweep algorithm, proposed by Gillet and Miller [26], to solve a vehicle routing problem (VRP). The solution of the VRP consists of *two phases*, namely, the *customer clustering* and solving a *traveling salesman problem* (TSP). In the first phase, the customers are sorted in an ascending order based upon their polar coordinate angles from the depot. By obeying the weight capacity

المنارة للاستشارات
www.manaraa.com

of the EVs, starting from the customer with the smallest angle, the customers are inserted in a single cluster. If violated, a new cluster is created for the remaining customers, and the process continues. The procedure terminates when all the customers are assigned in different clusters. For the second phase, a TSP is solved to generate the corresponding routing plans for each of the generated clusters. A pseudo-code of the modified Sweep heuristic is outlined in **Algorithm 1**.

Algorithm 1: Modified Sweep heuristic

```
Input: The longitude and latitude for customers and depot, the vehicle weight capacity, $\delta_e$,
  customer demand, $\gamma_{i\omega}$
Rank customers in the ascending order of polar angles with respect to depot
Create a cluster, $C_l \leftarrow$ , $l \leftarrow 1$
for $i \in I$ do
    if $\gamma_{i\omega} + \sum_{n \in C_l} \gamma_{n\omega} \leq \delta_e$ then
        $C_l \leftarrow C_l \cup \{i\}$
    else
        Start new cluster $C_{l+1} \leftarrow$
        $C_{l+1} \leftarrow C_{l+1} \cup \{i\}$
    end
end
for $C_l \in C$ do
    Solve a TSP on $C_l$ to obtain route $R_l$
end
Output: $Q_0 \leftarrow \cup_{l=1}^{|R|} R_l$
```

2.4.2.2 Iterative Greedy Heuristic for Charging Station Selection

Once the modified sweep heuristic generates an initial routing plan, the *iterative greedy* (IG) heuristic is utilized to allocate a set of charging stations in different routes from the candidate sites. In this section, first, we discuss the allocation cost of the charging stations, followed by the implementation of the IG heuristic to obtain a feasible route.

- ***Allocation Cost Analysis*****:** In the IG procedure, first, we remove all the located charging stations from the current solution and then reallocate them in an attempt to find a better

المنارة للاستشارات
www.manaraa.com

solution. Let $\mathcal{R} = \{r_1, r_2, ..., r_{|R|}\}$ be the routes obtained in the current solution. Charging stations with the least cost increment now needs to be inserted in the current routes to ensure the feasibility of the model. To serve this purpose, below, we provide a set of cost allocation strategies, which is used to select and insert a set of charging stations into the current partial routes.

(a) *Breaking point:* Let $r_l = \{n_o = o, n_1, n_2, ...,, n_m = o^{'}\}(r_l \in \mathcal{R})$ be the list of visited nodes in the l^{th} route of the current solution. We also define $n \in r_l$ to be the *breaking point* if it satisfies the following condition:

$$\{n|D^1_{nl\omega} < 0, n \in r_l\} \tag{2.50}$$

This implies that those nodes are unreachable by an EV $e \in \mathcal{E}$ due to battery capacity limitations. The first *breaking point* in route r_l, represented by $v^* = \{n|D^1_{n^*l\omega} < 0, D^1_{n^{'}l\omega} > 0, \forall n^{'} < n^*, (n^{'}, n^*) \in r_l\}$, signifies that all the nodes before v^* are reachable by EV $e \in \mathcal{E}$.

(b) *Node feasibility state:* In model **[EV-L]**, we introduce $D^1_{nl\omega}$ to be the maximal distance that EV $e \in \mathcal{E}$ could traverse after reaching node $n \in \mathcal{N}$ along the $r_l \in \mathcal{R}$ route. In order to further evaluate the feasibility status of the route r_l and its associated nodes, we define *node feasibility state*, denoted by w_{nl}, as follows:

$$w_{nl} = min\{D^1_{nl\omega}, 0\}, \quad n \in r_l \tag{2.51}$$

المنارة للاستشارات
www.manaraa.com

From (2.51), it could be observed that $w_{nl} \leq 0$. When $w_{nl} < 0$, it indicates that the node is not reachable and the corresponding route is infeasible. On the other hand, when $w_{nl} = 0$, it could be inferred that the node is reachable in route r_l. To summarize, *node feasibility state* represents the additional battery power required to visit node $n \in r_l$ and the necessity to allocate a charging station for recharging the batteries before arriving $n \in r_l$. Additionally, using the *node feasibility states* in route r_l, we compute the *worst node feasibility state* in route r_l as $w^*_l = min_{n \in r_l \setminus \{o\}} w_{nl}$. In each route $r_l \in R$, the smaller the w^*_l is, the worse the solution feasibility becomes.

(c) *Allocation Cost:* Once a candidate charging station $j \in \mathcal{J}$ is selected and inserted at position $\bar{n}$ after node n in route r_l, the allocation cost $f^{\bar{n}}_{jl}$ is used to evaluate the feasibility and improvement of the objective function value. To minimize the allocation cost of the charging station, eliminating more *breaking points* and/or gaining larger improvement among the whole *node feasibility state* is preferred. Let us now define $\bar{n}$ to be an insertion position for a charging station after node n, $g^{\bar{n}}_{j,l}$ be the respective *insertion gain*, $h^{\bar{n}}_{j,l}$ be the respective *insertion loss*, and $b^{\bar{n}}_{j,l}$ be the *extra penalty*. The insertion of a charging station $j \in \mathcal{J}$ at node $\bar{n}$ after node n in route r_l, denoted by $f^{\bar{n}}_{j,l}$, is defined as follows:

$$f^{\bar{n}}_{j,l} = \Phi 1(-g^{\bar{n}}_{j,l}) + \Phi_2 h^{\bar{n}}_{j,l} + \Phi_3 b^{\bar{n}}_{j,l}, \qquad j \in J, n \in r_l, r_l \in R \tag{2.52}$$

المنارة للاستشارات
www.manaraa.com

where

$$\Phi_1 + \Phi_2 + \Phi_3 = 1 \qquad \Phi_1, \Phi_2, \Phi_3 \geq 0$$

$$g^{\bar{n}}_{j,l} = \left(\sum_{n \in r_l \setminus \{o\}} (w^{'}_{nl} - w_{nl}) \right) \left(\frac{1 + |w^*_l|}{1 + |w^{*'}_l|} \right) \tag{2.53}$$

$$h^{\bar{n}}_{j,l} = d_{n_i,\bar{n}} + d_{\bar{n},n_{i+1}} - d_{n_i,n_{i+1}}, \qquad n_i, n_{i+1} \in r_l \tag{2.54}$$

$$b^{\bar{n}}_{j,l} = M|w_{\bar{n}l}| \tag{2.55}$$

where, $g^{\bar{n}}_{j,l}$ measures the improvement regarding the solution of r_l when station j is placed at position $\bar{n}$ after node n, and w_{nl} and w^*_l, respectively, represent the *node feasibility state* and *worst node feasibility state* before inserting the charging station j in route r_l. To obtain the *insertion gain*, we utilize equation (2.53), where the right hand side of the equation computes the total improvement with respect to the *node feasibility state* in route r_l. To obtain the *insertion loss*, we utilize equation (2.54), where n_i and n_{i+1}, respectively, denote the *predecessor* and *successor* of node positioned at $\bar{n}$. Finally, the *extra penalty*, $b^{\bar{n}}_{j,l}$, is calculated via equation (2.55), where M is a user-defined large number which we set to $M = 10^4$ in our experiments. When $w_{\bar{n}l} < 0$, the charging station $j \in \mathcal{J}$ at position $\bar{n}$ is deemed to be unreachable and is penalized via the infeasible insertion operator. Let us now define the a reachable charging station set, $\mathcal{J}^l_n \subset \mathcal{J}$, which is obtained as $\mathcal{J}^l_n = \{j \in \mathcal{J} | D^2_{nl\omega} \geq d_{nj}\}; \forall n \in r_l$. For any charging station in $\mathcal{J}^l_n$, if it is located after node n on route r_l, the extra penalty $b^{\bar{n}}_{j,l}$ is set to zero, i.e., $b^{\bar{n}}_{j,l} \leftarrow 0$.

للاستشارات المنارة

www.manaraa.com

- ***The Iterated Greedy (IG) Heuristic**:* This subsection introduces the IG heuristic, aiming to locate charging stations and maintain or improve feasibility in the routing decisions. First, a set of infeasible routes is identified. When by utilizing the least-cost allocation strategy, the best candidate charging stations with their respective positions are inserted. This process continues until all the routes become feasible. To the end, a *local search heuristic* is utilized to improve the current solution. **Algorithm 2** outlines the pseudo-code of this algorithm.

Algorithm 2: The Iterated Greedy (IG) algorithm

```
Input: Initial solution $Q_0$, and the initial cost of building a charging station $s_0 = \{\hat{s}_{j\omega}\}$
Initialize the cost of building a charging station $f_0$ and set $\Theta \leftarrow 0$
Eliminate all the located stations in the $Q_0$
$Q \leftarrow Q_0$
while $\Theta = 0$ do
    for $r_l \in R$ do
        Compute the worst feasibility state $w_l^*$
        if $q_l^* < 0$ then
            Select and insert the best stations
            Update the node feasibility state in $r_l$
            Update the station construction cost
        end
    end
    if all routes are feasible then
        $\Theta \leftarrow 1$
    end
end
$S \leftarrow$ Apply the local search procedure
Output: $Q$
```

Let Θ to denote the feasibility of the current solution, $s_0 = \{\hat{s}_{j\omega}\}$ to be the initial construction cost of the charging stations, and $\mathcal{R} = \{r_1, ..., r_l, ..., r_R\}$ to be the set of vehicle routes obtained in the initial solution. The IG algorithm assumes that the initial solution for model **[EV-SAT(PHA)]** is infeasible, i.e., $\Theta = 0$. At this point, all the currently located stations in

www.manaraa.com

$r_l \in \mathcal{R}$ are eliminated and the current solution Q is initialized to Q_0. Then, for each of the routes, the feasibility of the routes are evaluated based on the fact that they are not violated the battery driving range and the worst feasibility state w_l^* is determined. If a route $r_l \in \mathcal{R}$ is infeasible, i.e., $w_l^* < 0$, the IG heuristic starts by selecting and locating the charging stations. To select the best possible charging station locations, a segment of nodes $\Pi_l \in r_l$, referred to as *search zone*, is introduced, where all the predecessor nodes of the first *breaking point* until a charging station or depot are added to Π_l. At this point, for each of the nodes in $n \in \Pi_l$, the reachable charging station set $\mathcal{J}_n^l$ is determined, and the corresponding allocation cost $f_{jl}^{\bar{n}}$ is calculated for each station $j \in \mathcal{J}_n^l$. Note that nodes with empty reachable charging stations are discarded from Π_l. To obtain the best possible position to open the charging station, all the nodes in Π_l are sorted in ascending order based on the allocation $(f_{jl}^{\bar{n}})$ and revised construction costs $(\hat{s}_{j\omega})$ and position, indexed by $*\epsilon_1^{\rho_1} \times |\Pi_l|$, after node n is selected, where $0 \leq \epsilon_1 \leq 1$ is a random number and $\rho_1 \geq 1$ is a parameter to capture the randomness in the procedure (e.g., set to 10 in our implementation). Likewise, to position the best charging station location in $\mathcal{J}_n^l$, first set $\mathcal{J}_n^l$ is sorted in ascending order based on the allocation and construction costs, and position, indexed by $*\epsilon_1^{\rho_2} \times |J_n^l|$, after node n is selected, where $0 \leq \epsilon_2 \leq 1$ is a random number and $\rho_2 \geq 1$ is a parameter to capture the randomness in the procedure (e.g., set to 10 in our implementation). Following the placement of the stations $\bar{j}$ at position $\bar{n}$, the feasibility state of nodes in r_l are updated.

The iterations continue and the current solution is updated till all the respective routes become feasible (i.e., conforming the battery driving range of the EVs). At this point, a *local heuristic* is employed in an attempt to improve the solution quality of the current solution.

المنارة للاستشارات
www.manaraa.com

The local heuristic utilizes two neighborhood search operators, namely, the *EXCHANGE* and the *MOVE* operators. By utilizing the *EXCHANGE* operator, an opened charging station is replaced by another opened charging station. On the other hand, by utilizing the *MOVE* operator, an opened charging station is replaced by an unopened charging station. The procedure continues till a new feasible location with an improved objective function is found. As discussed earlier, the IG procedure first removes all the opened charging stations. Therefore, the selection of the new charging stations is strongly contingent upon the obtained vehicle routes. Further, the routes, obtained by the adaptive large neighborhood search (ALNS) heuristic (discussed in Section 2.4.2.3), is strongly affected by the opened charging station locations. With this, the proposed SIGALNS procedure exchanges information iteratively between the locating and routing phases in an attempt to improve the solution quality.

2.4.2.3 Adaptive Large Neighborhood Search (ALNS) Heuristic for EV Routing

The ALNS algorithm, proposed by Ropke and Pisinger [80], utilizes a set of insertion and removal operators by observing their historical successes to construct a new solution in the large neighborhood in an attempt to improve the solution quality. Below, we outline the steps involved in the ALNS algorithm.

- **Overall framework**: The overall framework of the ALNS algorithm consists of several major steps: creation of the *large neighborhood*, developing problem-specific *removal and insertion operators*, utilizing the *adaptive search mechanism*, *penalizing the objective function*, and obeying the *acceptance and termination criteria* [45].

المنارة للاستشارات
www.manaraa.com

In each iteration of the ALNS algorithm, first, n_r number of costumers are removed from the current solution (using a removal operator) and are added to a request bank. The n_r customers are selected randomly from the interval $[\vartheta_1 \times |\mathcal{I}|, \vartheta_2 \times |\mathcal{I}|]$, where $\vartheta_1, \vartheta_2 \in (0, 1)$ and $|\mathcal{I}|$ denotes the number of the customers. Theses removed customers are then reinserted into the routes by using an insertion operator. Note that a set of removal and insertion operators are defined at priory to perform the removal and insertion operations. An *adaptive search mechanism* is utilized that adaptively select the removal-insertion operators and adjust the operators' weight. The search process of the ALNS algorithm is divided into a set of *segments*, where each segment consists of v (e.g., $v = 50$) number of iterations. Within each iteration of the ALNS algorithm, a *roulette-wheel* mechanism is utilized to choose the respective removal and insertion operators. Let η_{ij} denotes the weight of operator i at segment j, which is selected with a probability of $p_{ij} = \eta_{ij}/\sum_{h \in \mathbf{H}} \eta_{hj}$, where $\mathbf{H}$ denotes the list of either removal or insertion operators and $\sum_{h \in \mathbf{H}} \eta_{h,j}$ represents the total weight of the respective operators at segment j. The initial weights of the operators $h \in \mathbf{H}$ are set to a small number (e.g., 10), which is then updated at the end of each segment as follows: if $\varphi_{ij} > 0$, $\eta_{i,j+1} = (1 - \chi)\eta_{ij} + \chi\tau_{ij}/\varphi_{ij}$; otherwise, $\eta_{i,j+1} = \eta_{ij}$, where $0 \leq \chi \leq 1$, referred to as a *reaction factor*, is a deterministic parameter (e.g., 0.3 in our implementation), and φ_{ij} and τ_{ij} represent the number of times the operator i has been selected at segment j, and the score of the operator i at segment j, respectively. Finally, the score τ_{ij}, initialized with zero, is enhanced by Δ_{ij} using the historical performance of the operator i at each iteration of segment j. For instance, Δ_{ij} could be increased by 50, 20, and 10, if a new best-known solution is found, the current solution improves, and the new solution is not improved but it

www.manaraa.com

can be accepted based on the feasibility conditions, respectively. Finally, using a *penalized objective function*, the objective function is penalized if the battery driving range of the EVs is violated.

$$O_{penalized} = \sum_{j \in J} \hat{s}_{j\omega} X_{j\omega} + \sum_{i \in N} \sum_{j \in N} \sum_{e \in E} c_{ije} d_{ij} V_{ije\omega} - M \sum_{l \in R} \sum_{n \in r_l} w_{nl} \tag{2.56}$$

where M is a user-defined big number (e.g., 10^4) and $w_{nl} \leq 0$ is the *node feasibility state* (introduced earlier). To define the *acceptance and termination criteria* of the ALNS algorithm, we follow the Simulated Annealing (SA) criterion as introduced by Adulyasak et al. [2]. Though a new better solution will always be accepted, a worse solution could also be accepted with a probability of $e^{(O(Q^{'})-O(Q))/T}$, where Q, $Q^{'}$, and T represent, respectively, the current solution, new solution, and current temperature of the SA. The temperature is first initialized (e.g., 10,000 in our study) and then updated as follows: $T_v = \Lambda T_{v-1}$, where Λ is the cooling rate of the SA method, which is set to 0.995 in our implementation. The overall ALNS algorithm terminates if one of the following criterion is satisfied: (i) maximum iteration limit (ITR^{ALNS}) or (ii) the maximum time limit ($TIME^{ALNS}$) is reached. Let Q_0, Q, $Q^{'}$, and Q^{*} to represent the initial, current, neighborhood, and the best-known solution, respectively. The outline of the overall ALNS algorithm is presented in **Algorithm 3**.

- **Removal operators:** We now discuss the removal operators that are utilized in this study.
  - *Random removal:* This operator randomly selects n_r customers from the current solution and adds them to the request bank.

المنارة للاستشارات
www.manaraa.com

Algorithm 3: Adaptive Large Neighborhood Search (ALNS) Algorithm

```
Input: Initial solution $Q_0$
$Q \leftarrow Q_0, Q^* \leftarrow Q_0$
$iter \leftarrow 1$
while $iter < ITR^{ALNS}$ do
    Select a pair of removal and insertion operators
    $Q^{'} \leftarrow Q$
    Apply the removal operator to $Q^{'}$
    Apply the insertion operator to $Q^{'}$
    if the acceptance is satisfied then
        $Q \leftarrow Q^{'}$
    end
    if $O(Q) < O(Q^*)$ then
        $Q^* \leftarrow Q$
    end
    Update the score and weight of each operatore
    $iter \leftarrow iter + 1$
end
Output:
        The best-known solution: $Q^*$
```

– *Basic worst removal:* To utilize this operator, first, we calculate the *removal gain* for each customer n, which can be obtained by finding the difference in the objective function value between the presence and absence of that respective customer, i.e., $(O(Q) - O_{-n}(Q))$ [30]. Since removal of the customer only affects the routing decisions (not the location decisions), the removal gain can be calculated as follows: $O(Q) - O_{-n}(Q) := d_{n-1,n} + d_{n,n+1} - d_{n-1,n+1}$, where $n-1$ and $n+1$ are the *predecessor* and *successor* nodes of customer n, respectively. Next, the customers are sorted based on the removal gain in descending order, and the customer indexed by $*\epsilon_3^{\rho_w} \times |\mathcal{I}|$, is eliminated from the respective route and added to the request bank, where, $0 \leq \epsilon_3 \leq 1$ is a random number, ρ_w is a pre-defined constant number, and $|\mathcal{I}|$ defines the total number of the customers in the current solution.

المنارة للاستشارات
www.manaraa.com

- *Related removal:* This operator, proposed by Shaw [83], removes the customers based on their similarity. First, an initial seed customer n is randomly chosen from the current solution. Then, the similarity between the seed customer n with other customers $n^{'}$ is calculated as follows: $m(n, n^{'}) := \zeta_1 d_{n,n'} + \zeta_2|\gamma_{n\omega} - \gamma_{n'\omega}| + \varsigma_{n,n'}$, where ζ_1 and ζ_2 are weights chosen from interval $(0, 1)$ and $\zeta_1 + \zeta_2 = 1$, and the term $|\gamma_{n\omega} - \gamma_{n'\omega}|$ denotes the difference in customer demands (absolute) between customer n and $n^{'}$. Finally, the last term of the equation, $\varsigma_{n,n'}$, is set to 1 if the two customers are on the same route; 0 otherwise. As can be seen, the smaller the value of $m(n, n^{'})$ is, the more similar customer n and $n^{'}$ becomes. We can now sort the customers in a descending order, and the customers, indexed by $*\epsilon_4^{\rho_r} \times |\mathcal{I}|$, are eliminated from the respective route and added to the request bank, where $0 \leq \epsilon_4 \leq 1$ is a random number, ρ_r is a pre-defined constant number, and $|\mathcal{I}|$ denotes the total number of customers in the current solution.

- *Advanced worst removal:* If a customer is removed from a route, it may result reducing the traveling distance and improving the feasibility of the solution. Thus, this operator calculates the *removal gain* for costumers, while simultaneously improves the feasibility state of the nodes as $O(Q) - O_{-n}(Q) := \alpha_1(d_{n-1,n} + d_{n,n+1} - d_{n-1,n+1}) + \alpha_2(\sum_{l\in R}\sum_{n\in r_l} w_{n,l} - \sum_{l\in R}\sum_{n\in r_l} w^{'}_{n,l})$, where $\alpha_1 + \alpha_2 = 1$, and $w_{n,l}$ and $w^{'}_{n,l}$, respectively, denote feasibility state of the nodes before and after the removal. Followingly, the customers are sorted based on the removal gain in descending order, and the customer indexed by $*\epsilon_3^{\rho_w} \times |\mathcal{I}|$, is eliminated from the respective route and added to the request bank.

المنارة للاستشارات
www.manaraa.com

  - *Station-based removal:* This operator first randomly chooses one of the opened charging station (as can be obtained from the current solution). Next, all the customers, connected to the selected station, are removed from the respective routes until n_c number of customers are removed. Readers are encouraged to review [98] for understanding the details about this operator.

  - *Single point removal:* Before introducing this operator, let us first define the concept of *service zone* of a charging station. Essentially, the partial routes between two nodes (e.g., charging stations, charging station and depot or the copy of the depot) are called the *service zone* of a charging station [98]. The main idea of this operator is to destroy the *service zone* of a node while maintaining feasibility of the newly constructed routing paths. The first step of this operator is randomly select a route, where at least one charging station is located. Afterward, one of the positions in the *service zone* of the respective route is randomly selected. Finally, the customers between the selected position and the respective charging station (or depot or the copy of the depot) are removed from the selected route.

- **Insertion operators:** By utilizing the removal operators, a set of customers could be removed from the existing solution of the current routes and added to the request bank. Then, a number of insertion operators, as discussed below, are utilized to reinsert all the customers in an attempt to improve the current solution.

  - *Basic greedy insertion:* This operator aims at inserting the removed customers from the request bank (R_b) into the current solution in such a way that the insertion leads

المنارة للاستشارات

www.manaraa.com

to the least objective function value increment. Let $\Delta O_{n,l} = O_{n,l} - O_{n-,l} = d_{n-1,n} + d_{n,n+1} - d_{n-1,n+1}$ to denote the increment in the cost after inserting node n in route r_l at its best inserting position. The inserted customer n^* can be determined as follows: $n^* = argmin_{n \in R_b}\{min_{r_l \in R}\Delta O_{n,l}\}$.

- *Basic regret-k insertion:* This operator reinsert the removed customers based on the largest regret values among the inserted positions [80]. For costumer $n \in \mathcal{R}_b$, let $\Delta O_{n,j}$ be the increment in the objective function value due to inserting n into j^{th} best route in its best position. Note that the increment in the objective function value could be calculated using the *Basic greedy insertion* operator. Using this operator, customer n^* could be selected as follows: $n^* = argmax_{n \in \mathcal{R}_b}\{\sum_{j=2}^{k}(\Delta O_{n,j} - \Delta O_{n,1})\}$, where $\Delta O_{n,1}$ denote the change in the cost after adding customer n into the best respective route. In our study, two cases of *Basic regret-k insertion* operator, namely, the *Basic regret-2 insertion* and the *Basic regret-3 insertion*, are implemented.

- *Advanced greedy insertion:* Note that the *Basic greedy insertion* only utilized the difference due to the traveling distance, i.e., $d_{n-1,n} + d_{n,n+1} - d_{n-1,n+1}$, to calculate the change in the objective function value. However, due to the limitations on battery driving range and weight capacity, the insertion of a customer in a given route could affect the feasibility of the current solution. As such, equation (2.57) is utilized

المنارة للاستشارات
www.manaraa.com

to compute the increment in the objective function value due to inserting customer $n \in \mathcal{R}_b$ in it's best position at route r_l, as shown below.

$$\Delta O^{new} = \alpha_3(d_{n-1,n} + d_{n,n+1} - d_{n-1,n+1}) + \alpha_4(\sum_{l \in L} \sum_{n \in r_l} w_{n,l} - \sum_{l \in L} \sum_{n \in r_l} w^{'}_{n,l})$$
$$+max\left\{ \left(\sum_{n \in r_l} \gamma_{n\omega} - \delta_l \right), 0 \right\} \times M \tag{2.57}$$

where, $\alpha_3 + \alpha_4 = 1$, and $w_{n,l}$ and $w^{'}_{n,l}$, respectively, denote the node feasibility states before and after the insertion. Using (2.57), this operator constructs new routes such that they satisfy the battery driving range limitation and the vehicle capacity constraints.

- *Advanced regret-k insertion:* The *Basic regret-k insertion* also utilizes the same equation (2.49), as used by the *Advanced regret-k insertion* operator, by replacing ΔO^{new} term with $\Delta O_{n,j}$, i.e., $\Delta O_{n,j} = \Delta O^{new}$, to calculate the regret values for this operator. Note that the two variants of the *Advanced regret-k insertion*, namely, the *Advanced regret-2 insertion* and the *Advanced regret-3 insertion*, are utilized as insertion operators in this study.

2.4.2.4 Algorithmic Framework of the hybrid Algorithm

In this section, first, we describe the algorithmic framework of the SIGALNS algorithm that is used to solve subproblem **[EV-SAT(PHA)]**, and then we outline the overall framework of the proposed hybrid decomposition algorithm to solve model **[EV-SAT]**.

The SIGALNS algorithm consists of three phases: *initialization*, *location*, and *routing* phases. Once the initialization phase is completed, the location and routing phases are implemented successively to generate the best-known solution for the model **[EV-SAT(PHA)]**. A pseudocode of

المنارة للاستشارات
www.manaraa.com

the SIGALNS algorithm is presented in **Algorithm 4**. The algorithm starts by generating an initial solution, Q_0, using the modified sweep algorithm. This initial solution is passed to the location and routing phases and the current solution, Q, and the best-known solution, Q^*, are fixed to Q_0 and the weights of the ALNS operators are initialized. At the beginning of each iteration of the SIGALNS algorithm, the opened charging station locations are eliminated from the current solution and then the location and routing subproblems are solved successively within the ALNS algorithm. Recall that the ALNS algorithm selects the newly constructed routes using the acceptance criterion provided by the Simulated Annealing (SA) algorithm. The entire SIGALNS algorithm procedure is continued until one of the two termination criterion are satisfied: (i) reaching the maximum iteration limit ($ITR^{SIGALNS}$) or (ii) reaching the maximum time limit.

Algorithm 4: The Framework of SIGALNS algorithm

```
Input: The distance between all the nodes $d_{nn'}$, $\forall(n, n') \in N$, customers' demand $\gamma_{i\omega}$,
the wight capacity of EVs $\delta_e$, $\forall e \in E$, battery driving range of EVs $s\hat{o}c^{\omega}(c, t)\theta$, where $c$ is
  charging time and $t$ is the ambient temperature
Implement modified sweep algorithm to obtain a initial solution $Q_0$
$Q \leftarrow Q_0, Q^* \leftarrow Q_0$
Starting the initial value of the removal and insertion operators for the ALNS algorithm
$iter \leftarrow 1$
while $iter < ITR^{SIGALNS}$ do
    $Q' \leftarrow Q$
    Remove all the located charging stations from $Q'$
    Apply the iterated greedy algorithm to $Q'$ to find out the updated located charging stations
    Apply the ALNS algorithm to $Q'$ to update the routing plans
    if the acceptance criterion is satisfied then
        $Q \leftarrow Q'$
    end
    if $O(Q) < O(Q^*)$ then
        $Q^* \leftarrow Q$
    end
    $iter \leftarrow iter + 1$
end
Output:
        The best-known solution for scenario $\omega$: $Q^*_\omega$
```

المنارة للاستشارات
www.manaraa.com

Algorithm 5 outlines the pseudo-code of the proposed hybrid algorithm.

Algorithm 5: Hybrid Algorithm

```
**Input**: $r \leftarrow 1, \epsilon, \{\zeta^{r}_{j\omega}\}_{j\in\mathcal{J},\omega in\Omega} \leftarrow 0, \kappa^{r} \leftarrow \kappa^{0}$, *terminate* $\leftarrow$ false
**while** *terminate = false* **do**
    **for** $\omega = 1$ *to* $|\Omega|$ **do**
        Solve the respective **[EV-SAT(PHA)]** using the SIGALNS algorithm (**Algorithm 4**) and
          obtain $\{X^{r}_{j\omega}\}_{j\in\mathcal{J}}$
        Calculate the consensus parameter: $\bar{X}^{r}_{j} \leftarrow \sum_{\omega=1}^{|\Omega|} \rho_{\omega} X^{r}_{j\omega}; \forall j \in \mathcal{J}$
    **end**
    **if** $(r > 1)$ **then**
        Update the largangian parameter: $\zeta^{r}_{j\omega} \longleftarrow \zeta^{r-1}_{j\omega} + \kappa^{r-1}(X^{r}_{j\omega} - \bar{X}^{r-1}_{j}); \forall j \in \mathcal{J}, \omega \in \Omega$
        Update the penalty parameter: $\kappa^{r} \longleftarrow \Delta^{p} \kappa^{r-1}$
    **end**
    **if** *the acceptance criterion is satisfied* **then**
        *terminate* $\leftarrow$ **true**
    **else**
        $r \leftarrow r + 1$
    **end**
**end**
**Output**:
        The best-known solution for location and routing decisions
```

2.4.3 Implementing Parallel Processing Techniques

As discussed in Section 2.4.1, in each iteration of the PHA algorithm, $|\Omega|$ number of individual scenario-specific subproblems are solved. Even though we employ a heuristic method, referred to as SIGALNS heuristic, to solve the location-routing subproblems, the overall algorithm may still find it difficult to solve realistic size problem instances of **[EV-SAT]** in a reasonable timeframe. In this sub-section, we develop a *synchronous master-slave* implementation for the proposed hybrid algorithm. The aim of this enhancement is to exploit the *multiprocessing* capabilities of the local computers and reduce the computational time in solving each iteration of the PHA algorithm. Note

المنارة للاستشارات
www.manaraa.com

that the parallel execution of the hybrid algorithm does not impact the quality of the PHA solutions, as the search process adheres to the same dynamics as in the sequential case.

In this implementation, the master is in charge of initializing and updating the Lagrangian and penalty parameters for the PHA. Then, it follows by allocating the scenario-specific subproblems, i.e., **[EV-SAT(PHA)]**, to the slaves. The slaves proceed by solving the respective subproblems using the SIGALNS algorithm. Once all the subproblems are solved by the slaves, the master collects the local information from the slaves and calculates the new overall solution. Then, if the termination criteria are not satisfied, the master updates the value of the penalty parameters and starts the next iteration; otherwise, the master terminates the implementation. The duties of the master and slave are summarized below.

Master:

- Creates a pool of the PHA subproblems
- Assigns each slave an equal number of PHA subproblems
- Check the load of slaves and adjusts the assignments
- Calculate the overall solution and update the penalty parameters

Slave:

- Solves the scenario-specific subproblems using the SIGALNS algorithm
- Store the optimal solution of the subproblems in a pool accessible by the master

2.5 Computational Study

This section first describes the data used in the proposed model formulation. Next, the computational performance of the solution approaches is discussed. Finally, an illustrative case study is

المنارة للاستشارات
www.manaraa.com

presented using Fargo, North Dakota (ND), as a testing ground. All numerical experiments are coded in Python 2.7 on a desktop computer equipped with an Intel Core i7 processor 3.60 GHz and a 32 GB RAM. The optimization solver used is GUROBI Optimizer 9.0.

2.5.1 Data description and parameter settings

We assume that a depot is located in the center of the test region (see Figure 2.2(a)). Then, by observing the different neighbors' population densities (>10,000 people) within 200 miles squared distance from the depot location, 25 customer locations are selected, as shown in Figure 2.2(a). Likewise, 50 potential charging station locations are selected by using the same selection criteria but for a population density of more than 5,000 (see Figure 2.2(b)). To calculate the distance and time between each origin-destination pair, we utilize a *google* tool, *Distance Matrix API*[1]. Our model uses *Tesla Model 3 Long Range* EV as a test case, which can travel up to $d_{max} = 322$ miles with a weight carrying capacity of δ_e =417 kg[2]. The weight of the customer demands ($\gamma_{i\omega}$) is generated randomly using a normal distribution with a mean of 60 and a standard deviation of 10. The fixed installation cost of a single port DCFC is set to be \$2,500, which is amortized over 10 years [84]. The unit distance cost is set to be $c_{ije} = \$1$.

After running several preliminary experiments, the following parameters are set for the ALNS and SIGALNS algorithms. For the SIGALNS algorithm, the following parameters are set as follows: $\Phi_1 = 0.07$, $\Phi_2 = 0.92$, and $\Phi_2 = 0.01$. We initialized different parameters of the ALNS algorithm as follows: $\vartheta_1 = 0.1$, $\vartheta_2 = 0.3$, $\rho_w = \rho_r = 10$, $\zeta_1 = 0.6$, $\zeta_2 = 0.4$, $\alpha_1 = \alpha_3 = 0.9$ and $\alpha_2 = \alpha_4 = 0.1$. Finally, for the ALNS and SIGALNS algorithms, the maximum number of iterations is fixed to 50 and 200, respectively.

[1] Available from: https://developers.google.com/maps/documentation/distance-matrix/start

[2] Available from: https://www.tesla.com/model3

المنارة للاستشارات
www.manaraa.com

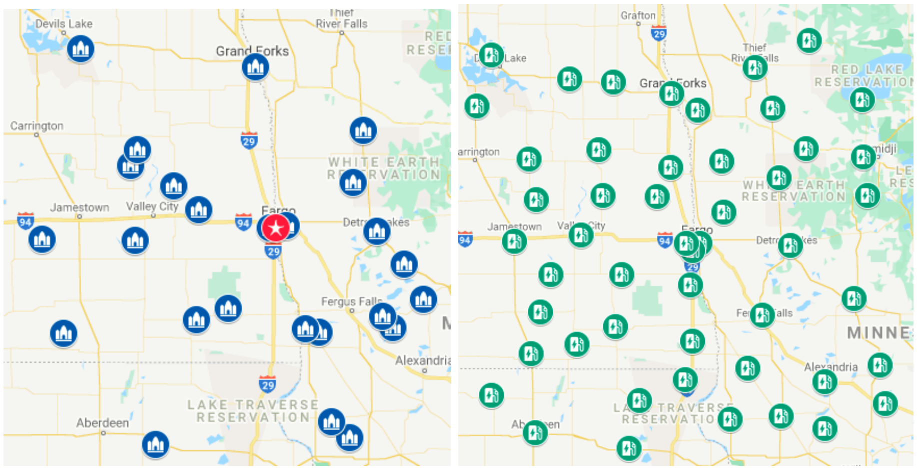

(a) Location of customers and depot (b) Potential location of the charging stations

Figure 2.2

Illustration of the dataset

2.5.2 Computational performance of the proposed algorithms

This section evaluates the computational performance of the proposed solution techniques in solving the model **[EV-SAT]**. To do so, we vary the number of customers, $|\mathcal{I}|$, and EVs, $|\mathcal{E}|$, to generate 5 different problem instances. Table 2.1 shows the number of variables and constraints associated with each test instance. For all these instances, the size of the potential charging station locations, $|\mathcal{J}|$, is set to be 50. In the following, the computational performance of the proposed solution techniques under these generated test instances is discussed.

First, we aim to explore `GUROBI` solver's performance in solving model **[EV-SAT]**. Note that we incorporated the variable fixing techniques and valid inequalities discussed in subsection 2.3.1 in reporting the solver performance. All the solution approaches introduced in this subsection are tested under three different temperatures: -10^oC, 10^oC, and 30^oC. Table 2.2 reports how the computational performance of the `GUROBI` and `PHA-SIGALNS` algorithm are varied under different

المنارة للاستشارات
www.manaraa.com

Table 2.1

Test instances for model **[EV-SAT]**

Instance	$\lvert\mathcal{I}\rvert$	$\lvert\mathcal{E}\rvert$	Variables			Total Constraints
			Binary	Continous	Total	
S1	5	1	3,242	171	3,413	9,518
S2	10	2	7,614	372	7,986	22,496
S3	15	3	10,079	593	10,672	35,831
S4	20	4	20,498	864	21,362	60,782
S5	25	5	29,310	1,155	30,465	86,990

temperature and test instances. The columns heading under $gap_1(\%)$ and $T_1(s)$ represent the optimality gap and solution time of `GUROBI`, respectively. Similarly, columns heading under $gap_2(\%)$, $T_2(s)$, and r_2 represent the solution gap[3], solution time, and number of iterations of the `PHA-SIGALNS` algorithm. In running the experiments, the optimality gap and time limit for `GUROBI` are set to 5% and 36,000 seconds, respectively. As shown in Table 2.2, the `GUROBI` solver is able to solve 10/15 instances by obeying the prespecified termination criterion. However, the average running time of the solver is considerably high, given the size of the test instances. As such, efficient solution methods are needed to provide quality solutions in a reasonable time.

We now evaluate the performance of the hybrid algorithm, referred to as the `PHA-SIGALNS` algorithm, in solving the instances of model **[EV-SAT]** under varying temperatures (see results in Table 2.2 for the performance of the algorithms under $-10\circ C$, $10\circ C$, and $30\circ C$ temperatures). It is worth mentioning that we run each test instance *five* times to obtain the best feasible solution and running time reported in Table 2.2. The corresponding results indicate that the proposed hybrid algorithm can find quality solutions, with an optimality gap of 1.1%, 2.2%, and 3.0% for the test instances, when the temperature is -10^oC, 10^oC, and 30^oC, respectively. Besides, the

[3] obtained by using this formula: $\frac{|Sol_{PHA\text{-}SIGALNS}-LB_{GUROBI}|}{LB_{GUROBI}}(\%)$, where $Sol_{PHA-SIGALNS}$ is the solution obtained by the `PHA-SIGALNS` algorithm and LB_{GUROBI} is the lower bound obtained by the `GUROBI` solver

المنارة للاستشارات
www.manaraa.com

PHA-SIGALNS algorithm can obtain such quality solutions in 5.3, 7.3, and 8.6 times faster than the GUROBI solver, when the temperature is -10^oC, 10^oC, and 30^oC, respectively.

Table 2.2

Performance of GUROBI and PHA-SIGALNS algorithm under different temperatures

		Gurobi		PHA-SIGALNS		
Temperature	*Instance*	$gap_1(\%)$	$T_1(s)$	$gap_2(\%)$	$T_2(s)$	r_1
-10$\circ C$	S1	2.3	**545.1**	1.1	2,310.6	6
	S2	2.7	3,843.3	1.5	**2,692.5**	7
	S3	4.9	26,965.2	0.9	**2,755.4**	9
	S4	4.9	32,659.9	1.6	**3,092.8**	6
	S5	6.1	36,000.0	0.6	**7,844.1**	12
	Average	4.2	20,002.7	1.1	**3,739.1**	8
10$\circ C$	S1	0.4	**387.8**	4.2	1,462.2	5
	S2	0.7	2,946.2	1.9	**1,844.5**	6
	S3	3.8	24,795.1	0.3	**2,973.1**	8
	S4	5.6	36,000.0	1.3	**2,584.2**	7
	S5	6.1	36,000.0	3.1	**4,849.2**	9
	Average	3.3	20,025.7	2.2	**2,742.6**	7
30$\circ C$	S1	1.2	**100.1**	3.0	899.3	3
	S2	0.7	**447.3**	4.8	1,320.5	5
	S3	4.5	20,224.2	3.4	**1,841.2**	5
	S4	4.9	36,000.0	2.2	**2,779.8**	7
	S5	5.9	36,000.0	1.8	**3,934.6**	8
	Average	3.4	18,554.3	3.0	**2,155.1**	5.6

To demonstrate the computation superiority of the parallelized hybrid algorithm, referred to as PHA-SIGALNS-Pl, over the basic hybrid algorithm PHA-SIGALNS, we further experiment with temperatures -10^oC, 10^oC, and 30^oC, as shown in Table 2.3. Note that the column headings $gap_3(\%)$, $T_3(s)$, and r_2 for the PHA-SIGALNS-Pl algorithm in this table represent the same definitions as provided by the PHA-SIGALNS algorithm in Table 2.2. As can be observed in Table 2.3, on average, the parallelized algorithm PHA-SIGALNS-Pl successfully reduced the computational time of the PHA-SIGALNS algorithm while maintaining a competitive solution quality. More specifically, such quality solutions in the PHA-SIGALNS-Pl algorithm are achieved

www.manaraa.com

in 2.6, 2.3, and 2.5 times faster than the `PHA-SIGALNS` algorithm. Overall, the `PHA-SIGALNS-Pl` algorithm consistently provides high-quality feasible solutions in a reasonable timeframe within our experimental ranges.

Table 2.3

Performance of PHA-SIGALNS and PHA-SIGALNS-Pl when temperature under different temperatures

		PHA-SIGALNS			PHA-SIGALNS-Pl		
Temperature	*Instance*	$gap_2(\%)$	$T_2(s)$	r_1	$gap_3(\%)$	$T_3(s)$	r_2
-10$\circ C$	s1	1.1	2,310.6	6	0.6	**653.8**	5
	s2	1.5	2,692.5	7	0.5	**1,008.5**	7
	s3	0.9	2,755.4	9	1.5	**1,217.2**	8
	s4	1.6	3,092.8	6	1.2	**1,524.3**	7
	s5	0.6	7,844.1	12.0	0.7	**2,706.1**	11
	Average	1.1	3,739.1	8.0	0.9	**1,422.0**	7.6
10$\circ C$	S1	4.2	1,462.2	5	3.6	**481.8**	4
	S2	1.9	1,844.5	6	2.1	**837.2**	6
	S3	0.3	2,973.1	8	1.8	**1,048.6**	7
	S4	1.3	2,584.2	7	2.9	**1,283.8**	6
	S5	3.1	4,849.2	9	3.8	**2,234.1**	10
	Average	2.2	2,742.6	7.0	2.8	**1,177.1**	6.6
30$\circ C$	S1	3.0	899.3	3	0.6	**331.4**	3
	S2	4.8	1,320.5	5	4.4	**647.7**	5
	S3	3.4	1,841.2	5	3.4	**654.2**	5
	S4	2.2	2,779.8	7	2.2	**1,040.4**	6
	S5	1.8	3,934.6	8	1.3	**1,493.8**	7
	Average	3.0	2,155.1	5.6	2.4	**833.5**	5.2

2.5.3 Sensitivity Analysis

This subsection performs a set of sensitivity analyses to assess the model performance and to draw managerial insights for the respective policymakers. To perform these experiments, the largest instance, namely, $S5$ (25 customers) from Table 2.1, is used. In all the experiments, we study the impact of ambient temperature along with other impacting factors such as charging time, initial

www.manaraa.com

SOC, the variability of SOC estimation parameters and mean value of the demand on the overall system performance. The key lessons learned from the experiments are summarized below.

- Figure 2.3 denotes the impact of ambient temperature and charging time on EV DCFC charging station location decisions and the overall system cost. For instance, when the charging time of the EVs is set to its base value (75 minutes) and the ambient temperature decreases from $10 \circ C$ (base ambient temperature) to $-10 \circ C$, the selection of the charging stations and the overall system cost increases by approximately 25%, and 24.2%, respectively. Figure 2.4 visualizes the EV DCFC charging station location decisions under different ambient temperatures. Likewise, if the ambient temperature remains fixed, but the charging time decreases, then more EV charging stations are getting selected. For instance, when the ambient temperature is set to its base value ($10 \circ C$) and the charging time of EVs increases from 75 minutes (base value) to 100 minutes, the selection of the charging stations decreases by approximately 20%, and 19.1%, respectively. The results clearly indicate that the EV DCFC charging station location decisions are highly sensitive to the ambient temperature and charging time.

- Figure 2.5 shows the impact of ambient temperature and the initial state of charge of EVs (soc_0) on the DCFC charging station selection decisions and the overall system cost. To run the experiments, we vary the ambient temperature between $-10 \circ C$ and $30 \circ C$ and soc_0 between 100 and 200 miles while keeping the recharging time fixed at 75 minutes (base value). The results in Figure 2.5 indicate that the EV DCFC charging station location decisions along with overall system cost are highly sensitive to both the ambient temperature

المنارة للاستشارات

www.manaraa.com

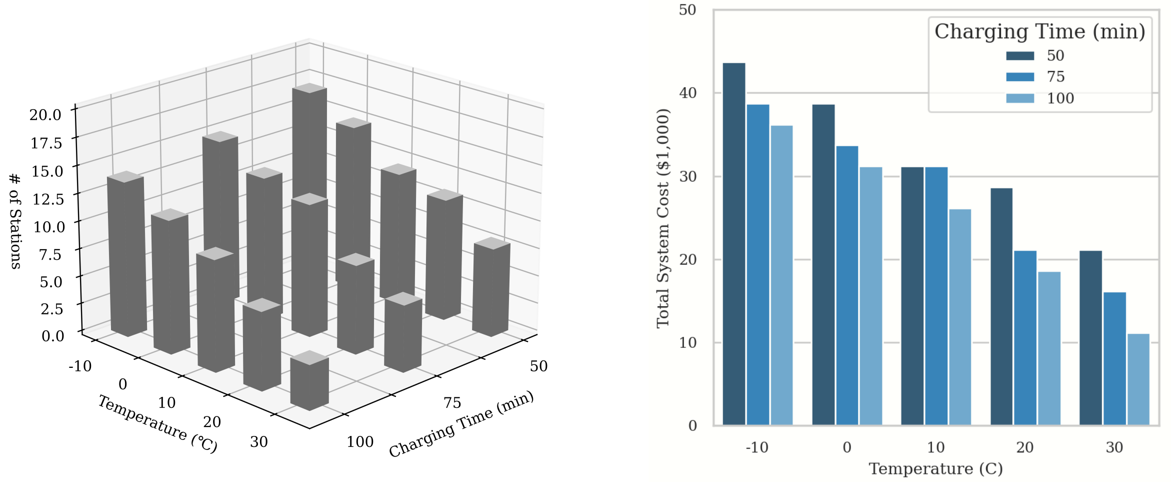

(a) Change in Station Selection

(b) Change in System Cost

Figure 2.3

Impact of temperature and charging time on EV DCFC charging station selection and system cost

and soc_0. For instance, when the ambient temperature is $10\circ C$ and the soc_0 decreases from 200 miles to 100 miles, the number of located EV DCFC charging stations and the overall system cost increases by approximately 62.5%, and 59.3%, respectively.

- The next experiments evaluate the impact of variations of SOC estimation parameters, namely, μ_1 and μ_2, as well as ambient temperature on the DCFC charging station selection decisions and the overall system cost (see Figure 2.6). At the same time, the soc_0 and charging time of EVs are fixed to their base values. Given the estimated values of λ_1, λ_2, and λ_3, to generate the base value of scenario-specific values of μ_1 and μ_2 (ambient temperature is fixed to $10\circ C$) [65], we utilize random distribution with a mean equal to 0.192 and 0.675, respectively, and variance equal to 40% of the respective mean. Note that for experiments referred to as *low* and *high* variability, the respective variance value is changed by 10% and 70% from their respective means. This experiment indicates that both the DCFC charging

المنارة للاستشارات
www.manaraa.com

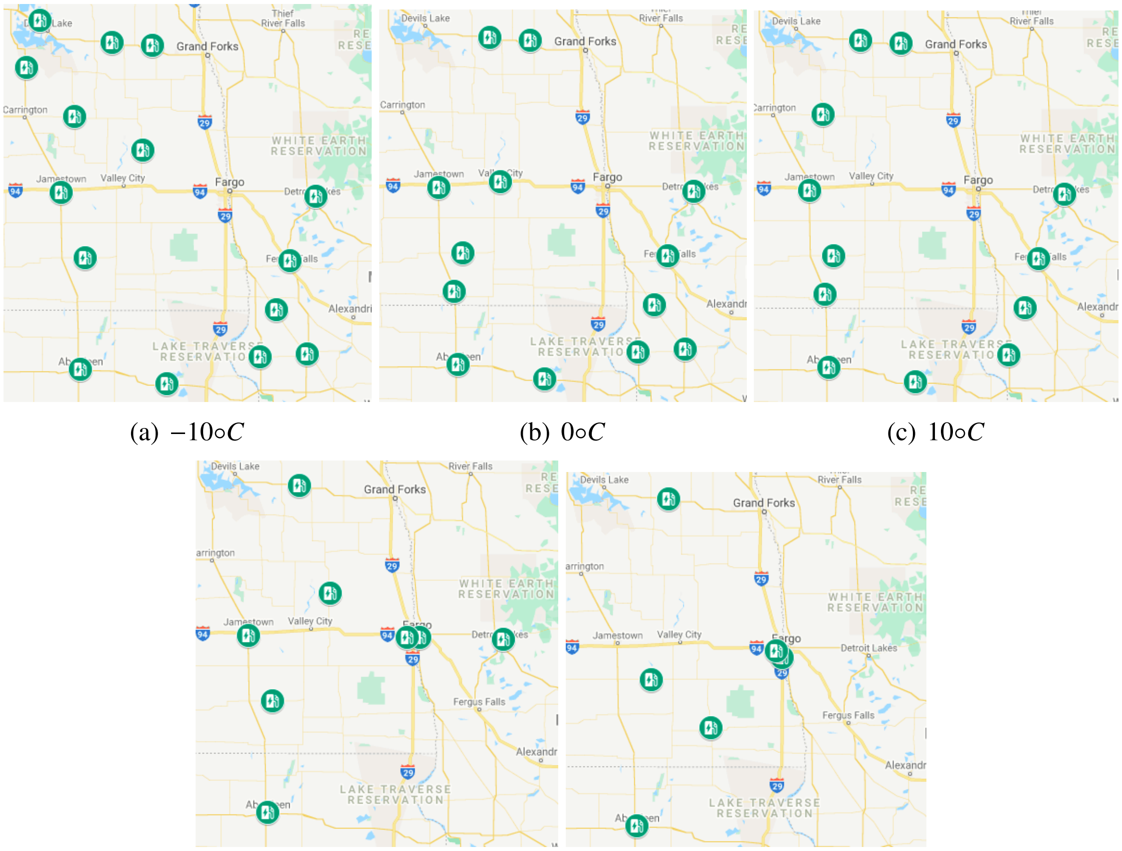

(a) $-10\circ C$ (b) $0\circ C$ (c) $10\circ C$

(d) $20\circ C$ (e) $30\circ C$

Figure 2.4

Illustration of charging station location decisions under different ambient temperatures

المنارة للاستشارات

www.manaraa.com

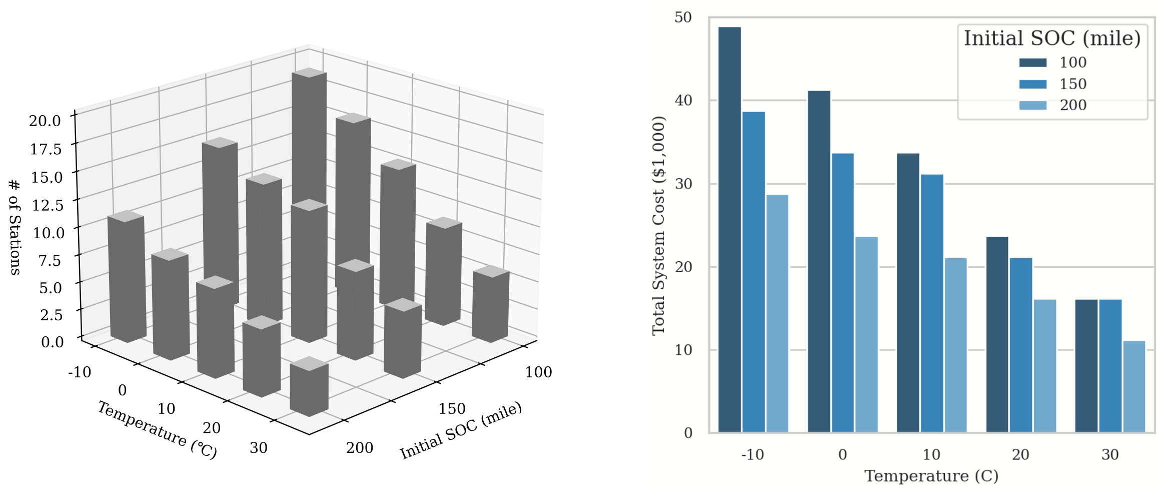

(a) Change in Station Selection

(b) Change in System Cost

Figure 2.5

Impact of temperature and initial SOC on EV DCFC charging station selection and system cost

station selection decisions and the overall system cost are susceptible to the variabilities present in the uncertain values of μ_1 and μ_2 parameters. For instance, for the case when the temperature is fixed to its base value ($10\circ C$) and the variabilities drops from high to low values, the located DCFC charging stations as well as the overall system cost decreases by 23.1% and 22.2%, respectively.

- In the final set of experiments, we assess the impact of the mean value of customers' demand and the ambient temperature on the DCFC charging station selection decisions and the overall system cost, while keeping the other parameters fixed to their base values. To run the experiments, we change the mean demand by −30% and 30%, respectively, to generate the *low* and *high* demand scenarios. The experimental results signify the importance of customers' demand on the DCFC charging station selection decisions and the overall system cost. For instance, when the ambient temperature is fixed to it's base value ($10\circ C$) and the

المنارة للاستشارات
www.manaraa.com

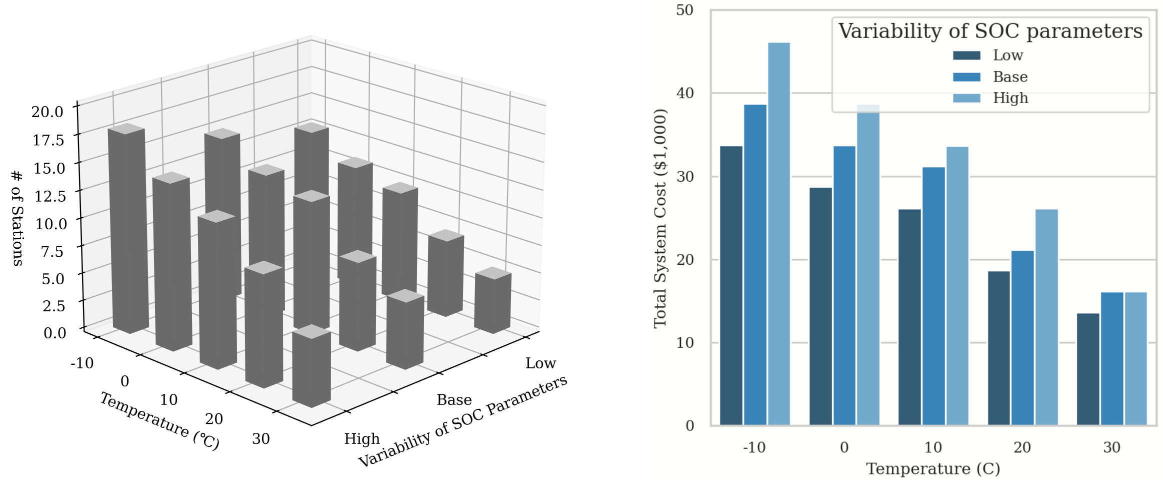

(a) Change in Station Selection

(b) Change in System Cost

Figure 2.6

Impact of temperature and SOC parameters on EV DCFC charging station selection and system cost

mean customers' demand drops from high to low values, the located DCFC charging stations and the overall system cost decreases by 15.3% and 15.9%, respectively.

المنارة للاستشارات
www.manaraa.com

CHAPTER III

CONCLUSIONS

3.1 Conclusion

The first chapter proposes a mixed-integer linear programming model to minimize the EV DCFC infrastructure and the associated routing decisions under fluctuating ambient temperature.Two highly customized heuristic approaches, namely, the two-phase Tabu Search-modified Clarke and Wright (TS-MCWS) algorithm and the Sweep-based Iterative Greedy Adaptive Large Neighborhood (SIGALNS) algorithm, are proposed to efficiently solve the optimization model. Both the algorithms' performance is tested under varying temperature, where SIGALNS are found consistent in providing high-quality feasible solutions in a reasonable timeframe. For instance, the SIGALNS algorithm is 2.7 and 2.4 times faster than TS-MCWS algorithm under 10 $\circ C$ and 30 $\circ C$, respectively. Results indicate that the EV DCFC siting decisions are highly sensitive to the ambient temperature. For instance, when the ambient temperature decreases from 10 $\circ C$ to -10 $\circ C$, the number of DCFC charging stations increases by approximately 141% (150 customers). The resultant siting decisions further increase the system cost by approximately 14.9%. We believe the insights gained from this study could help decision-makers efficiently design and manage DCFC EV logistic networks for cities that suffer from high-temperature fluctuations.

المنارة للاستشارات
www.manaraa.com

The second chapter proposes a two-stage mixed-integer programming model to formulate the EV DCFC infrastructure siting and the associated EV routing decisions under fluctuating ambient temperature and customer demand uncertainty. We then developed a highly customized solution technique PHA-SIGALNS, which combines Progressive Hedging algorithm with SIGALNS heuristic to efficiently solve the proposed optimization model in a reasonable timeframe. Further, we employ a *master-slave* architecture to speed up the solution time of the PHA-SIGALNS algorithm without sacrificing the solution quality. Testing the proposed algorithms' performance indicates that the parallelized heuristic outperforms other algorithms under different ambient temperatures. For instance, the parallelized heuristic, PHA-SIGALNS-PI, can solve the test instances 2.6 and 2.5 times faster compared to the PHA-SIGALNS algorithm, when the ambient temperature is $-10\circ C$ and $30\circ C$, respectively. Experimental results reveal that the EV DCFC siting and routing decisions are highly sensitive to fluctuations of the ambient temperature. For instance, it can be observed that if the ambient temperature drops from $10\circ C$ to $-10\circ C$, the number of located charging stations and the overall system cost is increased by 63.5% and 59.3%, respectively. We believe the managerial insights drawn from this study may help decision-makers designing a reliable and robust DCFC EV logistic network for a region with high weather variability.

Finally, we used Fargo city in North Dakota in both chapters as a testing ground to visualize the modeling results and to draw managerial insights.

للاستشارات المنارة
www.manaraa.com

3.2 Future Research Directions

This study paves the way to efficiently designing the DCFC EV logistic networks under ambient temperature and stochastic environment. This research can be extended in several directions. In VRP literature and reality, constraints such as time windows and battery swap stations (BSS) capacity are common problems; hence, we will consider such constraints in the formulation in future research. Second, it would be interesting to investigate how the stochasticity of a number of other parameters, such as travel time and EV load, impacts the model performance. Third, considering the uncertainty in travel times, the impact of the EV load on the battery depleting, and security of charging infrastructures issues [58, 59, 60], this study could bring greater benefits to DCFC EV logistic networks. Next, efforts will continue to developing more sophisticated solution techniques to efficiently solve the problem in a reasonable timeframe.then, the proposed model could be implemented in other geographic regions with varying climatic and traffic conditions to draw managerial insights for decision-makers. Finally, we will attempt to develop more efficient techniques to solve the larger instance of the problem in a reasonable time frame.These issues will be addressed in future studies.

المنارة للاستشارات

www.manaraa.com

REFERENCES

[1] A. Abdulaal, M. H. Cintuglu, S. Asfour, and O. A. Mohammed, “Solving the multivariant EV routing problem incorporating V2G and G2V options,” *IEEE Transactions on Transportation Electrification*, vol. 3, no. 1, 2016, pp. 238–248.

[2] Y. Adulyasak, J.-F. Cordeau, and R. Jans, “Optimization-based adaptive large neighborhood search for the production routing problem,” *Transportation Science*, vol. 48, no. 1, 2014, pp. 20–45.

[3] A. Aghalari, F. Nur, M. Marufuzzaman, and S. M. Puryear, “Designing a Reliable Inland Waterway Transportation Network under Uncertainty,” *arXiv preprint arXiv:2101.10120*, 2021.

[4] Aghalari A., Nur F., Marufuzzaman M., “A Bender’s based nested decomposition algorithm to solve a stochastic inland waterway port management problem considering perishable product,” *International Journal of Production Economics*, vol. 229, 2020, p. 107863.

[5] Aghalari A., Nur F., Marufuzzaman M., “Solving a Stochastic Inland Waterway Port Management Problem using a Parallelized Hybrid Decomposition Algorithm,” *Omega*, 2020, p. 102316.

[6] H. Asefi, S. Lim, M. Maghrebi, and S. Shahparvari, “Mathematical modelling and heuristic approaches to the location-routing problem of a cost-effective integrated solid waste management,” *Annals of Operations Research*, vol. 273, no. 1-2, 2019, pp. 75–110.

[7] R. Baldacci, A. Mingozzi, and R. Wolfler Calvo, “An exact method for the capacitated location-routing problem,” *Operations research*, vol. 59, no. 5, 2011, pp. 1284–1296.

[8] J.-M. Belenguer, E. Benavent, C. Prins, C. Prodhon, and R. W. Calvo, “A branch-and-cut method for the capacitated location-routing problem,” *Computers & Operations Research*, vol. 38, no. 6, 2011, pp. 931–941.

[9] R. W. Bent and P. Van Hentenryck, “Scenario-based planning for partially dynamic vehicle routing with stochastic customers,” *Operations Research*, vol. 52, no. 6, 2004, pp. 977–987.

[10] D. J. Bertsimas, “A vehicle routing problem with stochastic demand,” *Operations Research*, vol. 40, no. 3, 1992, pp. 574–585.

المنارة للاستشارات
www.manaraa.com

[11] G. Clarke and J. W. Wright, "Scheduling of vehicles from a central depot to a number of delivery points," *Operations research*, vol. 12, no. 4, 1964, pp. 568–581.

[12] G. B. Dantzig and J. H. Ramser, "The truck dispatching problem," *Management science*, vol. 6, no. 1, 1959, pp. 80–91.

[13] H. Das, M. Rahman, S. Li, and C. Tan, "Electric vehicles standards, charging infrastructure, and impact on grid integration: A technological review," *Renewable and Sustainable Energy Reviews*, vol. 120, 2020, p. 109618.

[14] H. Das, M. Rahman, S. Li, and C. Tan, "Electric vehicles standards, charging infrastructure, and impact on grid integration: A technological review," *Renewable and Sustainable Energy Reviews*, vol. 120, 2020, p. 109618.

[15] J. Dong, C. Liu, and Z. Lin, "Charging infrastructure planning for promoting battery electric vehicles: An activity-based approach using multiday travel data," *Transportation Research Part C: Emerging Technologies*, vol. 38, 2014, pp. 44–55.

[16] M. Drexl and M. Schneider, "A survey of variants and extensions of the location-routing problem," *European Journal of Operational Research*, vol. 241, no. 2, 2015, pp. 283–308.

[17] M. Dubarry, C. Truchot, M. Cugnet, B. Y. Liaw, K. Gering, S. Sazhin, D. Jamison, and C. Michelbacher, "Evaluation of commercial lithium-ion cells based on composite positive electrode for plug-in hybrid electric vehicle applications. Part I: Initial characterizations," *Journal of power sources*, vol. 196, no. 23, 2011, pp. 10328–10335.

[18] M. Dubarry, C. Truchot, B. Y. Liaw, K. Gering, S. Sazhin, D. Jamison, and C. Michelbacher, "Evaluation of commercial lithium-ion cells based on composite positive electrode for plug-in hybrid electric vehicle applications: III. Effect of thermal excursions without prolonged thermal aging," *Journal of the Electrochemical Society*, vol. 160, no. 1, 2012, p. A191.

[19] S. B. Ebrahimi, "A stochastic multi-objective location-allocation-routing problem for tire supply chain considering sustainability aspects and quantity discounts," *Journal of Cleaner Production*, vol. 198, 2018, pp. 704–720.

[20] S. Erdoğan and E. Miller-Hooks, "A green vehicle routing problem," *Transportation research part E: logistics and transportation review*, vol. 48, no. 1, 2012, pp. 100–114.

[21] M. S. Farham, H. Süral, and C. Iyigun, "A column generation approach for the location-routing problem with time windows," *Computers & Operations Research*, vol. 90, 2018, pp. 249–263.

[22] S. Fazayeli, A. Eydi, and I. N. Kamalabadi, "A model for distribution centers location-routing problem on a multimodal transportation network with a meta-heuristic solving approach," *Journal of Industrial Engineering International*, vol. 14, no. 2, 2018, pp. 327–342.

المنارة للاستشارات

www.manaraa.com

[23] K. M. Ferreira and T. A. de Queiroz, “Two effective simulated annealing algorithms for the location-routing problem,” *Applied Soft Computing*, vol. 70, 2018, pp. 389–422.

[24] M. Gendreau, G. Laporte, and R. Séguin, “An exact algorithm for the vehicle routing problem with stochastic demands and customers,” *Transportation science*, vol. 29, no. 2, 1995, pp. 143–155.

[25] M. Gendreau, G. Laporte, and R. Séguin, “A tabu search heuristic for the vehicle routing problem with stochastic demands and customers,” *Operations research*, vol. 44, no. 3, 1996, pp. 469–477.

[26] B. E. Gillett and L. R. Miller, “A heuristic algorithm for the vehicle-dispatch problem,” *Operations research*, vol. 22, no. 2, 1974, pp. 340–349.

[27] Gul S., Denton B.T., Fowler J., “A Multi-Stage Stochastic Integer Programming Model for Surgery Planning,” *Michigan Engineering*, 2012.

[28] A. Gupta, V. Nagarajan, and R. Ravi, “Approximation algorithms for VRP with stochastic demands,” *Operations Research*, vol. 60, no. 1, 2012, pp. 123–127.

[29] A. Gutierrez, L. Dieulle, N. Labadie, and N. Velasco, “A multi-population algorithm to solve the VRP with stochastic service and travel times,” *Computers & Industrial Engineering*, vol. 125, 2018, pp. 144–156.

[30] V. C. Hemmelmayr, J.-F. Cordeau, and T. G. Crainic, “An adaptive large neighborhood search heuristic for two-echelon vehicle routing problems arising in city logistics,” *Computers & operations research*, vol. 39, no. 12, 2012, pp. 3215–3228.

[31] J. Hof, M. Schneider, and D. Goeke, “Solving the battery swap station location-routing problem with capacitated electric vehicles using an AVNS algorithm for vehicle-routing problems with intermediate stops,” *Transportation Research Part B: Methodological*, vol. 97, 2017, pp. 102–112.

[32] J. Jaguemont, L. Boulon, and Y. Dubé, “A comprehensive review of lithium-ion batteries used in hybrid and electric vehicles at cold temperatures,” *Applied Energy*, vol. 164, 02 2016, pp. 99–114.

[33] Y. Ji, Y. Zhang, and C.-Y. Wang, “Li-ion cell operation at low temperatures,” *Journal of The Electrochemical Society*, vol. 160, no. 4, 2013, p. A636.

[34] M. Kabli, M. A. Quddus, S. G. Nurre, M. Marufuzzaman, and J. M. Usher, “A stochastic programming approach for electric vehicle charging station expansion plans,” *International Journal of Production Economics*, vol. 220, 2020, p. 107461.

[35] M. Kabli, M. A. Quddus, S. G. Nurre, M. Marufuzzaman, and J. M. Usher, “A stochastic programming approach for electric vehicle charging station expansion plans,” *International Journal of Production Economics*, vol. 220, 2020, p. 107461.

المنارة للاستشارات

www.manaraa.com

[36] F. Karamyar, J. Sadeghi, and M. M. Yazdi, “A Benders decomposition for the location-allocation and scheduling model in a healthcare system regarding robust optimization,” *Neural Computing and Applications*, vol. 29, no. 10, 2018, pp. 873–886.

[37] A. S. Kenyon and D. P. Morton, “Stochastic vehicle routing with random travel times,” *Transportation Science*, vol. 37, no. 1, 2003, pp. 69–82.

[38] M. Keskin and B. Çatay, “Partial recharge strategies for the electric vehicle routing problem with time windows,” *Transportation Research Part C: Emerging Technologies*, vol. 65, 2016, pp. 111–127.

[39] M. Keskin, B. Çatay, and G. Laporte, “A simulation-based heuristic for the electric vehicle routing problem with time windows and stochastic waiting times at recharging stations,” *Computers & Operations Research*, vol. 125, 2021, p. 105060.

[40] J.-G. Kim and M. Kuby, “The deviation-flow refueling location model for optimizing a network of refueling stations,” *international journal of hydrogen energy*, vol. 37, no. 6, 2012, pp. 5406–5420.

[41] Ç. Koç, T. Bektaş, O. Jabali, and G. Laporte, “The fleet size and mix location-routing problem with time windows: Formulations and a heuristic algorithm,” *European Journal of Operational Research*, vol. 248, no. 1, 2016, pp. 33–51.

[42] M. Kuby and S. Lim, “The flow-refueling location problem for alternative-fuel vehicles,” *Socio-Economic Planning Sciences*, vol. 39, no. 2, 2005, pp. 125–145.

[43] M. Kuby and S. Lim, “Location of alternative-fuel stations using the flow-refueling location model and dispersion of candidate sites on arcs,” *Networks and Spatial Economics*, vol. 7, no. 2, 2007, pp. 129–152.

[44] G. Laporte, F. Louveaux, and H. Mercure, “The vehicle routing problem with stochastic travel times,” *Transportation science*, vol. 26, no. 3, 1992, pp. 161–170.

[45] G. Laporte, R. Musmanno, and F. Vocaturo, “An adaptive large neighbourhood search heuristic for the capacitated arc-routing problem with stochastic demands,” *Transportation Science*, vol. 44, no. 1, 2010, pp. 125–135.

[46] G. Laporte and Y. Nobert, “An exact algorithm for minimizing routing and operating costs in depot location,” *European Journal of Operational Research*, vol. 6, no. 2, 1981, pp. 224–226.

[47] G. Laporte, Y. Nobert, and D. Arpin, “An exact algorithm for solving a capacitated location-routing problem,” *Annals of Operations Research*, vol. 6, no. 9, 1986, pp. 291–310.

[48] G. Laporte, Y. Nobert, and S. Taillefer, “Solving a family of multi-depot vehicle routing and location-routing problems,” *Transportation science*, vol. 22, no. 3, 1988, pp. 161–172.

المنارة للاستشارات

www.manaraa.com

[49] H. Lei, G. Laporte, and B. Guo, “The vehicle routing problem with stochastic demands and split deliveries,” *INFOR: Information Systems and Operational Research*, vol. 50, no. 2, 2012, pp. 59–71.

[50] Y. Li, P. Zhang, and Y. Wu, “Public recharging infrastructure location strategy for promoting electric vehicles: a bi-level programming approach,” *Journal of Cleaner Production*, vol. 172, 2018, pp. 2720–2734.

[51] S.-W. Lin, Z.-J. Lee, K.-C. Ying, and C.-Y. Lee, “Applying hybrid meta-heuristics for capacitated vehicle routing problem,” *Expert Systems with Applications*, vol. 36, no. 2, 2009, pp. 1505–1512.

[52] J. Lindgren and P. D. Lund, “Effect of extreme temperatures on battery charging and performance of electric vehicles,” *Journal of Power Sources*, vol. 328, 2016, pp. 37–45.

[53] R. B. Lopes, C. Ferreira, and B. S. Santos, “A simple and effective evolutionary algorithm for the capacitated location–routing problem,” *Computers & Operations Research*, vol. 70, 2016, pp. 155–162.

[54] J. Lysgaard, A. N. Letchford, and R. W. Eglese, “A new branch-and-cut algorithm for the capacitated vehicle routing problem,” *Mathematical Programming*, vol. 100, no. 2, 2004, pp. 423–445.

[55] H.-Y. Mak, Y. Rong, and Z.-J. M. Shen, “Infrastructure planning for electric vehicles with battery swapping,” *Management Science*, vol. 59, no. 7, 2013, pp. 1557–1575.

[56] Y. Marinakis, “An improved particle swarm optimization algorithm for the capacitated location routing problem and for the location routing problem with stochastic demands,” *Applied Soft Computing*, vol. 37, 2015, pp. 680–701.

[57] S. Martello and P. Toth, “Lower bounds and reduction procedures for the bin packing problem,” *Discrete applied mathematics*, vol. 28, no. 1, 1990, pp. 59–70.

[58] M. Marufuzamman, A. Aghalari, R. K. Buchanan, C. H. Rinaudo, K. M. Houte, and J. H. Ranta, “Optimal Placement of Detectors to Minimize Casualties in an Intentional Attack,” *IEEE Transactions on Engineering Management*, 2020.

[59] M. Marufuzzaman, A. Aghalari, R. Buchanan, C. H. Rinaudo, K. M. Houte, and J. H. Ranta, “Optimal Placement of Detectors to Minimize Casualties on a Manmade Attack,” *arXiv preprint arXiv:2101.10184*, 2021.

[60] M. Marufuzzaman, A. Aghalari, J. H. Ranta, and R. Jaradat, “Optimizing Civilian Response Strategy Under an Active Shooting Incident,” *IEEE Systems Journal*, 2021.

[61] R. Matulka, “Timeline: history of the electric car,” *Retrieved from United States Department of Energy Website: http://energy. gov/articles/historyelectric-car*, 2014.

المنارة للاستشارات

www.manaraa.com

[62] R. Matulka, “Timeline: history of the electric car,” *Retrieved from United States Department of Energy Website: http://energy. gov/articles/historyelectric-car*, 2014.

[63] P. Mirchandani, O. B. Madsen, and J. Adler, “Scheduling and location issues in transforming service fleet vehicles to electric vehicles,” *12th International Conference on Advanced Systems for Public Transport*, 2012.

[64] S. W. Moore and P. J. Schneider, *A review of cell equalization methods for lithium ion and lithium polymer battery systems*, Tech. Rep., SAE Technical Paper, 2001.

[65] Y. Motoaki, W. Yi, and S. Salisbury, “Empirical analysis of electric vehicle fast charging under cold temperatures,” *Energy Policy*, vol. 122, 2018, pp. 162–168.

[66] Mulvey J.M., Vladimirou H., “Applying the progressive hedging algorithm to stochastic generalized networks,” *Annals of Operations Research*, vol. 31, 1991, pp. 399–424.

[67] G. Nagy and S. Salhi, “Location-routing: Issues, models and methods,” *European journal of operational research*, vol. 177, no. 2, 2007, pp. 649–672.

[68] M. M. Nejad, L. Mashayekhy, D. Grosu, and R. B. Chinnam, “Optimal routing for plug-in hybrid electric vehicles,” *Transportation Science*, vol. 51, no. 4, 2017, pp. 1304–1325.

[69] R. Newell, D. Raimi, and G. Aldana, “Global Energy Outlook 2019: The next generation of energy,” *Resources for the Future*, 2019, pp. 8–19.

[70] J. Perl and M. S. Daskin, “A warehouse location-routing problem,” *Transportation Research Part B: Methodological*, vol. 19, no. 5, 1985, pp. 381–396.

[71] C. Prins, C. Prodhon, A. Ruiz, P. Soriano, and R. Wolfler Calvo, “Solving the capacitated location-routing problem by a cooperative Lagrangean relaxation-granular tabu search heuristic,” *Transportation Science*, vol. 41, no. 4, 2007, pp. 470–483.

[72] C. Prodhon and C. Prins, “A survey of recent research on location-routing problems,” *European Journal of Operational Research*, vol. 238, no. 1, 2014, pp. 1–17.

[73] M. A. Quddus, M. Kabli, and M. Marufuzzaman, “Modeling electric vehicle charging station expansion with an integration of renewable energy and vehicle-to-grid sources,” *Transportation Research Part E*, vol. 128, 2019, pp. 251–279.

[74] M. A. Quddus, M. Kabli, and M. Marufuzzaman, “Modeling electric vehicle charging station expansion with an integration of renewable energy and Vehicle-to-Grid sources,” *Transportation Research Part E: Logistics and Transportation Review*, vol. 128, 2019, pp. 251–279.

[75] M. A. Quddus, O. Shahvari, M. Marufuzzaman, J. M. Usher, and R. Jaradat, “A collaborative energy sharing optimization model among electric vehicle charging stations, commercial buildings, and power grid,” *Applied Energy*, vol. 229, 2018, pp. 841–857.

المنارة للاستشارات

www.manaraa.com

[76] M. A. Quddus, O. Shahvari, M. Marufuzzaman, J. M. Usher, and R. Jaradat, “A collaborative energy sharing optimization model among electric vehicle charging stations, commercial buildings, and power grid,” *Applied Energy*, vol. 229, 2018, pp. 841–857.

[77] M. A. Quddus, M. Yavuz, J. M. Usher, and M. Marufuzzaman, “Managing load congestion in electric vehicle charging stations under power demand uncertainty,” *Expert Systems With Applications*, vol. 125, 2019, pp. 195–220.

[78] M. A. Quddus, M. Yavuz, J. M. Usher, and M. Marufuzzaman, “Managing load congestion in electric vehicle charging stations under power demand uncertainty,” *Expert Systems with Applications*, vol. 125, 2019, pp. 195–220.

[79] Rockafellar R.T., Wets R.J.-B., “Scenarios and policy aggregation in optimization under uncertainty,” *Mathematics of operations research*, vol. 16, 1991, pp. 119–147.

[80] S. Ropke and D. Pisinger, “An adaptive large neighborhood search heuristic for the pickup and delivery problem with time windows,” *Transportation science*, vol. 40, no. 4, 2006, pp. 455–472.

[81] M. Schiffer and G. Walther, “The electric location routing problem with time windows and partial recharging,” *European Journal of Operational Research*, vol. 260, no. 3, 2017, pp. 995–1013.

[82] M. Schneider, A. Stenger, and D. Goeke, “The electric vehicle-routing problem with time windows and recharging stations,” *Transportation Science*, vol. 48, no. 4, 2014, pp. 500–520.

[83] P. Shaw, “A new local search algorithm providing high quality solutions to vehicle routing problems,” *APES Group, Dept of Computer Science, University of Strathclyde, Glasgow, Scotland, UK*, 1997.

[84] M. Smith and J. Castellano, *Costs associated with non-residential electric vehicle supply equipment: Factors to consider in the implementation of electric vehicle charging stations*, Tech. Rep., 2015.

[85] M. Soysal, M. Çimen, and S. Belbağ, “Pickup and delivery with electric vehicles under stochastic battery depletion,” *Computers & Industrial Engineering*, vol. 146, 2020, p. 106512.

[86] T. M. Sweda, I. S. Dolinskaya, and D. Klabjan, “Adaptive routing and recharging policies for electric vehicles,” *Transportation Science*, vol. 51, no. 4, 2017, pp. 1326–1348.

[87] E. M. Toro, J. F. Franco, M. G. Echeverri, and F. G. Guimarães, “A multi-objective model for the green capacitated location-routing problem considering environmental impact,” *Computers & Industrial Engineering*, vol. 110, 2017, pp. 114–125.

[88] D. Tuzun and L. I. Burke, “A two-phase tabu search approach to the location routing problem,” *European journal of operational research*, vol. 116, no. 1, 1999, pp. 87–99.

المنارة للاستشارات

www.manaraa.com

[89] C. Upchurch, M. Kuby, and S. Lim, "A model for location of capacitated alternative-fuel stations," *Geographical Analysis*, vol. 41, no. 1, 2009, pp. 85–106.

[90] T. Vidal, T. G. Crainic, M. Gendreau, and C. Prins, "Heuristics for multi-attribute vehicle routing problems: A survey and synthesis," *European Journal of Operational Research*, vol. 231, no. 1, 2013, pp. 1–21.

[91] F. Y. Vincent and S.-Y. Lin, "A simulated annealing heuristic for the open location-routing problem," *Computers & Operations Research*, vol. 62, 2015, pp. 184–196.

[92] Watson J.P., Woodruff D.L., "Progressive hedging innovations for a class of stochastic mixed-integer resource allocation problems," *Computational Management Science*, vol. 8, 2011, pp. 355–370.

[93] T.-H. Wu, C. Low, and J.-W. Bai, "Heuristic solutions to multi-depot location-routing problems," *Computers & Operations Research*, vol. 29, no. 10, 2002, pp. 1393–1415.

[94] R. Xiong, J. Tian, W. Shen, and F. Sun, "A novel fractional order model for state of charge estimation in lithium ion batteries," *IEEE Transactions on Vehicular Technology*, vol. 68, no. 5, 2018, pp. 4130–4139.

[95] R. Xiong, J. Tian, W. Shen, and F. Sun, "A Novel Fractional Order Model for State of Charge Estimation in Lithium Ion Batteries," *IEEE Transactions on Vehicular Technology*, vol. 68, no. 5, 2019, pp. 4130–4139.

[96] R. Xiong, Y. Zhang, H. He, X. Zhou, and M. G. Pecht, "A double-scale, particle-filtering, energy state prediction algorithm for lithium-ion batteries," *IEEE Transactions on Industrial Electronics*, vol. 65, no. 2, 2017, pp. 1526–1538.

[97] R. Xiong, Y. Zhang, H. He, X. Zhou, and M. G. Pecht, "A Double-Scale, Particle-Filtering, Energy State Prediction Algorithm for Lithium-Ion Batteries," *IEEE Transactions on Industrial Electronics*, vol. 65, no. 2, 2018, pp. 1526–1538.

[98] J. Yang and H. Sun, "Battery swap station location-routing problem with capacitated electric vehicles," *Computers & Operations Research*, vol. 55, 2015, pp. 217–232.

[99] X.-G. Yang, G. Zhang, S. Ge, and C.-Y. Wang, "Fast charging of lithium-ion batteries at all temperatures," *Proceedings of the National Academy of Sciences*, vol. 115, no. 28, 2018, pp. 7266–7271.

[100] M. H. F. Zarandi, A. Hemmati, and S. Davari, "The multi-depot capacitated location-routing problem with fuzzy travel times," *Expert Systems with Applications*, vol. 38, no. 8, 2011, pp. 10075–10084.

[101] M. H. F. Zarandi, A. Hemmati, S. Davari, and I. B. Turksen, "Capacitated location-routing problem with time windows under uncertainty," *Knowledge-Based Systems*, vol. 37, 2013, pp. 480–489.

المنارة للاستشارات

www.manaraa.com

[102] I. Zenginis, J. S. Vardakas, N. Zorba, and C. V. Verikoukis, “Analysis and quality of service evaluation of a fast charging station for electric vehicles,” *Energy*, vol. 112, 2016, pp. 669–678.

[103] B. Zhang, H. Li, S. Li, and J. Peng, “Sustainable multi-depot emergency facilities location-routing problem with uncertain information,” *Applied Mathematics and Computation*, vol. 333, 2018, pp. 506–520.

[104] P. Zhang, K. Qian, C. Zhou, B. G. Stewart, and D. M. Hepburn, “A methodology for optimization of power systems demand due to electric vehicle charging load,” *IEEE Transactions on Power Systems*, vol. 27, no. 3, 2012, pp. 1628–1636.

[105] S. Zhang, M. Chen, and W. Zhang, “A novel location-routing problem in electric vehicle transportation with stochastic demands,” *Journal of Cleaner Production*, vol. 221, 2019, pp. 567–581.

[106] Y. Zhao, L. Leng, and C. Zhang, “A novel framework of hyper-heuristic approach and its application in location-routing problem with simultaneous pickup and delivery,” *Operational Research*, 2019, pp. 1–34.

المنارة للاستشارات

www.manaraa.com